Democratic and Popular Republic of Algeria
Ministry of Higher Education and Scientific Research
A.MIRA-BEJAIA University

جامعة بجاية
Tasdawit n Bgayet
Université de Béjaïa

Faculty of Nature and Life Sciences
Department of Food Science
Biomathematics, Biophysics, Biochemistry and Scientometry Laboratory

THESIS

WITH VIEW TO OBTAIN THE DEGREE OF DOCTORATE

Domain: Natural and Life Sciences **Field :** Food Sciences

Speciality: Product Quality and Food Safety

Presented by

KRIBECHE Amina

Topic

Water purification using a plant by-product

Defended on : 07/10/2023

In front of the Jury composed of:

First & last name	Grade	Etablissement	
Mme BOULEKBACHE-MAKHLOUF Lila	Prof	Université de Bejaia	President
M. BEN HAMICHE Nadir	MCA	Université de Bejaia	Supervisor
M. MOUNI Lotfi	Prof	Université de Bouira	Reviewer
M. ZOUGGAGHE Fateh	Prof	Université de Bouira	Reviewer
Mme HAMRI-ZEGHICHI Sabrina	Prof	Université de Bejaia	Reviewer
M. BOUDRIES Hafid	Prof	Université de Bejaia	Reviewer

Academic year: 2022/2023

Democratic and Popular Republic of Algeria
Ministry of Higher Education and Scientific Research
A.MIRA-BEJAIA University

جامعة بجاية
Tasdawit n Bgayet
Université de Béjaïa

Faculty of Nature and Life Sciences
Department of Food Science
Biomathematics, Biophysics, Biochemistry and Scientometry Laboratory

THESIS

WITH VIEW TO OBTAIN THE DEGREE OF DOCTORATE

Domain: Natural and Life Sciences **Field :** Food Sciences

Speciality: Product Quality and Food Safety

Presented by

KRIBECHE Amina

Topic

Water purification using a plant by-product

Defended on : 07/10/2023

In front of the Jury composed of:

First & last name	Grade	Etablissement	
Mme BOULEKBACHE-MAKHLOUF Lila	Prof	Université de Bejaia	President
M. BEN HAMICHE Nadir	MCA	Université de Bejaia	Supervisor
M. MOUNI Lotfi	Prof	Université de Bouira	Reviewer
M. ZOUGGAGHE Fateh	Prof	Université de Bouira	Reviewer
Mme HAMRI-ZEGHICHI Sabrina	Prof	Université de Bejaia	Reviewer
M. BOUDRIES Hafid	Prof	Université de Bejaia	Reviewer

Academic year: 2022/2023

Don’t aim for success if you want it,

First do what you love and believe in,

And it will come naturally

David Forst

Acknowledgements

My dissertation work has been a long and rewarding journey. It has included many ups and downs. In the end, however, I managed to find my way back on track. Keeping the faith and finding the right track would not have been possible without the kind help of several people. It is now time to express my gratitude to those who have supported me during this journey.

I am forever grateful to my major advisor, Dr. Nadir BEN HAMICHE for the guidance, the undying patience, and assistance throughout these last five years. I cannot thank you enough for all the support, motivation, and patience you have provided to me repeatedly. I learned so much from you, you are the example to follow of work and perseverance. Your encouragements through the preparation of this work make me feel more confident.

I would like to express my gratitude to Pr. BOULEKBACHE –MAKHLOUF Lila, Pr. MOUNI Lotfi, Pr. ZOUGGAGHE Fateh, Pr. HAMRI-ZEGHICHI Sabrina, and Pr. BOUDRIES Hafid. Thank you all, for accepting to inspect my thesis work and document, thank you for the given attention and consideration. I am convinced that the time spent in the examination will help to enhance the quality of the work.

It is always impossible to personally thank everyone who has helped successful completion of this dissertation. To those of you without specifically name, my sincere thanks go to all of you.

I would like to thank all my friends and colleagues. Your company was encouraging, and the good atmosphere of mutual help that reigned in the laboratory permitted, largely, to carry out this work.

I save my deepest and warmest thanks to my family. My beloved parents, especially my mother there are no words to express my sincere gratitude to you for all the love and support during my life. My beloved brothers and sisters, thank you for always helping when needed and thank you for being such wonderful. Special thanks to my older brother for his support and encouragement which have always pushed me forward.

Amina

Table of content

Chapter III: coagulation –flocculation process

Chapter IV: Adsorption process

Part II: Material and methods

Section I

Seeds exploitation

Chapter I: Application in dam water treatment

Chapter II: Application in wastewater treatment

Section II

Seed husks exploitation

Part III: Results and discussion

Section I

Seed exploitation

Chapter I: application in dam water treatment

Chapter II: application in wastewater treatment

Section II

Seed husks valorization

List of Figures

List of Tables

List of Abbreviations

Adj-R^2 : Adjusted-coefficient of determination

ANN: Artificial Neural Network

BBD: Box-Behnken design

BOD: Biochemical Oxygen Demand

COD: Chemical Oxygen Demand

DSCP: dehulled Seeds Cake Powder

ED-XRF: Energy dispersive X-ray fluorescence spectrometry

EPA: Environmental Protection Agency

FFD: Full Factorial design

FT-IR: Fourier-transform infrared spectroscopy

ICP-MS: Inductively coupled plasma mass spectrometry

IUPAC: international union of pure and applied chemistry

IW: Inlet Water

KBr: Potassium bromide

KDa: Kilodalton

KeV: Electronvolt

Kj: Kilojoule

mA: milliamperes

MAE: Mean Absolute Error

MAPE: Mean Absolute Percentage Error

MB: Methylen Bleu

MFFF: Multilayer Full Feed Forword

MO: Moringa oleifera

MSE: Mean Squared Error

NTU: Nephelometric Turbidity Unit

OW: Outlet Water

pH: Hydrogen potential

R^2: Coefficient of determination

RMSE: Root-Mean-Square Error

RSM: Response Surface Method

rpm: round per minute

SEE: Standard error of Estimates

TSS: Suspended solids

UN: United Nations

µS/cm: microsiemens per centimetre

USCP: Unhulled Seeds Cake Powder

WWTP: Wastewater Treatment Plant

XRF: X-Ray Fluorescence

General introduction

General introduction

1. Background of the study

Water, as an essential element for all forms of life is not available in infinite quantities on our planet. It is the most important element of the mineral and biological world. It is very unevenly distributed on the planet **(spellman, 2007).** It covers more than 71% of the earth's surface. It is a necessary resource for all human activity and it is a key production factor in sustainable development **(Hinrichsen and Tacio, 2002)**. Water is becoming more and more central to strategic interests. All countries will, in the short or long term, have to deal with the problem of water scarcity **(spellman, 2007).** It is therefore necessary to have a better knowledge of existing water resources and their quality **(Alcamo et al., 2007).**

One of the serious problems in the world is the provision of clean drinking water, especially in developing countries. Providing potable water to many of the world's populations is a continuing challenge for governments and international bodies. It has been the focus of extensive global effort as exemplified by the United Nations millennium development goals and more recently in the sustainable development goals **(UN, 2022b).** It is currently estimated that a clean drinking water service was available to 74% of the world's population in 2020, up from 70% in 2015. In 2020, it was found that two billion people do not have access to properly managed drinking water systems, including 1.2 billion of whom do not even have the most basic level of service **(UN, 2022b).** These surface waters often contain pathogenic organisms that cause serious illness and death. These organisms include *Vibrio cholerae*, *poliovirus*, *Shigella, Campylobacter, E. coli*, and *Salmonella* recently estimated by the World Health Organization (WHO) state that contaminated water causes 485 000 diarrhoeal deaths each year **(WHO, 2022).**

There are many reasons why people do not have access to reliable, potable water, though in most cases it is a consequence of extreme poverty. The WHO has identified 22 countries where over 10% of the population relies on untreated surface waters. The majority of these 22 countries are in Sub-Saharan Africa where 10% of the population still rely on surface waters **(WHO, 2017).** In these areas where conventional water treatment options, such as chlorination, are not available or are too expensive, other traditional methods may be appropriate.

Population growth and economic development are putting unprecedented pressure on renewable but limited water resources, particularly in arid regions. The population of the globe

has expanded by more than three times since the middle of the 20th century. Massive urbanisation is expected to increase the world's population, which depending on the UN projects will reach 10 billion people by 2059 **(UN, 2022a).** It is also estimated that by 2025, 1.8 billion people will live in countries or regions with less than 500 m^3 of renewable water per year. According to prospective studies, pressures on resources are expected to increase and more countries will be in difficulty in the coming years. Thus, in 2025, almost half the population of the Mediterranean countries will be in a situation of water stress or scarcity **(FAO, 2007).**

When people use water, they not only consume it, but also release some of it into the environment. This is called wastewater **(Crotty, 2004).** This wastewater can contain various pollutants. Water pollution is defined as any physical or chemical change in the quality of water, while having a negative influence on the ecosystem and living organisms that makes the water unsuitable for the desired uses **(Crotty, 2004; Freeman, 2010).** Thus, water is said to be polluted when its composition is directly or indirectly modified by chemicals, industrial waste or other such as human action **(Freeman, 2010).**

In arid and semi-arid areas, where water is a limiting factor for plant production and where the needs linked to population growth and the increase in the standard of living are increasing, the volume of wastewater produced is increasing significantly and will continue to increase regularly. Under these conditions, wastewater can be considered an inexhaustible source. It is the only water resource that will grow in the future. It is therefore essential to take it into account and its use must therefore be integrated into the objectives of sustainable development, provided that it is purified **(Arnell, 2004; Alcamo, 2007).**

Urban wastewater treatment is part of a process to protect our environment and preserve our water resources. The choice of treatment process depends on the nature and the quantity of the water to be treated **(Huang et al., 2020).** However, wastewater treatment is almost absent in developing countries due to the high cost of investment and maintenance. There is therefore a need to find reliable, low-cost techniques that can effectively treat wastewater **(Mara, 2013).** There is a growing need to develop more environmentally friendly and appropriate wastewater treatment technologies whose performance is balanced by environmental, economic and societal sustainability (**Kalbar et al., 2016**). To this end, biological and natural processes in wastewater treatment could be a sustainable alternative in improving the quality of wastewater **(Kabore, 2011).**

2. Problematic

Access to safe drinking water is becoming a major concern in many parts of the world, particularly in rural areas where people are confronted to the poor management of water points, inadequate hygiene and sanitation, and the lack of appropriate disinfection methods at the family level. The production of drinking water requires the use of chemicals **(Alcamo, 2007),** as well as for wastewater purification **(Yin, 2010).** Various synthetic coagulants based on aluminium, iron salts and sodium carbonates are widely used, although their harmlessness to health in the event of long-term exposure can induce Alzheimer's and many other diseases **(Rondeau et al., 2000; Bondy and Campbell, 2018).** Unfortunately, the costs of conventional techniques used in treatment plants are not sufficient to solve the problem, especially in small communities. This has sparked worldwide interest in finding a safer and environmentally friendly alternative coagulant (**Yin, 2010; Gautam & Saini, 2020**). For this reason, several studies have been carried out to find ways of making coagulants from plants, in particular *Moringa oleifera.*

Plants have been used to treat water/wastewater for thousands of years **(Kansal & Kumari, 2014).** Nowadays, these natural alternatives are currently investigated and used as coagulants and disinfectants. Several plants have been considered as eco-friendly coagulants including *Capparidaceae*, *Papilionaceae* and *Moringaceae.* This last one, although very similar to the *Capparidaceae,* forms a family in their own right comprising a genus *Moringa* with 14 species including *Moringa oleifera***.** All of these plant materials exhibit coagulant or antibacterial properties. However, *Moringa oleifera* seeds are perfectly placed to achieve both **(Choy et al., 2014).** This tropical tree, which has enormous potential and beneficial properties for mankind, has considerable importance as a flocculant and disinfectant. Indeed, unlike other natural coagulants, *Moringa oleifera* seeds exhibit a natural and more effective flocculent activity with a turbidity reduction of up to 92-99% **(Ghebremichael et al., 2005).** It has been proven actually to be the best natural coagulant yet discovered which can, in fact, replace mineral flocculants, such as alumina sulphate, which is widely used worldwide **(Vilaseca et al., 2014),** by the presence of active cationic proteins, which acts as an adsorbent, coagulant and disinfectant agent **(Moulin et al., 2019).** This has given it the property to allow the treatment of drinking water, wastewater and factory effluents (**Kapse & Samadder, 2021; Vunainet al., 2019**).

3. Objective of the study

A good understanding of surface water purification processes is very useful for efficient water resource management. The focus was specifically on the use of the *Moringa Oleifera* seeds

as an effective coagulant in water and wastewater treatment using different processes. The principal aims of this work were:

- To identify the best ways of developing *Moringa Oleifera* seeds cake powder in a view of economic development, preserving the environment and improving biodiversity.
- To establish parametric coagulation-flocculation in water and wastewater treatment using the hulled and unhulled *Moringa Oleifera* seed cake powder;
- To valorise the *Moringa Oleifera* seeds by-products;
- To develop new applications for *MO* waste via the synthesis of new nanoparticles with adsorbent activity.

4. Adopted methodology

The treatment of raw water is complex and requires several steps. First, the coarse waste must be removed and then the suspended particles must be aggregated. The coagulation process is the main step. First, a coagulant is introduced, which neutralises the charge of the particles, and then a flocculent is injected to agglomerate these colloids. The water is then decanted, filtered and disinfected. This treatment is sometimes combined with other treatments such as adsorption, to deal with complex phenomena such as eutrophication. The adsorption process could also be considered as a main treatment, especially for dye removal. These two steps are brought together by adding the *Moringa Oleifera* seeds, which act as both coagulant and flocculent.

In one hand, this work aims firstly; to better document the effect of the influencing factors of coagulation-flocculation process for an optimum treatment according to different physicochemical parameters of water/wastewater and to evaluate, according to the obtained concentrations, the abatement of especially turbidity and suspended solids removal. The study also aims to evaluate the effect of the treatment on certain physicochemical parameters of sanitary interest, in particular nitrates, nitrites, phosphorus as well as heavy metals.

On the other hand, valorisation consists of moving away from the traditional linear economy model of taking natural resources and then throwing them away to a circular economy model where any material from one production process becomes the raw material for another process (**Dahiya et al., 2018**). Through this, the *Moringa oleifera* seeds wastes have been recovered for use in water purification as adsorbent. To achieve that, nanoparticles have been synthetised using *Moringa Oleifera* seeds waste and then tested in adsorption.

5. Manuscript Organisation

This thesis manuscript is structured into three principal chapters. The first chapter is devoted to a bibliographic synthesis on the different nails of the subject treated in this thesis, itself divided into 5 parts:

- Part A dealing with the problem of water pollution and it impacts on the environment;
- Part B presents a summary of the plant material used as coagulant, which is *Moringa oleifera.*
- Part C describes one of the most widely used water treatment methods, which is the coagulation-flocculation process, highlighting the different parameters reduced and/or influenced by this treatment process.
- Part D presents a second method of water treatment, namely adsorption.

The second chapter was designed on the adopted methodology to provide answers to the raised questions at the beginning of this dissertation. This chapter was divided on two main sections. The first one was devoted to the exploitation of the *Moringa Oleifera* seeds; its obtaining and the characterization of the prepared coagulants. This section has been divided in itself in two parts:

- Part A, dealing with the application of coagulation-flocculation process using *Moringa Oleifera* seeds cake powder in the treatment of surface water coming from the kissir dam located in the commune of Jijel, in which the coagulation-flocculation process effective parameters were studied using the Response Surface Method (RSM) and the neural networks (ANN).
- Part B, describing the application of the *Moringa Oleifera* seeds cake powder in wastewater treatment using the same approaches at the inlet and the outlet of Sidi Ali lebhar wastewater plant;

The second section has been reserved to the valorisation of *Moringa Oleifera* seeds waste via green synthesis of *Moringa Oleifera* nanoparticles and its application in the treatment of dye polluted water. In this section methylene blue was the target textile dye. Each part of this chapter has been consolidated by a scientific paper submitted or published. The obtained results have been then illustrated and discussed in the results and discussion section.

These chapters are also supplemented by a conclusion summarising briefly the main results and suggests research field for the coming years, since the scope of the subject merits further development.

Literature review

Literature review

Chapter I

Water pollution

1. Introduction

Governments and international organisations continue to face difficulties in providing clean water to many of the world's population. It has been the subject of intense worldwide effort, as demonstrated by the United Nations millennium development goals and, more recently, the sustainable development goals **(UN, 2022b).** Although people intuitively associate dirt with disease and the transmission of disease to pathogenic organisms in polluted water **(Gleick, 2002).** We now recognise that water pollution is a much broader threat and continues to pose serious health risks to the public and aquatic life. Water pollution is considered primarily a threat to human health due to the transmission of bacterial and viral waterborne diseases. In less developed countries, and in almost all countries in times of war, waterborne diseases remain a major threat to public health. In developed countries, however, water treatment and distribution methods have almost eradicated microbial contamination of drinking water (**Haseena et al., 2017).**

In this part of the Literature review, we discuss the sources of water pollution and the impact of this pollution on rivers, lakes and oceans, and the different process for water and wastewater treatment.

1.1. Water pollution definition

Water pollution or so-called aquatic pollution is the contamination of water bodies, usually as a result of human activities, in a way that adversely affects its legitimate uses **(Bhateria and Jain, 2016).** Water pollution reduces the capacity of the water surfaces to provide the ecosystem services that it would otherwise provide. Water surfaces include, for example, rivers, lakes, aquifers, oceans, reservoirs and groundwater **(Grizzetti et al., 2016).** Water pollution is therefore the result of the introduction of contaminants into these water surfaces. For example, the discharge of inadequately treated industrial wastewater into natural waters can lead to the

degradation of these aquatic ecosystems. All fauna and flora living in or exposed to polluted water can be affected. These effects can damage individual species and affect the natural biological communities of which they are a part. Water pollution can also lead to water-borne diseases in people who use polluted water for drinking, washing, bathing or irrigation **(Boelee et al., 2019).**

1.2.Water classification and pollution sources

Water can be classified based on several criteria **(Shmeis, 2018).** In this section water is classified based on its origin:

1.2.1. Underground water

When rain falls and seeps deep into the ground, occupying the cracks, pores and crevices of an aquifer (essentially a groundwater supply), it becomes groundwater. It is one of the least visible but most important natural resources. Almost 40% of the world's population depend on groundwater, pumped from the earth's surface, for their drinking water supply. For some people, especially in rural areas, it is their only source of fresh water. This groundwater is contaminated when pollutants such as pesticides and fertilizers from landfills and septic tanks, enter an aquifer, making them harmful to humans and environment. It can be then difficult, if not impossible, to remove contaminants from groundwater, and this leads to fatal and irreversible consequences. Once an aquifer is polluted, it may be unusable for decades or even thousands of years. Groundwater can also spread contamination far from the original source of pollution, seeping into rivers, lakes and oceans **(Harter, 2003).**

1.2.2. Surface water

Surface water, which makes up about 70% of the planet's surface, fills the oceans, lakes, rivers and all the other blue parts of the world map. Surface water from freshwater sources (i.e. sources other than the ocean) accounts for over 60% of the world's water supply **(Ward et al., 2020).** However, a large percentage of this water is at risk. According to the latest global water quality surveys, almost half of all rivers and more than a third of all lakes are contaminated and unsuitable for fishing, swimming and drinking. Pollution by nutrients including nitrates and phosphates represents the main type of contamination of these freshwater sources. Although plants and animals need these nutrients to grow, they have become a major contaminant due to agricultural waste and fertiliser run-off. Also, municipal and industrial waste discharges contribute much of their toxicity through their content of heavy metals, dyes and other toxic

pollutants. The waste that industry and individuals discharge directly into waterways represent also essential water pollution sources **(Borthakur and Singh, 2020).**

1.2.3. Oceans

Eighty percent of ocean pollution, or marine pollution, comes from land, both along the coast and far inland. Pollutants such as nutrients, chemicals and heavy metals are transported from farms, factories and cities by streams and rivers to bays and estuaries; from there they move to the sea and oceans. Meanwhile, marine debris, especially plastic, is blown away or washed down storm drains. The seas are also sometimes disturbed by oil spills and leaks (large and small) and are constantly absorbing carbon from the atmosphere. The ocean absorbs up to a quarter of carbon emissions from human activities **(Landrigan et al., 2020).**

1.2.4. Point source

When the contamination comes from a single source, this is called point source pollution. This includes wastewater (also known as discharges or effluents) discharged legally or illegally from a manufacturer, oil refinery or wastewater treatment facility, as well as contamination from leaking septic systems, chemicals and oil spills, and illegal discharges. The Environmental Protection Agency (EPA) regulates point source pollution by setting limits on what can be discharged from a facility directly into a water body. Although point source pollution originates from a specific location, it can affect miles of streams and ocean **(Wu & Chen, 2013).**

1.2.5. Non-point source

Non-point source pollution is represented by contamination from different sources. It can be agricultural runoff, stormwater, industrial wastewater or debris dumped into waterways by land. Pollution from non-point sources is the main cause of water pollution, but it is difficult to organise or control, while there is no single identifiable culprit **(Wu & Chen, 2013).**

1.2.6. Transboundary

Water pollution cannot be contained by a line on a map. Transboundary pollution occurs when contaminated water from one country enters the oceans of another country or continent. Contamination can result from a disaster, such as an oil spill, or from downstream contamination of industrial, agricultural or municipal discharges **(Guo, 2021).**

1.3. Impacts of water pollution

Water pollution poses major risks to both human health and environment **(Primack and Morrison, 2013).**

1.3.1. Impact on human health

Water pollution causes many contagious waterborne diseases that are the result of the fecal-oral route. The health risks resulting from water pollution include diseases such as cancer, diarrhoeal diseases, respiratory diseases, neurological disorders and respiratory diseases **(Halder & Islam, 2015; Haseena et al., 2017).** Poor people are vulnerable to disease due to poor sanitation, hygiene and water supply. Pregnant women are at greater risk and suffer adverse effects when exposed to contaminated water chemicals, resulting in increased rates of low birth weight **(Halder & Islam, 2015).**

1.3.2. Environmental impacts

Harmful ecosystems are based on a complex network of animals, plants, bacteria and fungi plants, which directly or indirectly interfere with each other. Damage to these organisms can create a chain effect and endanger entire aquatic environments. When water pollution causes an algal bloom in a marine environment, the newly introduced nutrient bloom stimulates plant and algal growth, reducing dissolved oxygen levels in the water. This lack of oxygen, known as eutrophication, suffocates animals and plants and can create "dead zones". In that zones water is essentially devoid of life. These harmful algal blooms can also in some cases create neurotoxins that affect wildlife of whales and sea turtles **(Mareddy, 2017).** Water is also contaminated with several toxic heavy metals and chemicals from industrial and municipal wastewater **(Behbahaninia et al., 2009).**

1.4.Polluted water treatment processes

In order to deal with these pollution problems and purify these polluted water resources, different water/wastewater treatment processes have been developed. These processes are classified into four different categories: physical, chemical, physico-chemical and biological treatment **(Saravanan et al., 2021).**

1.4.1. Physical processes

These methods such as filtration, sedimentation, flotation and skimming are used to eliminate solids where no chemical components are involved in the process **(Cheremisinoff, 1997).** One of the main techniques for physical treatment of water/wastewater is sedimentation, which deals with the suspension of insoluble/heavy particles in water/wastewater. Once the insoluble solids settle to the bottom, they can be separated from the pure water **(O'Melia, 1998).** After sedimentation water has to be filtrated. The sand filter is the most commonly used.

1.4.2. Chemical processes

As the name suggests, this technique involves the use of chemicals. Chlorine, an oxidising chemical, is often used to eliminate bacteria that break down water/wastewater by adding contaminants. Another oxidising agent used to purify wastewater is ozone **(Yargeau, 2012).** The chemicals also prevent bacteria reproduction in water **(Gupta et al., 2012).**

1.4.3. Physicochemical processes

Physicochemical treatment is one of the most effective basic processes for water treatment. Physicochemical treatment involves a range of techniques that can be carried out consecutively in a single or in separate unit. These processes are coagulation, flocculation, sedimentation, adsorption, membrane separation, and oxidation **(Gerba and Pepper, 2019).**

1.4.4. Biological processes

Several biological processes are used to break down the organic matter present in water/wastewater, such as soap, oils, waste, etc. In biological treatments, microorganisms metabolise the organic matter present in wastewater **(Yildiz, 2012).** Secondary treatments are required to remove solids from wastewater, but some dissolved nutrients such as nitrogen and phosphorus may persist. These biological processes are generally more economical, environmentally friendly, and efficient water treatment techniques **(Alenazi et al., 2020).** In this context, a number of natural products such as lime seeds **(Seghosime et al., 2017),** pods and seeds of tamarind **(Buenaño et al., 2019),** leaves of acorn **(Benalia et al., 2019),** peels of banana **(Zaidi, 2019),** Ipomoea batatas leaves **(Kusuma et al., 2021** *Moringa oleifera* seeds **(Ndabigengesere et al., 1995)** and many others have been used. The *Moringa oleifera* seeds however, are one of the typical natural plant-based coagulants that are extensively explored because of their effectiveness in treating turbid water **(Ndabigengesere et al., 1995).**

These producing coagulants may provide socioeconomic benefits to local populations that depends on agricultural economies, and can maintain a consistent supply of raw materials for the production of green coagulants. This is the case of *Moringa oleifera* seeds, rice starch**,** Nirmali seeds known by *S. potatorum* (nirmali), *Opuntia ficus indica* (cactus), *Plantago ovate*, *Trigonella foenum graecum* **(yin, 2010)**. The *Moringa oleifera* seeds contain more than just oil, and similarly to the cassava derivatives (Manihot spp), the waste generated during oil extraction can be employed as coagulants **(yin, 2010)**. Compared to other coagulants, this is regarded as a benefit. They are non-corrosive, which removes the possibility of pipe erosion, and have the potential to be carbon-neutral while manufacturing. At a rate that is nearly five times slower,

they can all generate sludge, and the produced sludge can be effectively degraded by biological processes because it is biodegradable **(Ndabigengesere et al., 1995).** Due to their low toxicity, it can be used safely as soil fertiliser, which lowers the cost of sludge management **(Choy et al., 2014).** With all of these advantages over other biomaterials, the *Moringa oleifera* seeds are an excellent coagulant for selection.

Chapter II

Moringa oleifera

1. Introduction

Since many years, there has been a substantial global worry about the need to create novel approaches for treating water/wastewater and supplying enough water to meet this need **(Qu et al., 2013).** Actually, water treatment using plants dates back thousands of years **(Kansal & Kumari, 2014),** and natural coagulants have long been traditionally used in water treatment **(Choy et al., 2014; Bratby, 2016)**. Scientific papers have identified several natural materials used for water purification VIZ plant seeds, fruit waste and bark. A number of effective coagulants are present in nature, which can be used either directly or after modification. The seeds of *Moringa oleifera* and *Strychnos potatorum*, as well as their leaves and the sap of *Opuntia ficus indica*, are among the plants that are frequently studied **(Yin, 2010; Kansal & Kumari, 2014).** All of these plant components have coagulant or antibacterial qualities, While *Moringa oleifera* seeds have both **(Choy et al., 2014).**

2. Source, origin and presentation of *Moringa oleifera*

The origin of *Moringa oleifera (MO)* is not really unknown, it was cultivated since antiquity. It is originated in India, south of the Himalayas. It has been naturalised in tropical and subtropical regions of the world, including many countries**.** Thanks to its exceptional medicinal and food virtues as well as its geographical distribution, different populations have attributed to this tree several names such as “tree of life”, “tree of paradise”, “horseradish tree”, “baguette tree” **(Chukwuebuka, 2015; Bidima, 2016; Abiyu et al., 2018; Bhattacharya et al., 2018).** The attributed names to *MO* in different countries are illustrated in **Table 1.** The *MO* originated in northern India is now widely distributed in tropical and subtropical countries, mainly in America, Africa, Oceania and Asia **(Figure 1) (Biswas Subrata Kumar, 2012; Oladoja & Pan, 2015; Zhigila et al., 2015; Saini et al., 2016; Brilhante et al., 2017)**. India is considered the largest producer with an annual production of between 1.1 and 1.3 million tonnes of seeds per year **(Bichi, 2013)**. In Africa, the tree has rapidly changed its status. Today, it occupies the place of a magical tree, which until recently was a hut tree, serving as a hedge or shade, sometimes as a medicinal or food-gathering plant **(Abderrezak & Alim, 2020).**

Figure 1. Geographical distribution of *MO* worldwide **(Saini et al., 2016).**

Table 1. List of some vernacular names for *MO* in some countries **(Bichi, 2013).**

Language	Designation
English	Moringa, horseradish tree, chopstick tree, Sujuna, ben tree, ben oil tree.
French	ben ailé, ben oléifère, benzolive, arbre radis du cheval; Spanish: ben, árbol del ben, paraiso, morango, Moringa
Spanish	ben, árbol del ben, paraiso, paraiso, morango, Moringa;
Portuguese	Acácia acácia, marungo, muringa, moringuiero; cedro (Brazil);
Arabic	ruwag, alim, halim, shagara al ruwag (Sudan);

3. Classification and Botanical description

The *MO* is a member of the *Moringaceae* family **(Bichi, 2013; Bidima, 2016).** With slender stems, in the form of flasks or as a tree or shrub. This family includes 13 currently known and morphologically different species. The *MO* is the most important species but also *Moringa stenopetala* and *Moringa massif* **(Abiyu et al., 2018).** The taxonomic classification of *MO* is illustrated in **Table 2.** The *MO* is characterised by tuberous taproots, which explains the plant's tolerance to drought conditions. Normally umbrella-shaped, the tree has a loose crown with graceful, airy foliage, whose feathery effect is due to the fine, innate division of the leaves. The leaves are densely packed at the top of the branches **(Bichi, 2013).**

In some cases, the *MO* tree can reach a height of 10 metres. It is a tree with pale grey or buff bark, sometimes smooth and sometimes rough. The trunk of the *MO* is 20 to 40 centimetres long. The fruits of the *MO* are elongated pods, divided into three valves **(Figure 2).** The pods are 10 to 15 centimetres long, brown in colour at the mature stage, and may contain up to 12 and 35 round seeds, surrounded by a semi-permeable brown shell. The seed shell is surrounded by

whitish wings extending from the base to the top. The abundant, pleasant-smelling *Moringa* flowers are white or cream in colour, sometimes with reddish spots **(Bidima, 2016).**

Table 2. Taxonomic classification of *MO* **(Mishra et al., 2011).**

Kingdom	Plantae
Sub kingdom	Tracheobionta
Super Division	Spermatophyta
Division	Magnoliophyta
class	Magnoliopsida
Subclass	Dilleniidae
Order	Capparales
Family	Moringaceae
Genus	Moringa
Species	Oleifera

Figure 2. Different vegetative and reproductive parts of *MO* tree; ***(a):*** field grown tree, ***(b):*** bundle of foliage, ***(c):*** flowers, and ***(d)*** fruit in pods **(Saini et al., 2016).**

4. Cultivation of the tree

The *MO* tree can grow in dry and impoverished areas **(Abiyu et al., 2018).** It can be grown in arid, semi-arid and hot areas, in temperatures between 25 and 35 °C, but can temporarily tolerate up to 48 °C as well as light frost conditions in subtropical areas, which allows it to be grown in several regions around the world including southern Algeria. It is drought tolerant and grows with annual rainfall between 250 and 3000 mm and at altitudes below 600 m. The *MO* tree can be grown in soils with a pH between 5.0 and 9.0, but grows best in neutral. It is also best suited to well-drained, sandy-clay soils, but can grow in clay soils without standing water. The soil does not necessarily have to be fertile, as the crop can also thrive in poor soil, starting to flower 8 months after planting and produce fruit within 15 months **(Pereira et al., 2015; Chukwuebuka, 2015; Abderrezak & Alim, 2020).**

5. Characteristics of *Moringa oleifera*

The *MO* has attracted the interest of scientists because of it chemical composition. The plant showed the presence of bioactive compounds showing the predominance of secondary metabolites such as phenolic acids, gallic acid, ellagic acid, chlorogenic acid, ferulic acid, glucosinolates, flavonoids, quercetin, vanillin and kaempferol, which give the plant special nutritional, pharmaceutical or antimicrobial properties. However, the content of these metabolites in *MO* extract varies according to geographical location, soil type, sun exposure and climatic conditions **(Brilhante et al., 2017). Table 3** shows the macro-nutrient composition of *MO* seeds.

Table 3. The *MO* macronutrient composition **(Brilhante et al., 2017).**

Nutrient components	MO (g/100g of plant material)		
	Leaves	Pods	Seeds
Proteins	25.0 – 30.3	6.7–43.5	29.4–38.3
Fats	00.1 – 10.6	0.1–05.1	30.8–41.2
Carbohydrates	00.1 – 43.9	0.1–38.2	00.1–21.1
Fibres	00.1 – 28.5	0.1–27.0	00.1–07.2

Table 4. The amino acids content in the different parts of *MO* tree **(Brilhante et al., 2017).**

	Amino acids	MO (g/100g of plant material)		
		Leaves	Pods	Seeds
Essentials	Arginine	0.4–1.8	0.36	4.5
	Histidine	0.1–0.7	0.11	2.3
	Leucine	0.4–2.2	0.65	6.7
	Lysine	0.3–1.4	0.15	1.5
	Méthionine	0.1–0.5	0.15	2.4
	Phénylalanine	0.3–1.6	0.43	4.0
	Thréonine	0.1–1.3	0.39	3.1
	Tryptophane	0.1–5.2	ND*	1.6
	Valine	0.4–1.4	0.54	4.3
Non-essentials	Alanine	1.8–3.0	ND	6.9
	Aspartate	1.4–2.2	ND	5.0
	Cystéine	0.01–0.10	ND	2.0
	Glutamate	2.5–2.5	ND	20.9
	Glycine	1.3–1.5	ND	10.9
	Proline	1.2–1.4	ND	4.5
	Serine	1.0–1.2	ND	4.4
	Tyrosine	0.01–2.60	0.08	1.6

ND : not determined*

Among the different nutrients of *MO* proteins represent the most important range occupying 25% of dry weight and at least 19 amino acids have been identified in this plant **(Anwar et al., 2007).** The amino acids content is shown in **Table 4.** The high nutritional content

of the leaves is due to the presence of the lipid compounds linoleic acid and palmitic acid **(Moyo et al., 2011).** Lipids are very abundant in the seed, mainly stearic acid, saturated palmitic acid and oleic acid, representing about 30% of the dry weight **(Abdulkarim et al., 2005).**

6. *Moringa oleifera's* applications

Thanks to its high quality composition, *MO* has a variety of applications including: pharmaceuticals, cosmetic, human food, animal fodder (processed leaves and cakes), alley cropping (biomass production), fertiliser (cakes), living fences, household cleaning products (crushed leaves), fuel wood, and others **(Chukwuebuka, 2015; Daba, 2016; Brilhante et al., 2017).** Since that, all parts of *MO* have become widely used, well adapted, and of great economic important **(Daba, 2016).** However, for many years, several studies have been looking at the potential of its seeds and pods for water treatment **(Camacho et al., 2017; Yamaguchi et al., 2021).**The most popular applications of *MO* are:

6.1.Nutritional applications

In Asia and Africa, the leaves, fresh pods (fruits) and seeds of *MO* are consumed and the roots are used as spice **(Velázquez-Zavala et al., 2016).** Protein, fibre, carbohydrates, amino acids, vitamins, carotenes, tocopherols and minerals have been identified in the plant, and the most abundant element is potassium **(Velázquez-Zavala al., 2016).** The obtained oil from the seeds has nutritional value and is suitable for frying due to its stability and high oleic acid content. In the leaf, linoleic acid is the most dominant acid, while in the rest of the plant it is palmitic acid **(Agoyi et al., 2014)** and even omega 3 and 6 acids **(Ayerza, 2012).** The leaves are very nutritive, thus new-borns and nursing mothers especially those from developing nations or regions where malnutrition is a problem are strongly advised to consume them. This is due to the increased risk of nutritional deficits in both classes. Infants are in a key developmental stage, and pregnant women and nursing moms require a steady supply of nutrients. It is known as the "Mother's Best Friend" due to its use to boost women's milk supply **(Estrella et al., 2000; Siddhuraju & Becker, 2003; Anwar et al., 2007).** For this, *MO* has been recommended by the United Nations (UN) to supplement the human diet **(Velázquez-Zavala et al., 2016).** It is also important to point out that numerous studies have demonstrated the versatility of *MO* 's major sections in producing foods for human consumption, such as cake **(Kolawole et al., 2013),** yoghurt **(Hekmat et al., 2015),** amla **(Karim et al., 2015),** weaning foods **(Arise et al., 2014)**, bread **(Chinma et al., 2014),** Soups **(Babayeju et al., 2014**) and biscuits **(Alam et al., 2014).**

6.2.Applications in the pharmaceutical field

One of the most beneficial trees in the world is the *MO*, which may be used for both medical and industrial reasons (**Khalafalla et al., 2010).** It contains over 90 chemical nutrients, including proteins, fats, carbohydrates and dietary fibre. In the tropical regions, it is used as a food source to overcome malnutrition, mainly in children and infants (**Brilhante et al., 2017).** It is traditionally used for the treatment of a number of diseases, including convulsions, diarrhoea, as a diuretic and stimulant in paralytic conditions, epilepsy, hysteria and high blood pressure **(Shah et al., 2011).** The medicinal uses/benefits of *MO* cannot be exhausted. This is because almost all parts of the tree have been used in traditional medical contexts. The flowers, leaves and roots are used for the treatment of ascites, rheumatism, venomous bites and as heart and circulatory stimulants in folk remedies **(Chukwuebuka, 2015).** Leaves have a very important role in reducing liver and kidney damage caused by the use of certain drugs such as gentamicin, pyrazinamide, rifampicin, isoziazide and acetaminophen **(Sharifudin et al., 2013; Toppo et al., 2015).** The oil is applied externally for skin diseases **(Chukwuebuka, 2015)**. The roots of the young tree as well as the root bark are rough and blistering **(Anwar & Bhanger, 2003).** The juice of the leaves is used in case of hiccups (emetic in high doses); the cooked leaves are given in case of flu. The root bark is used as an antiviral, anti-inflammatory and analgesic. The bark and flowers are hypoglycaemic. The seed infusion is anti-inflammatory, antispasmodic and diuretic, and is also used for venereal diseases. The seed infusion is anti-inflammatory, antispasmodic and diuretic, and is also used for venereal diseases **(Mishra et al., 2011).** *Moringa* supports also a healthy cardiovascular system, promotes normal blood sugar levels, neutralizes cancer-causing free radicals, provides excellent support for the body's anti-inflammatory mechanisms, enriches anemic blood and supports the immune system **(Mahmood et al., 2010; Razis et al., 2014).** It also improves eyesight, mental alertness and visual acuity. It has potential beneficial effects on malnutrition, general weakness, nursing mothers, menopause, depression and osteoporosis **(Mahmood et al., 2010).**

6.3.Applications in the energy field

Globally, the overuse of fossil fuels has led to rising energy demand as well as environmental problems like global warming. As a result, alternative energy or fuel sources need to be developed and improved. It has been suggested that bio-derived oil (biodiesel) could be used in addition to or in substitute of petroleum-derived oil. Due to the lack of sulphur and aromatic chemicals, biodiesel emits fewer monoxides, hydrocarbons, and particulates into the environment. More specifically, biodiesel can reduce developing countries' excessive

dependence on imported petroleum-based diesel **(Karmakar et al., 2010).** Approximately 45% of the weight of a *MO* seed kernel is oil. This oil can be consumed, used to make cosmetics, and for lubrication. Additionally, following prolonged storage, *MO* seed oil is resilient to oxidative decay **(Ofor & Nwufo, 2011).** The oil has potential for other industrial applications in addition to its current use in industry as a fine lubricant due to its fatty acid profile and high oleic acid content. It can therefore be used for biodiesel production **(Nayeripour & Kheshti, 2011).** The oil can be used as an alternative energy source that is accessible, technically feasible, economically viable and environmentally acceptable. It can be used as a biomass feedstock for the production of biodiesel **(Biswas, 2008).** Biofuels from this plant have reduced carbon monoxide emissions as well as hydrocarbon emissions **(Mofijur et al., 2014).**

6.4.Application in the cosmetic field

The *MO* oil has been presented as an excellent emollient and with high oxidative stability. As a natural product, *MO* seed oil has been commonly used for topical skin application since ancient times until today. It has been demonstrated that *MO* seed oil is effective at removing wrinkles from the skin and is a crucial component of perfumes and lotions **(Lalas & Tsaknis, 2002).** It is also used to moisturise and regenerate skin and in hair care products. Ancient Egyptians utilised the oil in ointments and skin preparations **(Mahmood et al., 2010).** Now, there is a growing trend to replace synthetic products and return to the use of natural oils in the cosmetic and pharmaceutical industries **(Kleiman et al., 2008).**

6.5.Cooking applications

The fruits of the young pods are very tasty and can be eaten boiled like beans. The dried seeds can be ground into powder and used to season sauces **(Foidl et al., 2001).** They can be eaten like peas, boiled or fried while still green. The *MO* seed oil is widely used as vegetable oil or for the production of soap and cosmetics **(Sánchez-mechado et al., 2010).** The *MO* roots are thick and soft. They are generally used to make a condiment similar to horseradish **(Stone et al., 2011).** The *MO* flowers can be eaten blanched or raw as an ingredient in a salad **(Foidl et al., 2001).** They can also be used to prepare a tea of very high nutritional value **(Price, 2007).** They are used in crushed form to make a paste which is then fried.

6.6. Application in water/wastewater treatment

Medicinal and nutritional applications are not the only ones to be developed for *MO*. The coagulant effect of *MO* seeds is one of the most important properties of the plant **(Brilhante et al., 2017)**, and the most frequently mentioned application of *MO* is the use of the seeds to clear

and purify water **(Ndabigengesere & Narasiah, 1998 a; Okuda et al., 2001),** but their use has been employed in different processes. The coagulation caused by the seeds may have been caused by adsorption or colloidal charge neutralisation **(Vieira et al., 2010; Vijayaraghavan et al., 2011).** The functional groups found in "side-chain amino acids of the proteins" from *MO* seeds are what cause water to become clearer **(Sotheeswaran et al., 2011).** As chemical coagulants used to purify water are dangerous to people and environment, frequently expensive and are linked to illnesses like cancer and Alzheimer's **(Mallevialle et al., 1984; Martyn et al., 1989).** Natural coagulants are used as a substitute for these synthetic coagulants. The *MO* seeds instead of chemical coagulants have been utilised to provide clean water **(Jahn et al., 1986).**

In the field of water treatment, *MO* seeds are used to reduce the concentrations of metals such as: copper, iron, zinc, aluminium, magnesium and lead. The advantage of using *MO* is that this treatment does not alter the pH, dissolved oxygen and hardness of the treated water; but it does slightly increase the total alkalimetric titre (TAC) and consequently the calcium ion content of the treated water **(Fatombi et al., 2007).** Additionally, *MO* seeds exhibit strong antibacterial properties, making them useful against a variety of bacterial and fungal organisms since they include active ingredients such polyelectrolytes and other proteins (**Ndabigengesere & Narasiah, 1998 b).** It also eliminates alkalinity, hardness and acidity **(Mangale et al., 2012).** For these purposes, *MO* seeds can act as a coagulant, flocculent or bio-adsorbent:

6.5.1. *Moringa oleifera* as a biocoagulant

The *MO* seeds act as a coagulant for organic matter suspended in water and are used in water treatment plants for natural cleaning before other cleaning processes. At this stage, the activity of *MO* seeds is more stable at different pH ranges compared to the activity of the conventional coagulant most commonly used in water treatment plants **(Okuda et al., 2001; Brilhante et al., 2017).**

As well, among the constituents of *MO* seeds, it can be mentioned that the basic polypeptide, which is more precisely a set of active cationic polyelectrolyte with a molecular weight of 12-14 kDa. Such a positively charged polyelectrolyte neutralises colloids in turbid waters since most of these colloidal materials are negatively charged. A single seed of *MO* may be sufficient to purify 1 L of slightly contaminated water, and two seeds for 1 L of heavily polluted water **(Foidl et al., 2001).**

Coagulation-flocculation is the most studied process involving the use of *MO* seeds, and results have shown that it is a natural coagulant with high efficiency, low cost and

environmentally friendly. However, studies have been increasingly intensified to understand how the coagulation mechanism occurs, identify the proteins that coagulate water pollutants, and isolation techniques **(Baptista et al., 2015; Boulaadjoul et al., 2018; Yamaguchi et al., 2021).**

6.5.2. *Moringa oleifera* as a bioflocculant

The *MO* seeds have been used as a potential bio-flocculent in several studies. The *MO* seeds were used as flocculent to remove heavy metals, algae, and volatile organic compounds from the liquid being treated. They are also used to clean vegetable oils, irrigation, tap water, and wastewater **(Kumari et al., 2006; Sengupta et al., 2012).**

The active component derived from the crushed and defatted seeds of *MO* seeds is a soluble protein that contains a natural cationic polyelectrolyte that causes flocculation. Conventional and developed methods have been used to obtain the *MO* seeds extract. The extraction have been carried out using solvents as Hexane, ethanol, etc. other advanced extraction techniques were used as supercritical liquid extraction (**Yusoff et al., 2019).**

6.5.3. *Moringa oleifera* as bioadsorbent

Due to the wide application of *MO* seeds for the above processes, the other parts of this plant can be considered as landfill waste. In this sense, some studies report the use of these materials for other types of water treatment, such as adsorption, which report their use as natural and chemically or thermally modified substances to remove various emerging pollutants, including heavy metals, dyes, pesticides, drugs. These studies have shown good removal of these pollutants, making *MO* an interesting precursor for the development of a promising technology **(Quesada et al., 2019; Cusioli et al., 2021).**

Chapter III

Coagulation-flocculation process

1. Introduction

Groundwater and surface water contain dissolved, suspended and colloidal particles. The part of the water containing suspended solids is separated using coagulation and flocculation. The coagulation-flocculation process is the most widely used process among the physicochemical treatments for water/wastewater. It involves the use of chemicals that can alter the physical state of colloidal particles (very fine particles < 10 µm in size), which helps to make them more stable and coagulable for further treatment or for membrane filtration. The suspended solids in water have a negative charge, and because they have the same surface charge, they repel one another when they are in close proximity. Because of this, suspended solids will remain in suspension and not clump together and settle out of the water, unless appropriate coagulation-flocculation is applied. This treatment method has been used for over a century in conjunction with biological treatment methods for water/wastewater treatment **(Zouboulis & Tzoupanos, 2010).** It has been successfully used for wastewater treatment, industrial water treatment, and wastewater sludge conditioning as part of pre-treatment while increasing efficiency at low costs. Physicochemical treatment can have a considerable influence on the biodegradation potential of organic matter in water/wastewater **(Teh et al., 2016).**

The effectiveness of the treatment depends on several aspects and on physicochemical properties of the water to be treated and the size of the suspended particles in that water. Very fine colloidal particles are highly stable and cannot be removed by physical or chemical techniques. The reason for this stability is that these materials have electrostatic surface charges of the same sign (usually negative). This indicates that repulsive forces are created between them, preventing their aggregation and sedimentation. It was therefore impossible to separate them by sedimentation or flotation (physical processes). However, separation by physicochemical treatments was possible. The coagulation-flocculation process was generally the most used in water/wastewater treatment to reduce or eliminate turbidity, colour, suspended solids and pathogens **(Barrera-Díaz et al., 2018).**

2. Physicochemical investigated parameters

2.1. Suspended solids (TSS) and colloidal particles

Solids are present in water in three main forms: suspended particles (or suspended solids), colloids and dissolved molecules. The suspended particles, such as sand, plant material and silts are classified by size from very large particles down to particles of a typical size of 10 µm. Colloidal particles are very fine particles, typically ranging from 10 nm to 10 µm **(Figure 3).** Dissolved molecules are present as individual molecules or ions **(Koohestanian et al., 2008).**

Suspended solids, abbreviated as TSS, are small solid particles that remain suspended in water as colloids or due to water movement. This parameter is used as an indicator of water quality. TSS is an important parameter, as various pollutants and pathogenic microorganisms are transported on the surface of particles. The smaller the particle size, the larger the total surface area per unit mass of particles, and the higher the pollutant load that is likely to be transported **(Turner & Millward, 2002).**

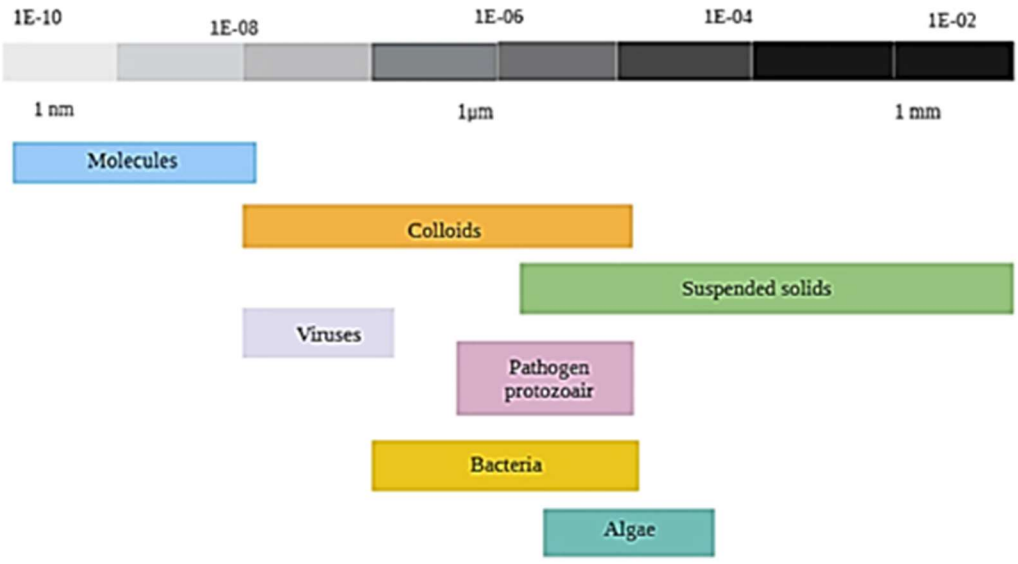

Figure 3. Size range of solids in water **(Koohestanian et al., 2008)**

Suspended solids are either of natural origin, linked to precipitation or of anthropogenic origin and then supported by atmospheric deposition and/or by municipal and industrial, urban, agricultural, or domestic effluents. TSS are linked to the soil use from which they originate and to the resulting phosphorus content, as well as to the mechanism of their transformation according to the season or the climatic and hydrological conditions. They include all undissolved matter in suspension in runoff water. In addition, TSS and solids transported in watercourses

derive from erosion of the outer surface of soils due to the movement of runoff water or rainwater **(Rosenwinkel et al., 2001).**

2.2. Affinity of colloidal particles for water

Colloidal particles in which the dispersed components have an affinity for the dispersing medium are called lyophilic, while those that repel the dispersant are called lyophobic. Lyophobic colloids are characterised by the absence of bonds between the dispersant and the dispersed phase. When the dispersant is water, these colloidal materials are called hydrophilic or hydrophobic, respectively. Hydrophilic colloids absorb water, swell and can give rise to a particular type of colloid known as a gel. Elsewhere, the liquid appears to be totally absorbed into the dispersed phase. A gel has the appearance of a solid. It is gelatinous and elastic, such as gelatine. These colloids are usually composed of macromolecules dispersed in water **(Eagland, 1973).**

2.3. Stability of colloids in water

The stability of colloidal materials is determined by the suspended particles remaining in water and depends on the interaction forces between the particles. These are particularly electrostatic interactions and Van der Waals forces, since they both contribute to the overall free energy of the system **(Bender, 1958; Eagland, 1973).**

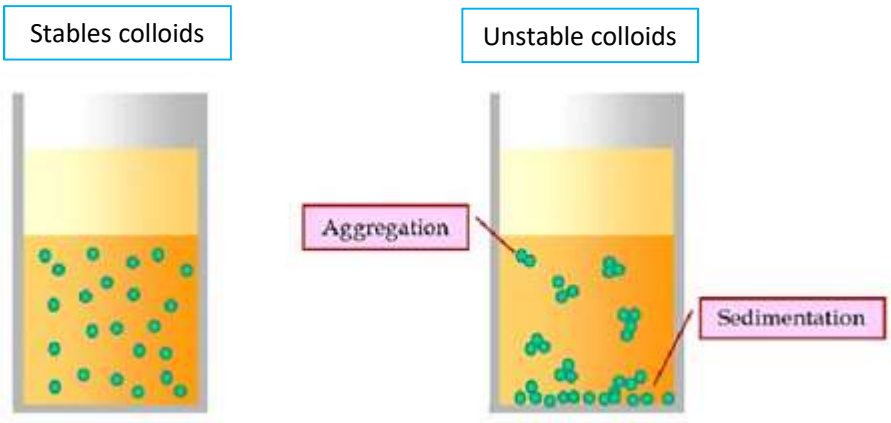

Figure 4. Examples of stable and unstable colloidal dispersion **(Rakshit et al., 2021).**

A colloid is stable if the interaction energy due to the attractive forces between the colloidal particles is less than kT, where k is the Boltzmann constant and T is the temperature. If this is the case, the colloidal particles will repel each other or have a weak attraction, and the particles will remain in suspension **(Figure 4).** If the interaction energy is greater than kT, the

attractive forces will prevail and the colloidal particles will start to agglomerate. This process is usually called aggregation, but also flocculation, and coagulation. Although these terms are often used interchangeably, they have different meanings in other definitions. In contrast, coagulation can be used to describe an irreversible and permanent aggregation where the forces holding the particles together are stronger than any external forces generated by agitation or mixing. Flocculation can be used to describe reversible aggregation involving weaker attractive forces, and the aggregate is usually called floc. However, the term precipitation is generally reserved to describe a phase change from a colloidal dispersion to a solid (precipitate) after a disturbance. Aggregation causes sedimentation or cremation, and the colloid become unstable. If one of these processes occurs, the colloid will no longer be a suspension **(Rakshit et al., 2021).**

3. Coagulation process

Coagulation represents the process of colloidal particles agglomeration; using chemicals such as aluminium sulphate, ferrous sulphate, ferric chloride, aluminium chloride, etc. It has been used in the past for the treatment of distillery wastewater. Chemical Coagulants with opposite charges to those of the suspended solids are added to the water to neutralize the negative charges on non-settlable solids (such as clay and color-producing organic substances). Coagulation is achieved by different mechanisms such as compression of the ionic layer, adsorption and neutralisation of the charge, particle entrapment-precipitation and inter-particle bridging, which reduces Zeta potential and consequently decreases the repulsive forces between the negatively charged colloidal particles **(Jiang, 2015).** In the last years, even natural coagulants called bio-coagulants like *MO*, *Cactus* and *Tanfloc* are used in coagulation process **(Amran et al., 2018).**

3.1. Compression of the double layer

In this mechanism, coagulants (ions) normally in high concentration are added to the system when similarly charged ions (negative charge) of the coagulants are repelled, but the positively charged ions are attracted by the initial charge of the colloidal materials, causing the compression of the diffuse double layer. As a result, the reduction of the diffuse double layer with a high concentration of counter ions of the coagulants causes the energy barrier of a colloidal system to be overcome, and eventually destabilised **(Rakshit et al., 2021).** The double electronic layer is illustrated in **Figure 5.**

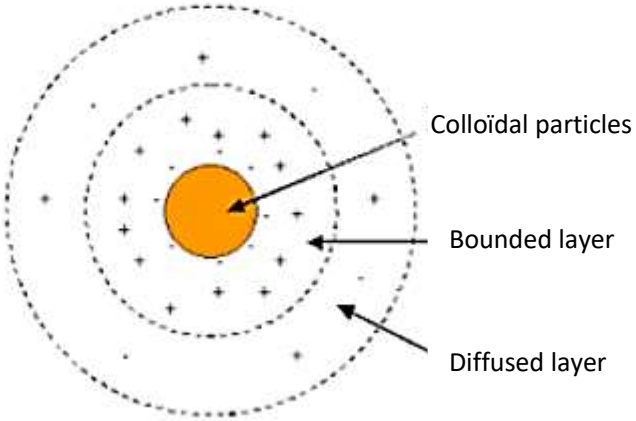

Figure 5. Double electronic layer **(Rakshit et al., 2021).**

a. Adsorption and neutralisation of charges

In this case, neutralisation of the colloidal particles charge is achieved by the addition of oppositely charged molecules that adsorb onto the outer surface of the colloidal particles. Once the charge is neutralized, the small suspended particles are capable of sticking together. These slightly larger particles are called micro-flocs, and are not visible to the naked eye. Water surrounding the newly formed micro-flocs should be clear. If not, coagulation and some of the particles charge have not been neutralized, and more chemical coagulants may need to be added. However, excessive addition of such molecules (coagulant) can lead to the restabilization of the system by the residual charges of the added molecules after having neutralized the initial charges of the colloidal particles **(Zheng et al., 2017; Rakshit et al., 2021).** The neutralisation charge, the particle flocculation, the bridging and adsorption are illustrated in **Figure 6.**

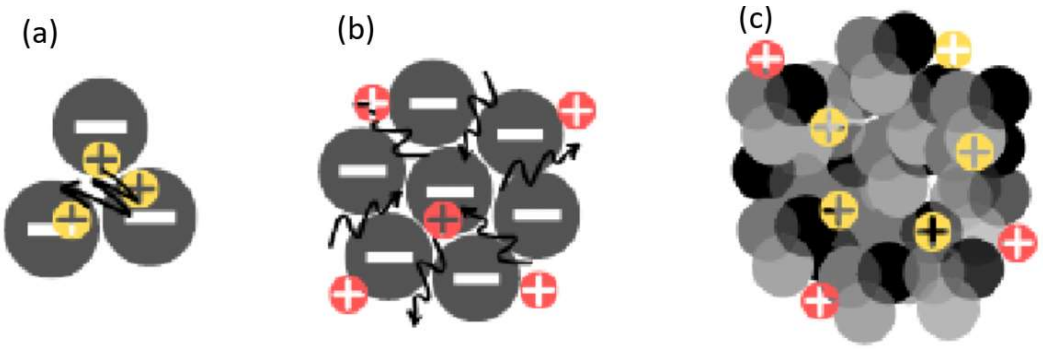

Figure 6. Illustration of (a) neutralisation charge, (b) bridging and adsorption, and (c) particle flocculation **(Zheng et al., 2017).**

b. Particle trapping and precipitation

In this mechanism, the added metal salts such as aluminium sulphate, ferric chlorides, and calcium oxides, precipitate as hydroxides, in which the colloidal particles become trapped and precipitate **(Dongyu et al., 2018) (Figure 7).**

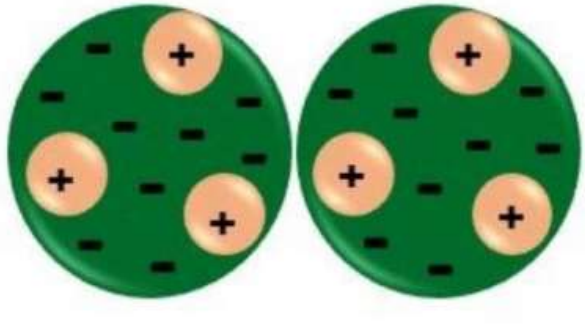

Figure 7. Colloidal particle trapping **(Koshani et al., 2020)**

c. Inter-particle bridging

This mechanism was proposed by Lamer in 1963, where long-chain charged polymer molecules are added to a colloidal system (water to be treated). This mechanism is based on the theory that one charged end of the polymer molecule attaches to a site on a colloidal particle and the other end extends to the bulk solution. If the other end attaches to another colloid, then an effective bridge between two colloidal particles has occurred **(Figure 8),** resulting in their precipitation together **(Koshani et al., 2020).**

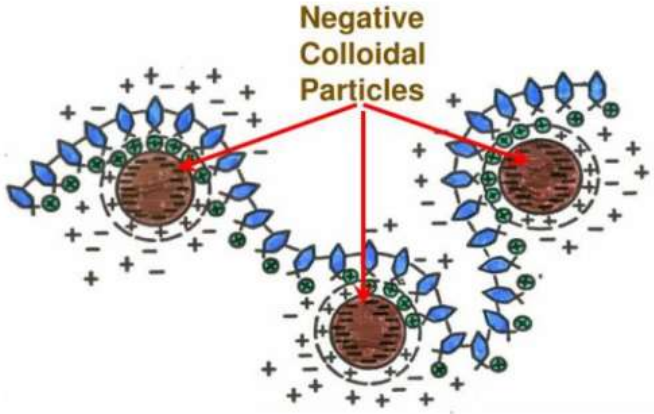

Figure 8. Bridging between colloidal particles **(Koshani et al., 2020).**

4. Flocculation process

Flocculation is a water treatment process in which suspended solids and colloidal particles form larger particles, called macro-flocs to be removed from water. This process can occur simultaneously, or by adding chemicals. These chemical compounds are characterised by a high molecular weight such as polymers (polyelectrolyte, polyglutamic acid, polyaluminium chloride, chitosan etc.) that allow the agglomeration of colloidal particles **(Chong, 2012).**

5. Parameters influencing coagulation-flocculation

Factors influencing coagulation-flocculation include the source, composition load, size, shape and density of suspended particles, which vary considerably. The correct application of coagulation-flocculation processes and the selection of coagulants depend on understanding the interactions between these parameters **(Bratby, 2016; Saritha et al., 2017).** The main parameters influencing the coagulation-flocculation process are:

5.1. Water pH

The pH measurement of water samples is a very vital. Chemical parameter that defines the acid or alkaline properties influences similarly the turbidity level of water samples **(Gautam et al., 2021).** The pH of water plays a fundamental role in the kinetics of the coagulation reaction. Most water treatment plants using chemical coagulants adjust the pH of raw water by adding acid solutions or CO_2. The predominance of a particular hydrolysis species during destabilization is very largely dependent on the pH value. For a given colloidal suspension, it is logical to consider that there is a particular hydrolysis species that are most effective for destabilization, either by virtue of the charge carried or the absorptivity of the species. Adjusting the pH to a range where the most efficient coagulant hydrolysis species are formed is essential to produce optimal coagulation. Lower pH values, between 5.5 to 7.5, can be used to retain the positive hydroxyl of hydrolysed species of the chemical coagulant. Higher pH values would give hydroxide salts a chance to be generated and precipitate afterwards. Hence, the pH values may dictate the coagulation mechanism in question. Generally, it is not allowed to have a final pH of the treated water much below 6.5 to avoid problems caused by the acidity of the water. On the other hand, the pH of the raw water can be adjusted before treatment by the coagulation-flocculation process, but it cannot be controlled during the reaction **(Bratby, 2016).**

5.2. Turbidity

Turbidity is generally caused by suspended matter, such as clay, silt and finely divided organic and inorganic matter. In addition, it can include biological organisms such as algae, zooplankton, cyanobacteria, and filaments. It is considered as the measurement of the relative clarity of water **(Davies-Colley & Smith, 2001)**. It is recommended that turbidity must be reduced as low as possible, depending on the type of water. Turbidity is not a direct measure of the concentration of suspended solids in water, but rather it is a measure of the light scattering impact caused by these particles. Since several parameters affect the intensity of light scattering intensity, such as particle size, distribution, shape, refractive index and adsorption capacity, of the particles, they could change its measurement value **(Kitchener et al., 2017).** Turbidity is a good indicator of water quality. The species causing turbidity could have different consequences on raw water quality; inorganic particles such as silt, clay and natural precipitants. All these particles can increase or decrease the pH and the alkalinity of water/wastewater, and can be sources of micronutrients and influence the Zeta potential. Although organic species as well as animal debris and humic substances, could be sources and of micro-organisms. They give taste and odour, serve as precursors for the formation of chlorine or ozonated compounds, can form complexes with toxic elements, affect pH and finally could protect colloidal materials. The presence of organic matter in water can lead to a high demand for disinfectant, an increase in several water characteristics such as chemical oxygen demand (COD) and biochemical oxygen demand (BOD), and as results, a decrease in water quality, and a high dose of coagulant will be required **(Davies-Colley & Smith, 2001)**.

5.3. Temperature

Industrial discharges have different temperatures depending on the nature of the process and the reason for using the water. Similarly, raw water from rivers and lakes undergoes seasonal variations in temperature throughout the year. This can have a direct impact on the various characteristics of water, in particular density, viscosity and Zeta potential **(Bratby, 2016).**

5.4. Coagulant concentration

Regardless of the type or the nature of the used coagulant, the concentration can be increased or decreased depending on the type and the value of turbidity and other effluent parameters **(Bratby, 2016).** The dosage of the coagulant, particularly metal coagulants, has a significant impact on the mechanisms responsible for particle destabilisation later **(Teh et al., 2016).** The common trend is that the dose increases with increasing turbidity and decreasing temperature. However, an excessive dosage of coagulant will lead to a decrease in turbidity

removal **(Dotto et al., 2018).** In general, inadequate or excess dosages of coagulants or flocculants can lead to poor performance of coagulation-flocculation process. In addition, a higher amount of coagulant has a negative effect by producing additional sludge that needs to be treated later **(Teh et al., 2016).**

5.5. Coagulation stirring speed

The importance of agitation speed and its effect on the coagulation-flocculation process is often hidden by chemical overdosing in water treatment plants. This parameter can play an important role in the coagulation-flocculation process because operators can manipulate or change the speed and the time of mixing. The fast stirring provides the necessary kinetic energy for the particles to overcome the energy barrier and allow collision between colloidal particles **(Bratby, 2016).** Several stirring times can be set. During the rapid mixing (coagulation) ranging from 0.5 to 5.0 minutes, the dispersion of the coagulant in wastewater is carried out, but also the initial stage of coagulation in the water/wastewater is carried out too. In this initial stage of coagulation, the particles collision will take place and consequently the formation of aggregates will take place too **(Bratby, 2016).**

5.6. Flocculation Stirring speed

Stirring, commonly referred to mixing, is an important stage in the coagulation-flocculation process used to treat water and wastewater. Both quick and slow mixing are possible. To guarantee homogeneous coagulant dispersion into effluent for effective treatment, rapid mixing is primarily used **(Teh et al., 2016).** Mixing is essential, especially when treating wastewater with high turbidity level, as it speeds up the adsorption and floc formation by increasing the likelihood of particle collisions. In the flocculation step, the floc sweeping and bridging mechanisms will take place **(Bratby, 2016).** For this, the stirring speed of flocculation is different and lower than that of coagulation. The Fast and slow mixing time has an effect on the size and strength of formed flocs. Greater floc growth was possible with relatively shorter quick mixing times, but the flocs were less shear resistant (less compact), whereas treatments with longer fast mixing times produced stronger but smaller flocs. For this, the choice of the appropriate mixing regime by treatment plants can improve the coagulation-flocculation process.

5.7. Agitation type

Agitation in the coagulation-flocculation process can be modified either by changing the type of mixer or by changing the agitation mode in terms of time and intensity. Researchers have found that the geometrical shape of the agitators' propellers plays an important role in the

flocculation process, while others have shown that the flocculation kinetics depends on the type of mixers **(Teh et al., 2016).**

5.8. Settling time

The overall efficiency of the process is influenced by the strength and settling speed of the flocs created during the coagulation-flocculation treatment **(Teh et al., 2016).** The flocs serve as a medium for settling and separating treated effluent from suspended particles in wastewater, which transports them to the wastewater's bottom. It is not ideal to produce little flocs during the coagulation-flocculation process because of their fragility, slower settling velocity, and difficulties in separating them from the effluent **(Bhatia et al., 2006; Renault et al., 2009).** The type of coagulant or/and flocculent used in the treatment as well as the type of water/ wastewater have a significant impact on the settling capacity of flocs formed following the coagulation-flocculation process. Flocs settling is highly dependent on the floc size generated during the treatment. Larger floc sizes can be produced using flocculants, which leads to quick settling. The main mechanisms for forming macroflocs from mechanically bridged microflocs during rapid settling remain polymer adsorption and bridging involving long-chain polymers during flocculation **(Teh et al., 2016).**

6. Coagulants and flocculants

The success of coagulation-flocculation process does not only depend on these parameters but also on the right choice of the utilized coagulants and flocculants. Chemicals, specifically coagulants or flocculants are introduced to water to play a significant part in the coagulation-flocculation process **(Pang et al., 2011).** For this, understanding the aqueous chemistry after the addition of coagulants and flocculants to the raw water is considered a key parameter for evaluating the performance of the utilized products **(Yin, 2010).**

6.1. Coagulants

The coagulation and flocculation entail the addition of chemicals to change the physical state of dissolved and suspended materials and make it easier for sedimentation to ensure their removal **(Verma et al., 2012)**. The different coagulants used for the treatment of dam water, industrial or municipal wastewater are classified in two categories according to their nature:

- Chemical coagulants
- Natural coagulants (bio-coagulants)

6.1.1. Chemical coagulants

Aluminium sulphate, ferric sulphate, and cationic polyelectrolytes are examples of coagulants that work by bringing the colloidal system's Zeta potential down to a level where the colloidal particles can collide and eventually coalesce as a result of gradual agitation. Anionic and non-ionic polyelectrolytes can greatly facilitate the construction of much larger flocculated particles that will settle more rapidly and produce less turbid effluent. In this way, anionic and non-ionic polyelectrolytes are called "coagulant aids" or "auxiliary coagulants" **(Ranade & Bhandari, 2014).** When aluminium sulphate ($Al_2(SO_4)_3 18H_2O$) dissolves in water, some of the aluminium goes into true solution as the trivalent aluminium ion (Al^{3+}). If there are colloidal particles with a negative surface charge, the trivalent aluminium ions, as well as other aluminium species such as $Al(OH)_2^+$ and $Al(OH)^{2+}$, will be attracted to these negatively attracted charged surfaces and remove the negative surface charge, which means that they will remove the Zeta potential **(Harif et al., 2012).**

In one hand, there are other metal salts that dissolve to produce trivalent ions, such as aluminium chloride, ferric sulphate, and ferric chloride. These metals are able to coagulate colloidal suspensions with similar efficiency to that of aluminium sulphate. In the other hand, salts that produce divalent ions after dissolution, such as manganese sulphate or calcium chloride, have also an effect on reducing the Zeta potential and possible coagulation, but with much lower efficiency than the difference in ionic charge **(Tang et al., 2016).**

6.1.2. Natural coagulants

Natural coagulants, or so-called bio-coagulants, have gained popularity in the field of water and industrial wastewater treatment due to their advantage over chemical coagulants. Natural coagulants are derived from plants (whether plant or not), animals or microorganisms. Now, several effective coagulants that are of plant origin are identified. The most common coagulants include *MO* seeds*, Hibiscus sabdariffa* (Roselle seeds), *Dolichos lablab* (Hyacinth bean), Nirmali seeds, watermelon seeds and cactus species. The disadvantages of chemical coagulants have led to the search for alternative coagulants from a natural source that are environmentally friendly and sustainable in their use and production. The main advantages of natural coagulants are that they are renewable, biodegradable, non-toxic and cost-effective. Although many studies have proven the effectiveness of bio-coagulants in wastewater treatment applications. However, their use on an industrial scale is still tentative **(Gautam & Saini, 2020).** Bio-coagulants contain functional groups that contribute to the surface charge. The molecular weight of the natural coagulant is very important for the bridging of particles. If the molecular

weight of the bio-coagulant is higher, it can form solid bridges with colloidal particles and leads to the formation of strong flocs and possibly improving sedimentation **(Ang et al., 2020).**

Natural coagulants are composed of carbohydrates, proteins and lipids. The main building blocks are polymeric polysaccharides and amino acids. According to previous research, the main mechanisms governing coagulation activity are charge neutralisation and polymer bridging **(Wibowo & Nurcahyo, 2021).** Natural coagulants have different mechanisms of action, like adsorption and charge neutralisation, inter-particles bridging, adsorption and bridging, and charge neutralisation and bridging (**Yin, 2010**, **Vijayaraghavan et al., 2011; Saranya et al., 2014; Kumar et al., 2017).**

6.2. Flocculants

The main function of a flocculent is to make suspended particles stick together very strongly after coming into contact (after the coagulation stage). This effect is achieved by the use of very high mass polymers, capable of forming molecular bridges between adjacent surfaces. Chemical flocculants are very effective and widely used in industry. For large-scale use, a flocculent must meet certain key requirements: it must be effective, relatively low cost environmentally safe and readily available. According to this, flocculants are divided into too main groups; inorganic flocculants and the organic polymeric flocculants. Only certain inorganic flocculants such aluminium sulphate and ferric salts can be used on a large scale as coagulants and flocculants. Many other effective organic flocculants have been developed, but none are as cheap as the commonly used inorganic salts **(Chatsungnoen & Chisti, 2019).**

6.2.1. Organic flocculants

Organic flocculants are mainly polymers. Polymers with an anionic or cationic charge can behave as polyelectrolytes. The non-ionic polymers are uncharged. They can be synthetic or natural. The natural polyelectrolytes include cationic polysaccharide starch, chitosan (cationic polymer) and poly-γ-glutamic acid polypeptide (cationic polymer). Among the synthetic polyelectrolytes, polyacrylamides (cationic or anionic) are widely used. Polyelectrolytes work by combining neutralisation of the cell surface charge and surface of particles to form flocs **(Ajao et al., 2018)**.

The effectiveness of polyelectrolyte flocculants is influenced by the following factors: the molecular weight or chain length of the polymer; the density of the molecule; the dose used; the concentration of biomass; the ionic strength, solution pH; and stirring speed in the fluid. Higher molecular weight polyelectrolytes (longer chain polymers) are better bridging agents. A high

charge density tends to unfold the polymer molecule, which improves its ability to surface charge on suspended particles and its bridging performance (**Niaounakis & Halvadakis, 2006; Ajao et al., 2018).**

Cationic polyelectrolytes such as chitosan can induce effective flocculation of colloidal particles in fresh wastewater at low doses. A dose of chitosan in the range of 1-10 mg/L can be very effective. The flocculation efficiency decreases in more saline environments, as in these environments the polymer molecule tends to fold back on itself, requiring a higher dosage. The pH of 7 is optimal for flocculation, in low salinity media (**Yang & Wang, 2018).**

6.2.2. Inorganic flocculants

Inorganic salts of multivalent metals are effective flocculants as they are efficient coagulants. Aluminium-based flocculants include aluminium sulphate, aluminium chloride, sodium aluminate, aluminium chlorohydrate and polyaluminium chloride. Iron flocculants include ferric chloride, ferric sulphate, ferrous sulphate and ferric chloride sulphate. A high dose of the inorganic flocculent is generally required for flocculation of suspended particles in a medium with a high ionic concentration compared with the concentration required for flocculation in a freshwater medium. Aluminium salts are generally more effective than ferric and zinc salts due to the fact that the low ionic radius of aluminium results in a higher surface charge density **(Chatsungnoen & Chisti, 2019).**

Chapter IV

Adsorption process

1. Introduction

Adsorption is one of many techniques that are successfully used for the removal of different pollutants **(Carmen & Daniela, 2012).** This unit operation is important in many natural and industrial systems, such as fundamental biological studies, separation and purification processes, upgrading of chemical compounds, catalysis and waste treatment processes. It can replace other separation processes and contribute effectively to eliminate pollutants from aqueous solutions **(Jena et al., 2004).** Several parameters can intervene in the adsorption phenomenon, which can act separately or simultaneously. The complexity and diversity of adsorption mechanisms make the study of this process more difficult **(Hu & Xu, 2020).**

2. General information on adsorption

Adsorption is a mass transfer process which is a phenomenon of sorption of gases or solutes onto solid surfaces. The adsorption on solid surfaces is explained by the fact that molecules or atoms have residual surface energy due to unbalanced forces. When some substances interact with the solid surface and make collision between each other, they are attracted by some unbalanced forces and remain on the solid surface **(Wang & Guo, 2020).** The term "adsorption" comes from Latin. It means that material's molecules can lead, at the end of the phenomenon, to the accumulation or elimination of the molecules of phase "A", in the vicinity of the zone of contact with phase "B". In other words, adsorption is a separation method in which natural or synthetic adsorbents are used, such as precipitates of iron or aluminium hydroxides, ion exchangers, metal oxides such as iron, manganese and titanium, zeolites, activated carbon and natural red clay **(Ćurko et al., 2016).** Due to its low cost and great effectiveness, adsorption is commonly used as separation method, particularly in environmental remediation **(Wang & Guo, 2020).** Adsorbent materials are characterized by maximum surface area covered by a minimum volume of adsorbent. The efficiency of the adsorption process is determined by the physical and chemical properties of the soluble substances and the solid surface **(Figure 9).** The adsorbent materials commonly used include activated carbon, zeolites, aluminium, scavengers, lignite coke and; bentonite **(Kosmulski, 2001; Ćurko et al., 2016).**

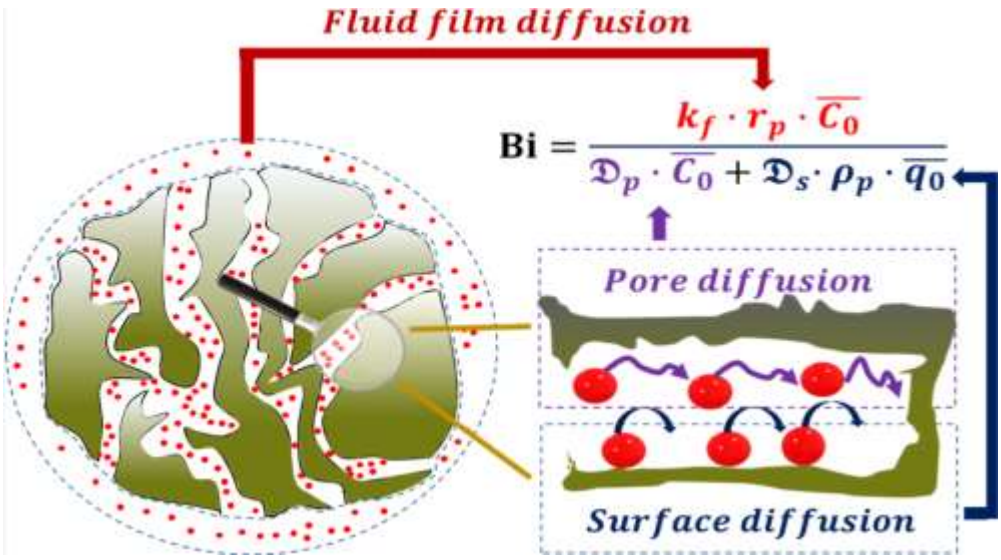

Figure 9. Illustration of the adsorbent, the adsorbate and the active sites (pores) **(Inglezakis et al., 2020).**

3. Types of adsorption

According to the different adsorption forces, the adsorption process can be divided into two categories: physical adsorption and chemical adsorption **(Hu and Xu, 2020; Wang & Guo, 2020).**

3.1.Physical adsorption

Physisorption involves physical attraction resulting from electrostatic interactions and relatively weak non-specific Van der Waals forces having low adsorption energy of no more than 40 kJ/mol. Physically adsorbed molecules can diffuse along the surface of the adsorbent and are generally not bound to a specific location on the surface. While these molecules are weakly linked, physisorption is easily reversible and exothermic **(Webb, 2003; Kecili & Hussain, 2018; Wang & Guo, 2020).**

In contrast to chemical adsorption, physical adsorption, under favourable temperature and pressure conditions, will take place on all surfaces. It can even end up with the formation of several layers of adsorbed molecules **(Wang & Guo, 2020).**

3.2.Chemical adsorption

Chemical adsorption, also known as chemisorption on solid materials is achieved by high electron sharing between the adsorbent surface and the adsorbate to create a covalent or ionic bond. As such, chemical adsorption is not fully reversible and requires high energy to be regenerated **(Webb, 2003; Bell et al., 2010).** Chemical adsorption, however, is highly selective

and only occurs between certain adsorbent and adsorbed species and only if the surface of the adsorbent is chemically active and cleaned of previously adsorbed molecules **(Webb, 2003).**

Indeed, in the typical case, this mechanism only takes place if the adsorbent can come into direct contact with the surface. It is therefore a single layer process**.** Exceptions may exist if the adsorbent is highly polar such as ammonia (NH_3) **(Webb, 2003).**

Physical and chemical adsorption can occur on the same surface simultaneously; a layer of molecules can be physically adsorbed on a lower chemically adsorbed layer, and sometimes the same surface can exhibit physisorption at a given temperature and chemisorption at a higher temperature **(Webb, 2003).** Physical adsorption and chemical adsorption are not isolated and often occur together. In wastewater treatment technology, most of adsorption process is the result of several types of adsorption processes. Due to the influence of the adsorbents, adsorbates and other factors, a certain form of adsorption may dominate over the other **(Hu and Xu, 2020). Table 5** shows a comparison between both adsorption categories.

Table 5. Comparison between physical and chemical adsorption **(Kecili & Hussain, 2018; Hu and Xu, 2020).**

	Adsorption categories	
	Physical adsorption	**Chemical adsorption**
Adsorption force	Van der Waals force	Chemical bonding strength
Selectivity	Non-selective adsorption	Selective adsorption
Adsorption layer	Single or multilayer	Monolayer
Adsorption temperature	Low temperature	High temperature
Adsorption speed	Rapid	Slow
Stability	Unstable	Stable

4. Description of the adsorption mechanism

Adsorption defines the property of certain materials to fix molecules or ions to their surface in a more or less reversible way. The utilized compounds have a porous structure giving them a large specific surface. The pollutants are therefore physically and/or chemically bounded to the active sites found on the pores of the adsorbent. Once the adsorbent is saturated, it will need to be regenerated. This implies physical and/or chemical and sometimes even thermal treatments to break the bonds formed between the adsorbed elements and the adsorbent. In addition, the adsorbent regeneration is done in order to restore all or part of the adsorbent and its adsorption capacity. The adsorbent regeneration allows its reuse and thus reduces operating costs **(Webb, 2003; Kecili & Hussain, 2018).**

5. Adsorption kinetics

Generally, adsorption represents a dynamic phenomenon. It is considered to be the partition of a solute containing a liquid phase into a solid phase made up of all the solid constituents in the form of an adsorbent. Desorption is simply the reverse phenomenon **(Wang and Guo, 2020).**

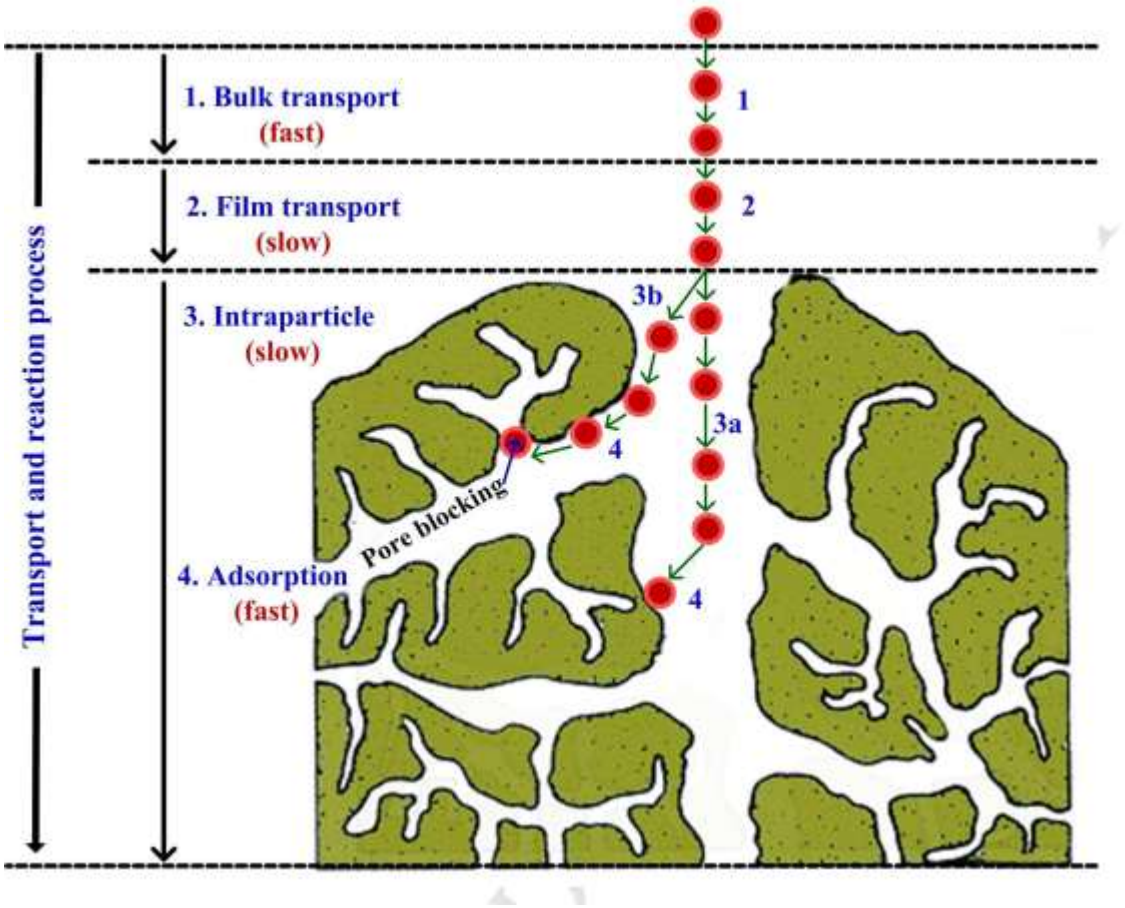

Figure 10. Transport processes during adsorption by a porous adsorbent **(Tran et al., 2017).**

The transfer from a liquid phase (containing pollutants or contaminants to be eliminated) to a solid phase is necessary for the adsorption process. This transfer requires retention of suspended and soluble molecules in the aqueous solution. The mentioned retention is observed through contact at the adsorbent surface. Adsorption consists in four main phases **(Qiu et al., 2009).**

- Transfer of molecules (very fast);
- Displacement of the pollutant molecules in the aqueous phase contact with the adsorbent (fast);

- Diffusion of water into the adsorbent under the influence of the concentration gradient (slow);
- Adsorption of pollutants or particles into the microporous of the adsorbent (very slow).

The transport processes during adsorption by a porous adsorbent is illustrated in **Figure 10.** The study of the kinetics and thermodynamics of the adsorption process is crucial in order to estimate the adsorption mechanism. For these reasons, adsorption kinetic models such as pseudo-first order, pseudo-second order are widely applied to adsorption systems **(Kecili & Hussain, 2018).**

6. Adsorption isotherms

The adsorption isotherm is represented by a curve of the quantity of the adsorbed pollutants on the surface of the adsorbent. This curve is function of the adsorbate concentration or the partial pressure at a constant temperature. These isotherms are used to obtain precise information on the interactions between the molecules to be adsorbed and the surface of the adsorbents **(Kecili & Hussain, 2018).** According to the classification of IUPAC (International Union of Pure and Applied Chemistry), adsorption isotherms can be categorized into six types based on the isotherm shape of adsorbate-adsorbent pairs **(Al-Ghouti & Da'ana, 2020).** The most used isotherms are:

6.1.Langmuir Isotherm

In 1932, Irving Langmuir presented the adsorption model that bears his name "Langmuir Isotherm" **(Kecili & Hussain, 2018).** It is the most widely used isotherm. This adsorption isotherm model was originally developed for the description of gas adsorption on solid phase adsorbate. According to Langmuir theory, adsorption process onto a solid surface is based on a kinetic principle in which a continuous bombardment process of molecules onto the surface with corresponding molecules' desorption or evaporation from the surface with zero accumulation rate at the surface **(Al-Ghouti & Da'ana, 2020).** This isotherm simulates the monolayer adsorption of the adsorbate onto a homogenous adsorbent surface. The constants of the Langmuir isotherm have specific physical meanings that can successfully describe the maximum capacities and the surface properties of the adsorbent **(Guo & Wang, 2019).** This isotherm is based on the following main approaches **(Kecili & Hussain, 2018):**

- Adsorption occurs at specific binding sites which are located on the surface of the adsorbent.

- All adsorption sites on the adsorbent surface are identical.
- Adsorption will take place on a single layer or so-called monolayer of the adsorbed molecules.
- There is no interaction between the adsorbed pollutants on the surface of the adsorbent.

6.2. Freundlich Isotherm

The Freundlich isotherm model, however, is used to describe another hypothesis of multi-layer adsorption of heterogeneous molecules on the adsorbent surface **(Kecili & Hussain, 2018).** It is used to represent nonlinear adsorption phenomenon. It is one of the most widely used isotherms in adsorption **(Wang & Guo, 2020).** Freundlich isotherm model expression defines the heterogeneity of the surface as well as the exponential distribution of the active sites and the active sites energies. The Freundlich model describes the adsorption condition at which the equilibrium coverage fraction is about 50%. This model was originally developed for animal charcoal adsorption. It demonstrated that at different concentrations of the solution, the ratio of the adsorbate onto certain adsorbent mass was not constant **(Al-Ghouti & Da'ana, 2020).** Both chemical and physical adsorption can be represented by the Freundlich isotherm **(Wang & Guo, 2020).**

7. Parameters influencing adsorption

The adsorption process depends on various factors that can influence the retention kinetic and the capacity of the adsorbate on the adsorbent. For a better adsorption, the following parameters should be optimised:

7.1.Effect of pH

The pH of a solution is one of the key parameters influencing the adsorption capacity of different pollutants **(Pokhrel & Viraraghavan, 2008).** Pollutants have different behaviours in aqueous solutions and, consequently, their efficiency in removing different contaminants. Variations of solution pH can impact not only the degree of protonation but also the properties of the surface (charge and functional groups) of the adsorbent **(Olatunji et al., 2015).**

7.2.Temperature effect

Temperature is also considered as an important parameter for the study of adsorption process. This factor is directly involved on the mechanism of adsorption. Basically, there are two major effects of temperature on the adsorption process **(Olatunji et al., 2015).** The increase of temperature involves the increase of adsorbate molecules diffusion through the outer boundary

layer into the inner pores of the adsorbent particles **(El-Rahman et al., 2006).** For the same reason, the change in the temperature of the adsorption system results in a change in the equilibrium capacity of the adsorbent for a particular pollutant **(Wang et al., 2005).** Therefore, if the adsorption rate increases with increasing temperature, the mechanism controlling the process is considered endothermic. Otherwise, the adsorption process is exothermic **(Olatunji et al., 2015).**

7.3.Effect of contact time

The contact time affects the adsorption process considerably. The study of the pollutant adsorption on a solid support in aqueous solution involves the determination of contact time which corresponds to the adsorption/desorption equilibrium or to a state of equilibrium or of saturation of the support by the substrate. In addition, the contact time can influence the economic efficiency of the process as well as the adsorption kinetics. Therefore, contact time is another performance factor governing the adsorption process **(Iftekhar et al., 2018).** Variations in contact time lead to changes in the optimal adsorption efficiency of pollutants **(Olatunji et al., 2015).**

7.4.Effect of the initial concentration of the adsorbate

This is another important parameter that determines the amount of adsorbate to be linked to a particular adsorbent. The removal efficiency of a pollutant and the adsorption capacity of each adsorbent depend strongly on the relationship between the pollutant and the adsorbent. This last one, in turn, is a function of the initial adsorbate concentration in the solution and the pores or adsorption sites existing on the adsorbent surface **(Yagub et al., 2014).**

7.5.Effect of ionic strength

Ionic strength is the difference between the effective concentration (activity) and the analytical concentration of a solution. This difference is due to Coulombic interactions between the different ions of the solution under study. The greater the number of ions in solution and the greater their charge, the greater the difference is.

Industrial and natural water contains a lot of salts. These can have a considerable effect on the adsorption and therefore the elimination of certain organic and inorganic pollutants. The effect of ionic strength on adsorption depends on the type of the adsorbent and the adsorbate. For example, in the adsorption of phosphate, increasing the ionic strength of the solution increases the adsorption of phosphate to magnetite particles. It was also observed that the polyelectrolyte

dissolved in the presence of phosphate at high ionic strength presents a globular structure which is preserved after adsorption with substantial effects on the buildup of the multilayer system **(Zappi et al., 2019).**

Material and methods

Material and methods

Experimental work schedule

This chapter outlines the different materials and methods used to carry out this work. Specific experimental designs and procedures are presented in the relevant chapter. All laboratory work was performed at the University of Bejaia with the majority undertaken in Laboratory of ecology and hydraulics laboratory.

In order to encourage energy efficiency and renewable energy sources, the Algerian government created a national program for integration of beneficial vegetation, for the years 2011–2030. The *MO* tree was one of the trees introduced and planted in the Algerian Sahara. The *MO* implantation was very successful due to its rapid growth, climatic adaptation to the Sahara, fertilizing impact on the nutrient-poor soil, and fruit production after one year of establishment **(Boulal et al., 2019).** Based on the presented background, it is obvious that the growing of *MO* trees in Algeria could lead to new research in fields like environmental protection through the use of the *MO* seeds in water and wastewater treatment. Its usage as a flocculent and or coagulant is both cost-effective and advantageous because, unlike other materials, it helps to preserve the environment. This work has been divided into three main parts. The work schedule for this thesis is illustrated in **Figure 11.**

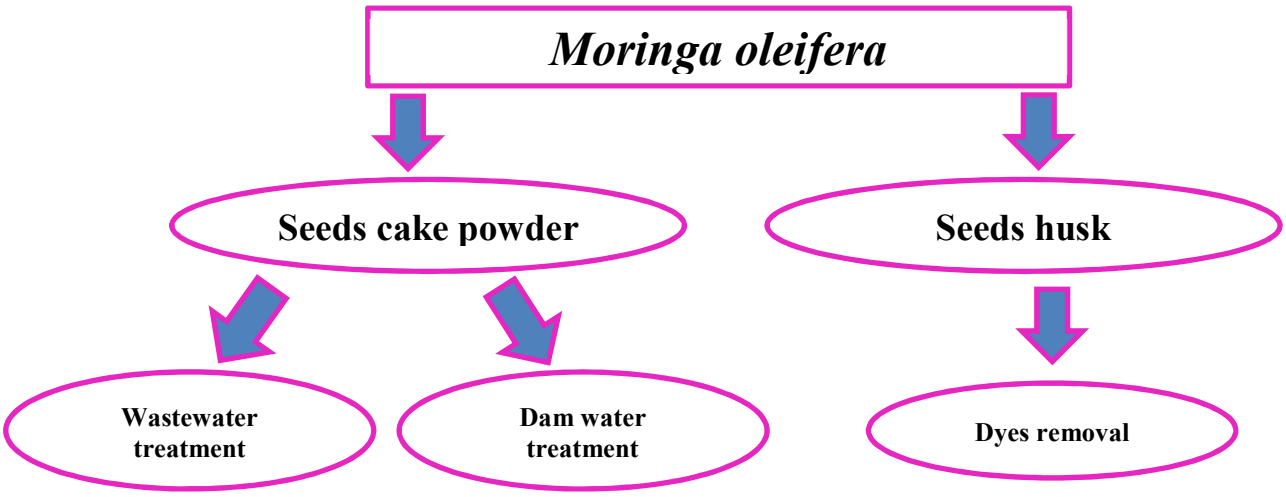

Figure 11. Experimental work schedule

Section I

Seeds cake powder exploitation

1. Introduction

In this section the seeds of *MO* have been used after oil extraction in the coagulation-flocculation process. The obtained *MO* seeds coagulant was used in dam water purification and urban wastewater treatment. The principal idea in this section is to operate the hulled and unhulled seeds in water clarification because of long time required for husking the seeds as well as the amount of labour required. In order to achieve these objects, the experimental work was structured as:

- Obtaining the *MO* seeds powder;
- Characterization of the *MO* seeds powders;
- Application in dam water and wastewater treatment.

2. Coagulant powder preparation

Two coagulants have been prepared. For this purpose, good quality and dry *MO* seeds were harvested in Jun 2018 from Tamanrasset region in southern Algeria. The *MO* seeds have been sorted to get rid of impurities and parasitized seeds. The seeds were then dried at 25°C for 4 hours to decrease the humidity and facilitate oil extraction. The utilized seeds were divided into two groups: shelled and unshelled seeds.

In order to get the defatted *MO* seeds cake powder the method of cold pressing has been selected. Cold pressing was performed with a cold press machine. Given that the solvent extraction method has drawbacks such as being hazardous, expensive, and causing a lot of environmental damage, cold pressing method was applied to extract the abundant vegetable oil from the *MO* seeds. The usage of mechanical systems is justified by their ecological benefits and their capacity to adapt to ongoing operations **(Richter et al., 1996).** This method has the advantage that it is easy to use, has quick process realisation, which results in a short process time, use of small amounts of raw materials, application of various oilseeds, and low cost. Rich press cake providing protein is also produced as a by-product **(Singh & Bragale, 2000).** For all these reasons, cold expression method was chosen for the *MO* seeds defatting **(Figure 12).**

Figure 12. Cold extraction of the *MO* seeds oil.

The defatted cake (the solid phase) was collected, milled and sifted through 0.5mm sifter. Two types of coagulant powder were obtained and named *MO-DS* and *MO-NDS* for the *MO* hulled and unhulled *MO* seeds, respectively **(Figure 13).** The soft obtained powder has been stored in hermetically sealed glass jars and stored at +4°C until use.

Figure 13. The *MO* seeds cake powder preparation.

3. Coagulant *powder* characterization

The characterization and the evaluation of seeds and plant tissue is turning into increasingly more essential method to achieve fundamental understanding of plant physiology as well as the determination of its structural framework **(Budevska et al., 2003).** The physicochemical richness of the *MO* seeds cake powder can widely affect its structural framework, as well as the understanding of its mechanism of action. The aim of the characterization work is to elucidate the disposition of different functional groups of two kinds of *MO* seeds cake powder. Thereupon, samples were characterized by Fourier Transform

Infrared spectroscopy (FT-IR), the X-ray fluorescence (XRF). A detailed elemental analysis of the plant was completed by the inductively coupled plasma mass spectrometry analysis (ICP-MS).

3.1.Structural analysis

3.1.1. Fourier Transform Infrared spectroscopy analysis

The FT-IR analysis was carried out to explore the surface functional groups of the obtained samples. The FT-IR spectra were recorded on Thermo-scientific, Nicolet 6700 FTIR system with a DTGS-KBr (Deuterated Triglycine Sulphate with potassium bromide) detector. About 3 mg of the *MO* seeds cake powder already stored at +4°C were homogenised with 100 mg of KBr by means of an agate mortar and pestle, the powder was pressed into pellets using a KBr press (ICL international, USA). FT-IR absorption spectra were recorded in the 4000–400 cm^{-1} range. The data were collected at 8 cm^{-1} resolution, and each spectrum was a result of 64 scans. The different positions of the vibration bands of the main functional groups and inorganic compounds identified in this work were presented on spectra in the section results and discussion.

3.2.Elemental analysis

3.2.1. X-ray fluorescence analysis

The elemental analysis was carried out using the X-ray fluorescence (XRF) technique in order to examine the microelements and traces elements in the *MO* seeds cake powder samples. This analysis was conducted to explore the *MO* seeds powders content of heavy metals. The *MO* seeds cake powder samples were compressed in a standardised sample chamber under standardised conditions. Analysis was conducted using energy dispersive X-ray fluorescence (ED XRF). A dispersive energy X-ray fluorescence spectrometer (HORIBA, XGT-5000) was used to analyze the plant tissue in both samples. A maximum current of 0.380 mA and a voltage of around 50 keV were both reached by the device.

3.2.2. The inductively coupled plasma mass spectrometry analysis

The inductively coupled plasma mass spectrometry (ICP-MS) method was used to conduct the multi-elemental analysis. To eliminate organic material, both *MO* seeds cake powders were burned at 600°C for two hours in a muffle furnace. Each sample was digested using a solution of (1+1) HNO_3 and (1+4) HCl, totalling around 1g. The acid digestion was carried out in triplicate. The analysis was performed by ICAP RQ Thermo Qtegra with CETAC ASX-560 configuration.

The analysis was conducted on Cr, Mn, Fe, Ni, Cu, Zn, As, Cd, and Pb **(US-EPA, 1994).** The resulting calibration curves were used to calculate mineral element concentrations.

Chapter I

Application in dam Water treatment

1. Application goals

The specific aim of this part of the study is to apply the use of the obtained coagulants in dam water purification by coagulation-flocculation process. Through this, the efficiency of both coagulants was identified by modelling turbidity removal for the simulated dam water using dehulled and unhulled *MO* cake powder extract, and determining the parameters that influence the process to produce the best performance. Also, evaluating the relative efficacy of RSM and ANN methods, as well as illuminating the connections between the process parameters were important aspects of this part.

2. Sampling

The sampling operation was carried out on a daily basis. Water samples were collected from Kissir dam situated in Jijel town (36° 47′ 29″ North and 5° 40′ 46″ East) of Algeria, over the period from December 2021 to March 2022 **(Figure 14).** The Kissir dam water is located in a mountainous area. Becoming operational in 2011, the dam is used to supply drinking water to the town population counting more than 637 000 inhabitants.

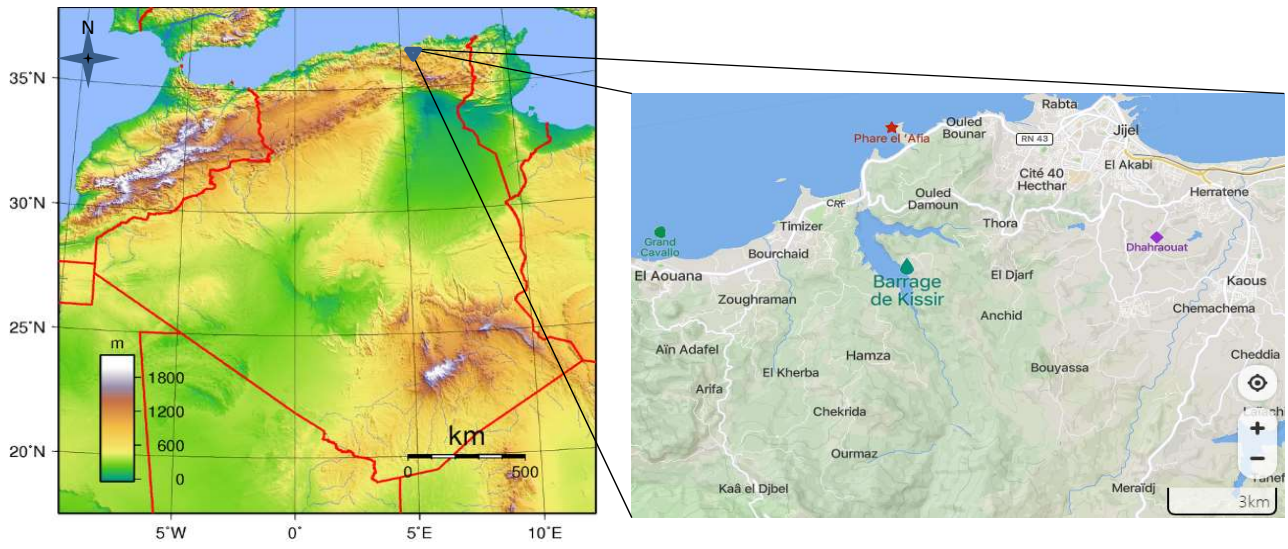

Figure 14. Location of the Kissir dam.

The dam can hold 60 million m^3 of water, which is mostly utilised for agricultural and drinking water. The dam managers had difficulties to deal with the turbidity level which

increases during the heavy rainy season. For this, turbidity was among the most important parameters in the study. Sampling was done in clean bottles, at a rate of 12 litres per day. Once at the laboratory, the *MO* seeds cake powder coagulation-flocculation method is used to treat these materials. **Table 6** displays the physicochemical properties of the captured raw water that were investigated.

Table 6. Physicochemical characterization of the used raw water**.**

Parameter	Raw water values	Algerian norm for potable water (JORADP, 2011)
pH	7.79 ± 0.03	≥ 6.50 and ≤ 9.00
Conductivity	200.00 ±1.55	200.00 – 2800.00 µS/cm
Turbidity	9.30 ± 1.82	< 5.00 NTU

3. Coagulant solution preparation

The *MO* seeds cake aqueous solution has been prepared according to **Baptista et al (2015)**, by dissolving 20 g of dehulled or unhulled *MO* seeds cake powder in 1 litre of deionised water. The mixture was vigorously stirred for 30 minutes, producing a milky-looking pale liquid as a result. This liquid has been filtrated using the filter1 to get a clear *MO* seeds solution. This aqueous solution was daily, prepared before each use **(Figure 15).** The doses of the used *MO* seeds cake solution are taken from this stock solution.

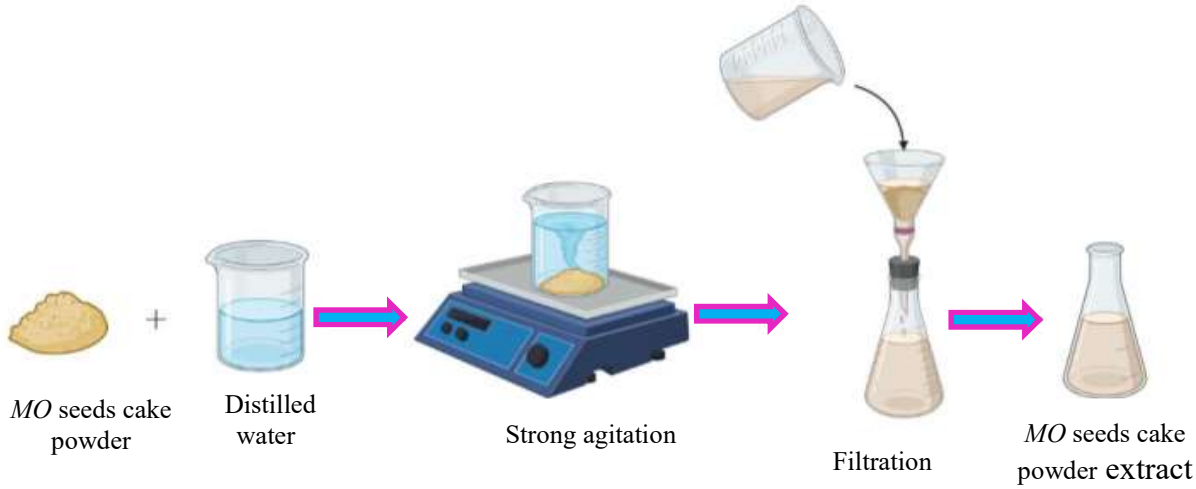

Figure 15. Preparation of the *MO* seeds cake powder solution.

4. Water treatment methodology

In order to optimise the coagulation-flocculation process, the Jar Test method was used **(Figure 16).** To ensure quality control and repeatability of readings, the test was run in triplicates.

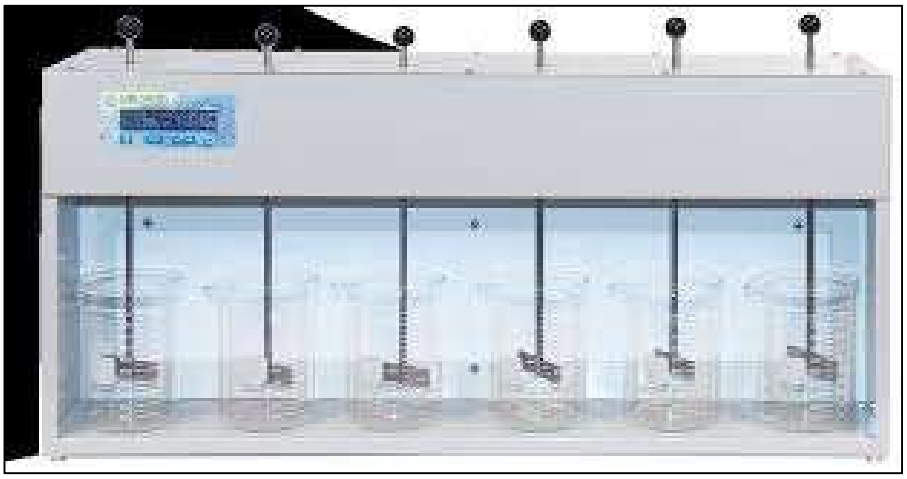

Figure 16. The applied jar test in the *MO* seeds cake powder efficiency trials.

One litre of dam water was used for each trial. Both preparations of *MO* seeds cake solution were used, each at increasing concentrations. The coagulant doses have been fixed through preliminary trials, which are based on the analysis of the influencing factors of coagulation-flocculation process. The influencing parameters were individually examined in single factor experiments to cut down on the amount of the experimental work. The concept was to maintain a constant value when one variable wasn't being researched. To achieve this, the employed concentration of the *MO* seeds cake solution in each test has ranged between 10 and 50 ml/L. The doses of 10 to 50 ml per 1000 ml of raw water were derived from a stock solution of 20 g/L. The stirring speed was ranging between 100 and 250 rpm for the fast stirring and between 20 and 80 rpm for the low stirring. Water samples were homogeneously mixed and kept in touch with the coagulant thanks to the quick mixing. However, slow mixing allowed the suspended matter to collide with enough energy to break through the energy barrier and bind together to form a bigger colloid. The treated water was let to settle for 30 to 120 minutes. These parameters were all tested with both coagulants. Before any physicochemical analysis, all samples were filtered. **Table 7** illustrates the coagulation-floculation process set parameters.

Table 7. Factors and levels for FFD (in coded and uncoded levels of variables)

Factors	Code	Minimum (- 1)	Maximum (+1)
Dosage	X_1	10 mL	30 mL
Fast mixing	X_2	100 rpm	200 rpm
Slow mixing	X_3	40 rpm	80 rpm
Settling time	X_4	30 min	90 min
Seeds kind	X_5	USCP*	DSCP**

**: unhulled seeds cake powder, **: dehulled seeds cake powder*

5. Experimental optimization

In order to determine the parameters influencing the coagulation-flocculation process using both coagulants, the response surface method and the neural network method were used.

5.1.Response surface methodology

5.1.1. Experimental design

To assess the impact of coagulation-flocculation operational parameters on turbidity removal, pH, and conductivity fluctuations, five main factors were picked: VIZ coagulant dose, fast mixing, low mixing, settling time and seeds kind. The impact of these five chosen components and their interactions were studied using a two-level full factorial design **(Goupy and Creighton, 2006; Mukerjee and Jeff Wu, 2010)**. Actually, widely developed linear models are applied in different areas of control engineering. But as most of the real time systems are ill-defined and uncertain in nature, system modelling based on conventional linear system tools is not appropriate for such systems. Chemical, electrical power, water treatment and other largescale industrial plants are complex systems consisting of many interconnected subsystems presenting a wide range of different properties. Factorial design is the statistical technique employed here for designing experiments where several factors (main factors) are controlled and their effects are investigated at each of two levels, as well as their interactions. This makes it an effective instrument that, in comparison to other experimental designs, offers the most thorough understanding of the behaviour of the system. It comprises the greater precision in estimating the overall main factor effects and interactions of different factors **(Jankovic et al., 2021).** In full factorial design every setting of every factor appears with every setting of every other factor. They are also, strong candidates in examining treatment variations. This mathematical model includes the assessment of linear influence of the individual factors and also the influence of factor interactions. This type of experimental design is known for its easy procedure, flexibility and low set up cost **(Ahmad et al., 2007).** It requires a good choice of factors number, if greater than 5 it gets more complicated and the interactions are misinterpreted. However, through the choice of 5 factors, there were enormous diversity in combinations, and because of that it was easy to explain, dissect, and ascribe the response amount variation to every potential cause, giving the process a nearly realistic representation. The FFD model can be then used as reliable benchmarks for comparing the characterization of other designs **(Jankovic et al., 2021).**

In the FFD method, many experiments could be integrated into one rather than doing a number of individual experiments. In an experiment, each of the input variables was normally

assigned to two levels. These levels are referred to as high (+1) and low (-1), respectively. **Table 7** shows the experimental and coded levels discovered during preliminary tests, as described in the section on jar test investigations. In this work, the coagulation-flocculation process using *MO* seeds cake powder was modelled using 35 runs, three of which were in centre points.

Turbidity, pH, and conductivity measurements were used to determine treatment effectiveness. According to **Haaland (1989),** the effect of a factor is defined as the change in response produced by change in the level of the factor. For the experimental design, the obtained polynomial equation is shown below (Eq.1):

$$Y = b_0 + b_1X_1 + b_2X_2 + b_3X_3 + b_4X_4 + b_5X_5 + b_{12}X_1X_2 + b_{23}X_2X_3 + b_{25}X_2X_5 + b_{35}X_3X_5 \quad \text{(Eq. 1)}$$

5.1.2. Validation

Once the optimum values have been obtained and in order to evaluate the models' suitability, further water treatment trials were carried out under the FFD's ideal predictions. The experimentally collected data was contrasted with the regression model's anticipated values. At this point, the idea was built on doing experiments using brand-new parameters, evaluating the results, and contrasting the various response values with the expected values. Experiments were conducted in triplicate.

5.2.ANN Methodology

5.2.1. ANN Modeling technique

The ANN modelling technique is an advanced data-driven modelling technique that is skilled at simulating the complex and nonlinear interactions among the observable data sets without necessitating a complete physical understanding of the natural systems. It has an adaptable mathematical topology **(Adamowski and Sun, 2010).** The ANN research has advanced significantly since the 1980s, and ANNs are now used extensively **(Ding et al., 2013).** The core idea behind the ANN technique is inspired by the brain's learning mechanisms and derives from an analogy of incredibly simplified mathematical models of biological neural networks **(Jean et al., 2004; May and Sivakumar, 2009).** The biological brain is fundamentally different from the traditional digital computer in its structure and information-processing methods. The biological brain is significantly more sophisticated and superior than traditional computers in many ways. The ability of a biological brain to "learn" and "adapt," which a

traditional computer lacks, is its most important point of differentiation. Conventional computers execute predetermined tasks based on "programs" or "softwares" that have been installed into them **(Sazli, 2006).** The ANN method is able to generalize from historical data and examples to come up with meaningful explanations for problems **(Jean et al., 2004; May and Sivakumar, 2009).** It provides important assistance with data organization, classification, and summarization. Additionally, it aids in identifying patterns in the incoming data, makes few assumptions, and produces highly accurate predictions. Due to its accuracy, adaptability, robustness, effectiveness, and efficiency in solving modelling problems, artificial neural network (ANN) technology is a potentially promising alternative tool for recognition, classification, and forecasting in almost all fields of science and engineering **(Khataee & Kasiri, 2011).** ANNs are also, adaptable nonlinear information processing systems with a number of properties like self-adaptation, self-organization, and real-time learning that incorporate a number of processing units **(Ding et al., 2013).** The ANNs structure includes three or more layers in their construction, including an input layer, one or more hidden layers, and an output layer. The input layer's function is to communicate the input data pattern to the neurons in the first hidden layer. The neural network's output layer responds to a specific input by producing an output. The initial layer provides the input data to the intermediate hidden layers, which may consist of just one hidden layer. Based on the activation function and network architecture, these serve in a variety of ways as a group of feature detectors. For this reason, the most important and difficult step in creating an ANNs-based model is choosing an appropriate neural architecture. To maintain the model within controllable scales, the modeller should select an effective testing method that can be applied to a wide range of alternatives. Network topology, training method, and input selection are the primary presumptions that need to be defined **(Anctil et al., 2004).**

5.2.2. Data collection and the Artificial Neural Networks building

For the coagulation–flocculation process modelling using the artificial neural network method, the multilayer full feed forward (MFFF) was used. The fluctuations in conductivity, pH, and turbidity removal were anticipated. An input layer of five neurons, two hidden layers, and a three-neuron output layer made comprised the ANN architecture. The number of iterations was set at 600. The building of multiple neural networks with various transfer functions (Hyperbolic-tangent, Gaussian, and Linear) allowed for iteratively determining the output layers. This step is extremely important since transfer functions are one of the main building blocks of the ANN process. The transfer function is in charge of transforming input signals into output signals. If the incorrect transfer function is selected, the transfer operation may fail **(Ghasemzadeh et al.,**

2018). On one hand, because of its simplistic nature, the trained ANN cannot accurately represent the relationship between the input and output variables. However, creating ANN models with too many neurones results in over-fitting issues. This implies that a trained ANN has a constrained ability to generalise the model. On the other hand, an inadequate number of neurons results in a poorly fitting model **(Khataee & Kasiri, 2010).** Generally, the data set are distributed on three principal stages, which are training, validation and testing. For this reason, the network topology used in this investigation had two hidden layers. In this work, the learning algorithm used 70% of the experimental data for training, 15% for validation, and 15% for testing. This was used to evaluate the model's generalisation ability and its predictive capability for hidden data that wasn't used for training.

Chapter II

Application in wastewater treatment

1. Introduction

In this section, both prepared *MO* seeds cake powder coagulants are used in the optimization of at Sidi Ali Lebhar wastewater treatment. For this purpose, the RSM and the ANN method were also utilized. A scientific paper in relation with this part has been already submitted.

2. Sampling

From December 2020 to June 2022, sampling was carried out daily at the Sidi Ali Lebhar wastewater treatment plant situated in Bejaia, Algeria (36.7 and 36°43'14.96″ North and 5°04'37.82″ East). Due to the plant's proximity to the Mediterranean Sea, the treated wastewater is dumped right into the water **(Figure 17).** This makes the subject of wastewater treatment at this plant a topical one.

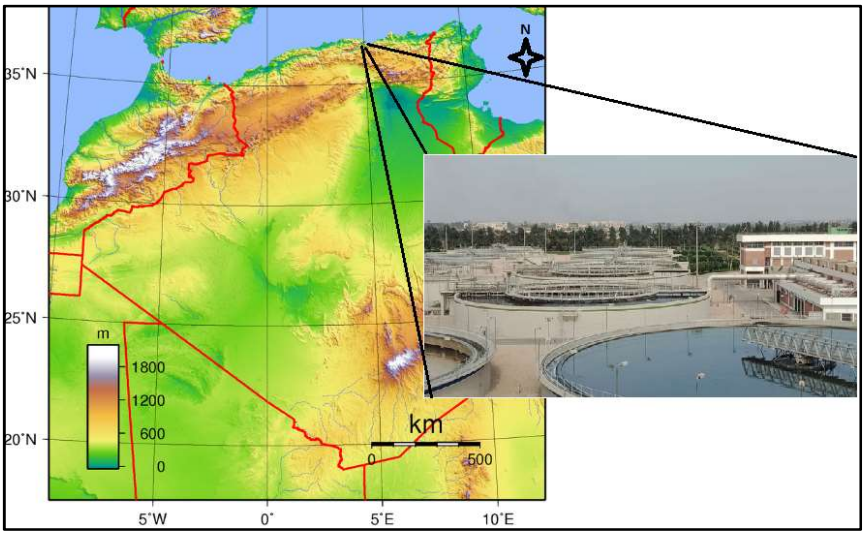

Figure 17. The Sidi Ali Lebhar wastewater treatment plant location.

On average, the Sidi Ali Lebhar wastewater treatment plant (WWTP) handles 31,000 m^3 of wastewater per day that is discharged by the citizens of Bejaia. The treated wastewater by the WWTP comes from domestic and industrial activities in Bejaia city. It is in fact a domestic wastewater treatment plant, and is of the low-load activated sludge type, because the most of the

city's industrial activities are in food industry and the received pollution by the WWTP is biodegradable. It is appropriate to treat this biodegradable pollutants using activated sludge.

Samples were collected at the entrance of the wastewater plant after the de-oiling/sanding stage, and at the exit of the plant before discharge, which gives raw wastewater noticed here as inlet water (IW), and outlet water (OW). The average volume of wastewater generated in one working day is 12 m^3 **(Figure 18).**

Figure 18. Sampling operation in the inlet and outlet of the wastewater treatment plant.

(a): de-oiling tank, (b): purified wastewater at the outlet of the plant, (c): sampling operation.

3. Wastewater treatment methodology

3.1.Response surface methodology

3.1.1. Jar test conditions

To optimise the coagulation-flocculation process using both *MO* seeds coagulants, the Jar test was carried out. To guarantee quality control and repeatability of results, the test was carried out in triplicates. The *MO* seeds cake solution was utilised in both forms, each at concentrations that increased by 10 ml, from 60 ml to 100 ml. For quick stirring, the speed ranged from 100 to 200 rpm, while for slow stirring, it ranged from 20 to 60 rpm. Rapid stirring took place for 2 to 4 minutes, whereas slow stirring took place for 10 to 30 minutes. The rapid mixing procedure ensured homogenous mixing of the suspended materials and maintained contact with the coagulant. To overcome the energy barrier and come together to form a larger colloid, gradual mixing enabled the suspended matter to collide with sufficient energy.

3.1.2. Preliminary trials

It entails employing both *MO* seeds cake preparations to optimise the coagulation-flocculation process influencing parameters in wastewater treatment plant. Each element was investigated independently, and the effects of the process parameters were initially examined

independently in single-factor trials. In order to reduce the overall experimental work, a variable was kept constant while it was not under investigation. Fast and low mixing were maintained at 100 and 20 rpm for 2 and 10 minutes, respectively, to examine how the concentration of the coagulant affected the mixing process. The coagulant dosage and low mixing were set at 70 ml and 20 rpm, respectively, to examine the impact of quick mixing on the coagulation-flocculation process. However, fixing the coagulant dose and fast mixing at 70 ml and 100 rpm, respectively, allowed for an investigation into the impact of low mixing. The preliminary tests were also performed in triplicates.

3.1.3. Experimental design (Box-Behnken optimisation set up)

The *MO* seeds cake powder dosage (X1), quick mixing (X2), and slow mixing (X3) represent the independent factors in this study. The interactions between these factors were evaluated using the RSM based on Box Behnken design (BBD).

BBD is a class of rotatable or nearly rotatable second-order designs based on three-level incomplete factorial designs. It has been shown that BBD is significantly more efficient than three-level full factorial designs and marginally more efficient than other RSM designs. The absence of combinations for which all elements are concurrently at their highest or lowest levels gives BBD an advantage. Therefore, these designs are helpful in preventing trials carried out under difficult circumstances, for which disappointing findings might occur. However, they are not indicated for circumstances when we would prefer to know the reactions at the extremes **(Ferreira et al., 2007).**

The preliminary investigation was used to define the limit values for each factor. The response model in the BBD is represented by suspended solids (Y). The experimental data were fitted into the quadratic model using the generalised form of second-order multiple regression as in **equation 1** to ascertain the relationship between the variables (X1), (X2), and (X3) and the response (Yi).

$$Y = \beta_0 + \sum_{i=1}^{n} \beta_i X_i + \sum_{i=1}^{n} \beta_{ii} X_i X_i + \sum_{i=1}^{n} \beta_{ij} X_i X_j \qquad \text{(Eq. 2)}$$

The coefficients for the intercept, linear, quadratic, and interaction effect term are β_0 , β_i , β_{ii} and β_{ij}, respectively . X_i and X_j are the independent variables in coded form. The number of independent variables is n. The steps are established in the diagram below, which is a replica of the experimental design. **Figure 19** depicts the diagram of the experimental design.

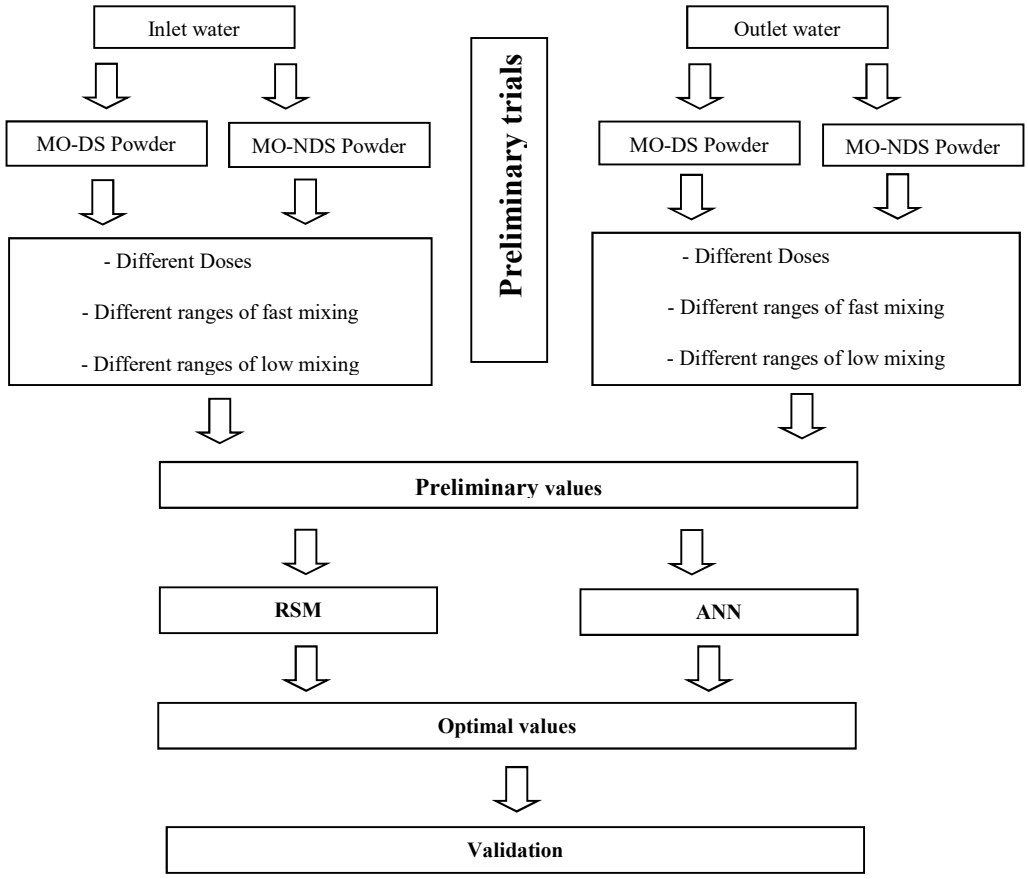

Figure 19. Diagram of experimental design.

3.2.Artificial Neural Network methodology

3.2.1. Data collection for ANN design set up

As indicated in the previous section, a model's over-fitting issues arise when there are too many neurones used to create coagulation-flocculation ANN models. However, the trained ANN's simplifications make it impossible to depict the relationship between the input and output variables with accuracy.

In this section of the study, the input layer of the ANN design was made up of three neurons, whereas the output layer was made up of two hidden layers and one neuron. The final choice of output layers was made after creating numerous neural networks with different transfer functions (Hyperbolic-tangent, Gaussian, and Linear). Since transfer functions are one of the fundamental pillars of the ANN process, this stage is crucial because if the wrong transfer function is selected, the transfer procedure might not succeed **(Ghasemzadeh et al., 2018).** TSS removal was predicted using the multilayer full feed forward (MFFF), using 900 iterations. The learning algorithm for TSS removal in this section employed 75% of the experimental data as

training set and 25% as validating set. This was used to evaluate the model's generalization ability and its predictive capability for hidden data that wasn't used for training.

3.3.Validation for generalization

Validation for generalization was applied for both techniques (RSM and ANN). Additional wastewater treatment trials were conducted at the ideal conditions predicted by the BBD and ANN models to confirm that the derived models were adequate. Models have then been used to test their effectiveness on other parameters and gauge their generalizability. The following variables were tested: lead (Pb), cadmium (Cd), and zinc (Zn) heavy metals, nitrates (NO^{3-}), nitrites (NO^{2-}), phosphorus (PO_4^{3-}), chemical oxygen demand (COD) and biochemical oxygen demand (BOD). The best conditions were used in triplicate for confirmation trials.

Cahpter III

Seed husks valorization

1. Introduction

People have always used dyes for clothing, food and home decoration. Since ancient times, they have extracted dyes from plants, such as indigo, and from animals, such as carmine extracted from cochineal. The use of these natural dyes continued until the first half of the 19th century. They were gradually replaced by synthetic dyes, which are suitable for many specific uses.

Dyes represent an important class of synthetic organic compounds used in many industries, particularly textiles **(Magdalane et al., 2017).** As a result of the wide use of dyes in industry, large amounts have been discharged into industrial wastewaters. The direct release of this wastewater into water bodies, such as lakes, rivers, etc., pollutes the water and harms the flora and fauna. Different types of dyes are found in textile industry effluent, however due to their high molecular weight and complicated structures, they have very limited biodegradability (**Pala and Tokat, 2002**; **Kim et al., 2004; Gao et al., 2007).** Furthermore, the biological treatment processes are disturbed by the direct discharge of this industrial effluent into sewage networks. These effluents cause biological reactors to create high quantities of inorganic salts, acids, and bases, increasing treatment costs **(Gholami et al., 2001; Babu et al., 2007).**

Methylene blue is a cationic dye. It is the most widely used dye for cotton, wood, silk and many other materials. It is also very difficult to eliminate, requiring potential treatments to eliminate it and purify the wastewater containing it. Among several processes to treat industrial liquid waste, the adsorption technique is the most favourable and most widely used to eliminate textile dyes. This method has become the method of choice, the most effective and the easiest to use **(Ahmed & Dhedan, 2012)**. Due to this, research projects are focusing on the use of suitable materials to enhance this dye removal, mainly those that are low cost, locally available, highly biodegradable and, above all, organically produced **(Karim et al., 2010)**.

After the hulling of the *MO* seeds, an enormous quantity of seed waste is obtained. Recycling this waste would seem to be an excellent way to improve high effectiveness of all parts of the *MO* seeds in water treatment. The choice of nanoparticles (NPs), which have been

used increasingly in recent years, is based on their high adsorption capacity. The NPs enable pollutants to be isolated quickly and easily **(Giakisikli & Anthemidis, 2013).** They have demonstrated a high level of performance in wastewater treatment **(Xu et al., 2012)**, thanks to their large exchange surface, superior reactivity and photo-catalysis **(Dutta et al., 2014).**

The aim of this section is to recover the waste from the *MO* seeds, a low-cost agricultural waste, by using in polluted water treatment. It involves synthesising a cellulose-based NPs using *MO* seed waste in order to obtain biodegradable products that can be easily used in water treatment, particularly for decolourising textile industry wastewater. The effectiveness of these materials in reducing one of the most persistent pollutants, methylene blue is investigated, offering a new process for treating coloured water based on the use of organic nanoparticles. For this reason, cellulosic based nanoparticles were prepared chemically using *MO* seed waste.

2. Methylene blue importance and characteristics

Actually, the toxicity of dyes could therefore be linked to the reduction of dissolved oxygen in these environments. In addition, their very low biodegradability, due to their high molecular weight and complex structures, gives these compounds a toxic character that may be high or low. As a result, they can persist in this environment for a long time, causing major disruption to the various natural mechanisms that exist in the flora (self-purification capacity of watercourses, inhibition of the growth of aquatic plants, etc.) and fauna (destruction of a category of fish, micro-organisms, etc.). The dye considered in this study is Methylene blue (MB), which is often used to study the performance of adsorbents in general. This dye was chosen because it is organic, cationic and has a known average size (15 Å), with a complicated aromatic structure **(Rafatullah et al., 2010; Hamed et al., 2014).** MB (or methylthioninium chloride) has the chemical formula of bis-(dimethylamino)-3,7 phenazathionium chloride, with the empirical formula C_{16} $H_{18}CIN_3S$. **Figure 20** shows the chemical structure of MB**.**

In addition to the environmental pollution risks, there is a major risk for human health. This dye harms both human and animal eyes permanently. Direct contact with this dye can also result in local burns, nausea, vomiting, mental health problems, and methemoglobinemia. Respiratory function may be also hampered by this substance **(Mahmoud et al., 2012).** For this reason, MB has been selected to be treated in this section. Dye choice for this study meets also other criteria:

- High solubility in water;

- Low vapour pressure;
- UV/visible spectrophotometer analysis;
- cationic structure;

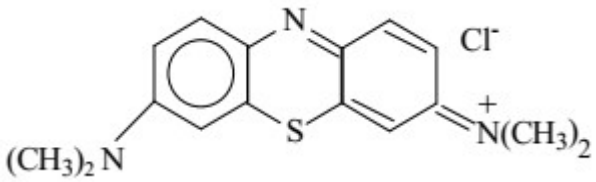

Figure 20. Methylene bleu structure.

All the properties and physicochemical characteristics of the chosen dye are summarised in the **Table 8.**

Table 8. Physico-chemical characteristics of methylene blue

common name	**Methylene bleu**
Molar weight	319,85 g/mol
Water solubility	High
Utility	Disinfectant and dye in bacteriology
vaporising pressure	Low

a. Preparation of Methylene bleu solution

MB (a cationic dye), taken as a model pollutant, is used without any prior purification. The solutions are prepared by dissolving quantities of the dye in distilled water. The solution is prepared by dissolving 100mg of MB in one litre of distilled water. The calibration curve was established by successive dilutions of the stock solution. The absorbance measurements were carried out using a UV/visible spectrophotometer type UV-3100PC with a maximum wavelength of 662 nm.

3. Characterisation of *Moringa oleifera* seed waste

The *MO* seed waste (peel) was characterised using FTIR, to confirm its cellulosic nature. This represents the basis for the choice of the type of materials synthesised subsequently.

4. Nanotechnology

Adsorption is a successful method for removing colours from wastewater among the various physical and chemical treatment procedures **(McRobb & Holt, 2008)**. Due to their high surface to volume ratio, nanoparticles have emerged as having the greatest potential for organic

chemicals adsorption particularly colours, from wastewaters and sewage tanks **(Hernandez et al., 2015; Ahmadi et al., 2017)**. Because of this, interest in nanotechnology research and development has greatly expanded **(Igwebe et al., 2018)**. Nanoparticles are known by their outstanding qualities, including their huge surface area, small size, high stability, high reactivity, and diverse chemistry for further functionalization **(Ihsanullah, 2020).**

4.1. Nanoparticles synthesis

The synthetized NPs in this study are cellulosic in nature. The NPs synthesis involves several stages such the extraction of cellulosic material, pre-treatment processes (alkali and bleaching treatments) and the final preparation of NPs.

4.1.1. Extraction of cellulose fibres from *MO* seeds husks

The *MO* seed husks were ground using an electric mixer. The obtained powder was then sieved (500µm) to obtain a homogeneous powder.

In order to extract the cellulose from *MO* seed husks by using alkaline and bleaching techniques, hemicelluloses and lignin were extracted sequentially from the raw material **(Moriana et al., 2016; Vallejos et al., 2016; Shaheen & Emam, 2018).** The *MO* seed husks powder was boiled in water for 20 min at 100°C to remove hemicellulosic materials. Alkaline treatment was carried out using 50g/L of the boiled *MO* seeds husk powder with 1.0 M NaOH solution for 2h at 80°C under mechanical stirring. The remaining alkaline sample was then bleached for 1 hour at pH 4.5 and 100 °C using sodium chlorite (2.5% w/v) in a material to liquor ratio of 1: 20 after being thoroughly rinsed with hot water. In order to get rid of any leftover or unreacted chemicals, the bleached cellulose was ultimately washed three times in boiling water before being dried in an oven. At this stage purified cellulose was obtained **(Figure 21).**

4.1.2. Preparation of Cellulose nanocrystals (CNC)

Under the influence of an ultrasonic approach, sulfuric acid was used to hydrolyze the pure cellulose. In order to perform the hydrolysis, 10 g of pure cellulose were suspended in 10 ml of 60% (w/w) sulfuric acid. In order to facilitate hydrolysis, this suspension was maintained at 60 °C under sonication for 60 min. To stop the reaction right away after hydrolysis, the suspension was diluted five-fold with cold distilled water to stop the reaction. The crystals were then separated from the suspension by centrifuging it at 12,000 rpm for 10 min before being decanted. Sonication caused the solid aggregates in the suspension to break apart. To get rid of any

remaining sulphate salts, the residual materials were then rinsed with distilled water and the combination centrifuged once more. Using dialysis tubing (MWCO 10,000), free acid in the dispersion was removed by dialysis against distilled water. The neutrality of the dialysis effluent served as evidence for this. The ensuing CNC suspension was stopped. After being frozen, samples were freeze-dried into powder form at -60 °C and 0.1 mbar, a pressure that won't damage the cellulose nanostructure **(Figure 21).**

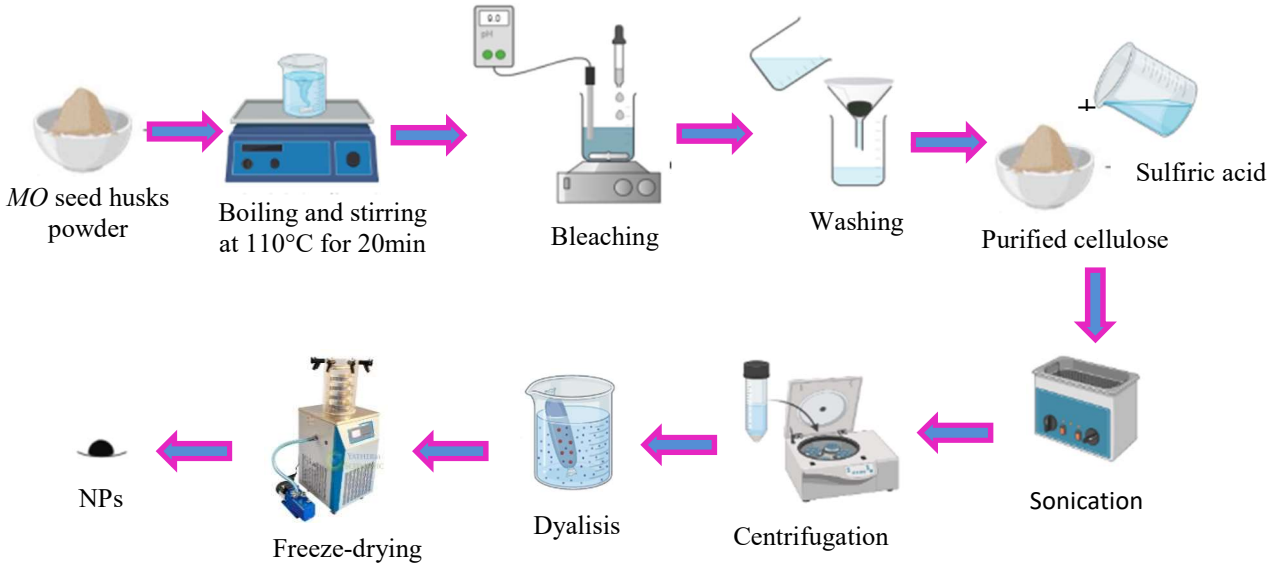

Figure 21. Nanoparticles synthesis.

5. Characterization of the obtained adsorbent

The characterization of both adsorbents has been carried out by the determination of the apparent density (ρa), the real density of adsorbents (pr), the adsorbents porosity and the zero load point (PHPZC). FTIR and SEM were also used for structural characterization.

5.1. The apparent density (ρa)

0.5 g of NPs was filled separately in a graduated cylinder. The volume covered by each matrix was noted. After being weighed, the bulk density is calculated using the equation below **(Chaouche, 2014).**

$$pa = \frac{m_1}{\mathrm{Vt}} \qquad \text{(Eq. 3)}$$

Where, $\boldsymbol{m_1}$**:** Material mass (g)

$\boldsymbol{Vt}$ **:** Apparent volume (cm^3)

5.2. The real density of the adsorbent (pr)

0.2 g of the studied adsorbent (NPs) is placed in a tared pycnometer. It was then filled with methanol (**Vm**) until a total volume (Vt) was reached. Vt corresponds to the total mass. The real density is calculated according to equation below:

$$pr = \frac{m_1}{\mathrm{Vt}} \qquad (\mathrm{Eq.}\,4)$$

The volume of methanol is calculated according to equation (5) as follows:

$$Vm = \frac{m_2}{\mathrm{pM}} \qquad (\mathrm{Eq.}\,5)$$

The volume of the material is calculated according to the equation (6):

$$V1 = Vt - Vm \qquad (\mathrm{Eq.}\,6)$$

$\boldsymbol{m1}$: Material weight (g)

m2 : Weight of methanol (g/mol)

Vr : Real volume of material (cm^3)

Vt : Total volume of pycnometer (cm^3)

ρM: Methanol density (g/ $cm^{3)}$

Vm : Volume of methanol (cm^3)

V1 : Material volume (cm^3)

5.3.The adsorbent porosity

The adsorbent porosity is calculated using the apparent and real densities according to the equation below:

$$\boldsymbol{\varepsilon = 1 - \left(\rho_{app} - \rho_{réelle}\right)} \qquad (\boldsymbol{Eq.7})$$

5.4.The pH zero load point (pHpzc)

The pHpzc is an important parameter to characterise adsorbents. It is used for surface charge determination. It was examined based on the standard method. For this effect, 250 mL of 0.01 M NaCl solution as an electrolyte was positioned in a vessel. Then, in 6 Erlenmeyer flasks,

25 mL of the electrolyte was introduced and the pH was adjusted to the required value (2.00, 4.00, 6.00, 8.00, 10.00, and 12.00) by adding 0.1 M NaOH or 0.01 M HCl. The suspension is then stirred for 24 hours, after which its final pH (pHf) is measured. The suspension was subsequently filtrated and the final pH was determined. The point of zero charges (pH_{PZC}) was found at the intersection point by plotting the initial pH versus the final pH **(Nandi et al., 2009).**

6. Characterization of the obtained material

Material characterisation is the process of defining the physicochemical properties of one or more components of materials. The characterisation techniques are used for a variety of reasons, such as identifying materials and detecting the presence of impurities, or knowing the external or internal structure of a product. Characterisation can also be a useful first step before carrying out a more intensive study of identifying impurities by eliminating certain variables from the investigation.

The characterization for the obtained material has been carried out using the FTIR analysis, and the SEM analysis. The FTIR analysis for the obtained materials was performed as indicated in section I of the study. The SEM analysis (Hitachi S-3400 scanning electron microscopy) was performed under 50, 20 and 10µm magnification. The SEM analysis was coupled to the EDX analysis giving a semi-quantitative analysis of the adsorbent.

7. Adsorption tests

The elimination of MB by adsorption using the synthetized NPs prepared using *MO* seed husks under the effect of several factors was studied. The batch adsorption process was carried out for this purpose. The MB solution concentration, the material concentration, and pH of the studied solution were carried out in a batch. The concept is based on bringing a dose of adsorbent into contact with a solution volume of 100 ml under agitation at 500 rpm. Next, a sample is recovered at a given stirring time. The sample is filtered through 0.45 µm filter paper and centrifuged if essential **(Figure 22).**

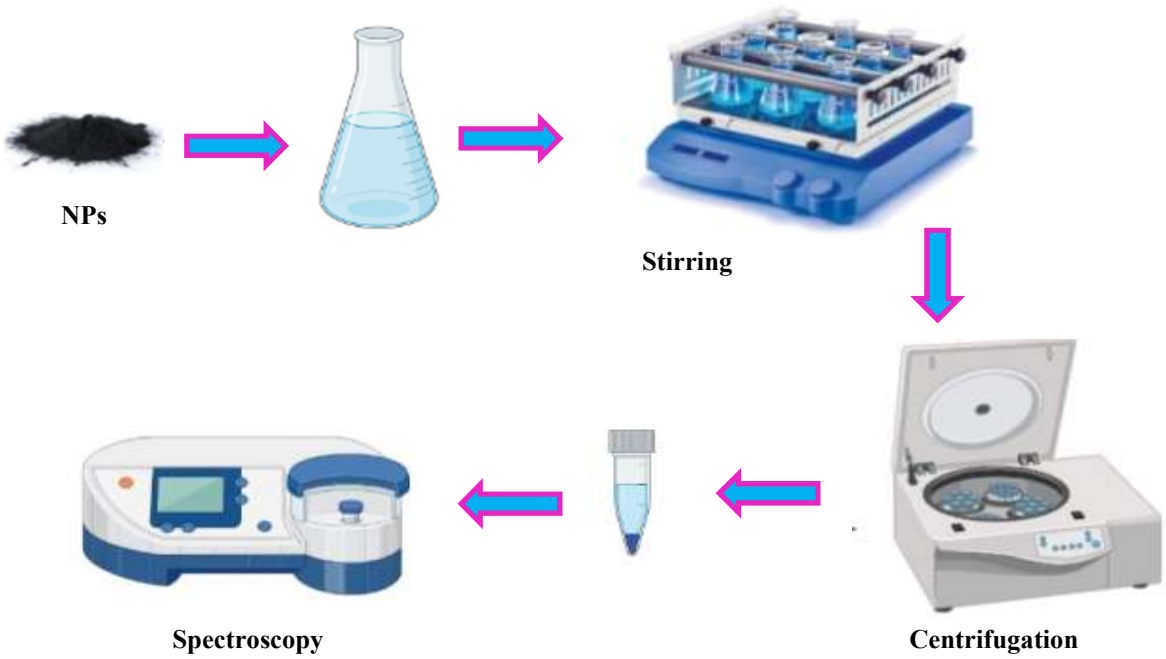

Figure 22. Batch adsorption process for dye removal.

7.1.Bio-sorbent masse effect

The bio-sorbent dose is one of the parameters that have a major effect on the adsorption process. In order to determine the optimum dose of the studied adsorbent on dye removal several tests have been carried out. The effect of adsorbent mass on MB adsorption was studied by varying the bio-sorbent dosage. Different concentrations of NPs (5; 15; 30; 45; 65, 80, 95, 110 mg) were used. Tests were carried out on 20 ml of dye solution, and the performance was tested under magnetic stirring for 24 hours. After stirring, the residual solution was separated by centrifugation at 5000 rpm for 5 minutes. The supernatant was recovered and analysed at 662 nm using a UV-visible spectrophotometer.

7.2.Bio-sorbent pH effect

The influence of pH solution on the adsorption of MB by NPs was studied. The experiments were carried out by introducing 110mg of NPs into 20ml of the 100mg/l MB solution. The effect of pH on MB adsorption was studied over a pH range from 2 to 11. The pH was adjusted using 0.1 M NaOH and 0.1 M HCl solutions. The mixture was then stirred for 24 hours. The supernatant was then recovered and analysed by UV-visible spectrophotometer at wavelength 620nm.

7.3.Effect of initial concentration of MB

From the evaluation of the quantity of the adsorbent giving maximum adsorption, it is useful to study the variations in this adsorption yield for the same quantity of adsorbent (m) at variable initial concentrations C_0 of MB. This is a crucial parameter to establish since it tells us the ideal concentration at which MB can be absorbed from aqueous medium. This was done while keeping adsorbent dose and MB solution pH stables.

7.4.Adsorption kinetic

To determine the time required to reach equilibrium for the adsorption of MB using the obtained NPs (110mg), we put 20ml of MB solution at 100mg/l in a beaker under magnetic stirring for 2h. The supernatant was recovered after centrifugation and absorbance measurements were carried out at different contact times, ranging from 15 min to 120 min. Kinetic models are used to examine the rate of the adsorption process and the potential rate controlling step. The pseudo-first-order rate equation is expressed as demonstrated by **Bulut et al (2007).**

$$Log(q_e - q_t) = Log(q_e) - \frac{K_1}{2.303}t \qquad \text{(Eq. 9)}$$

Where qe and qt are the amounts of MB adsorbed (mg/g) at equilibrium and time t (min), respectively, and k_1 is the rate constant of adsorption (min^{-1}). Values of k_1 were calculated from the slope of plots of log (q_e - q_t) against (t) at different concentrations. The pseudo-second-order rate equation is given as (**Bulut et al., 2007**):

$$\frac{t}{q_t} = \frac{1}{K_2\, q^2} + \frac{t}{q_e} \qquad \text{(Eq. 10)}$$

Where k_2 is the second order rate constant (mg^{-1}, min^{-1}), q_t and q_e are the amounts of MB adsorbed on the adsorbent (mg/g) at equilibrium and at time (t), respectively.

8. Chemical analysis

The multi-elemental analysis was performed by inductively coupled plasma mass spectrometry (ICP-MS). The analysis was conducted by ICAP RQ Thermo Qtegra with CETAC ASX-560 configuration. Samples preparation has been carried out as indicated in **US-EPA (1994).** Standard Methods were used to analyse the following parameters in both raw and processed water: TSS, BOD, COD, NO_3^-, NO_2^-, PO_4^{-3}, BOD, conductivity and pH were determined as described by **Rodier et al (2009).** Absorbance was measured in a UV–VIS

spectrophotometer (PerkinElmer). Moreover, turbidity was measured by using HANA HI 88713-ISO Turbidimeter. Conductivity and pH were measured using HANNA HI 98129 COMBO. Heavy metals concentration was determined by atomic absorption spectrometry (AAS) method with flame, as described in **Rodier et al (2009),** using Thermo Scientific ICE 3000 Series AA Spectrometer. From standard stock solution (1000 mg/L), several calibration solutions for lead, cadmium, and zinc were created. Five distinct concentrations of each element, ranging from 0.5 to 7 ppm, were created **(Nand et al., 2012).**

9. Statistical analysis and softwares

The RSM and ANN were built using the JMP (Trial Version 10, SAS, USA) programme, which was used to analyse all the outcomes. To evaluate the model's applicability and significance, the obtained data were statistically analysed using an ANOVA test. Significance was judged by determining the probability level that the *p*-value calculated from the data is less than 5%. The sufficiency of the model was evaluated using $R^2$and adjusted-R^2 **(Myers *et al.* 2009)** for FFD. For the ANN model, R^2 and RMSE were determined to identify the best ANN model by comparing evaluated values for the model. The validation graphics were designed using Origin Pro 8.5. kinetic and adsorption test's graphics were also designed using Origin Pro 8.5. The FT-IR spectra have been analysed by OMNIC software. The processing and the superimposition of spectra were carried out with OriginPro 8.5.

Results and discussion

Results and discussion

1. Introduction

In this part of thesis; the obtained results during the experimental work are presented and discussed in details. Material characterisation is the process of defining the physicochemical properties of one or more components of a substance or product. The characterisation techniques are used for a variety of reasons, including identifying product materials and detecting the presence of impurities, or knowing the morphology or the external or internal structure of a product. Characterisation can also be a useful first step before carrying out a more intensive study to identify impurities by eliminating certain variables from the investigation.

In this study various structural and elemental techniques were used to identify the functional groups of raw and modified materials. This explains the ability of using these materials as coagulants.

2. Raw material characterization (*MO* seeds cake powder)

2.1.Structural analysis

2.1.1. Fourier Transform Infrared spectroscopy analysis

From the obtained spectra, it turned out that the FT-IR spectrum of the *MO-DS* gives as many peaks as in *MO-NDS* spectrum, which gives the same structural composition.

Regarding the obtained spectra illustrated in **Figure 23**, The Strong broad centred at about 3347 cm^{-1} may be attributed to the OH stretching. This strong broad of OH is additionally attributed to presence of water in samples which have been used without prior drying. This alcohol function returns to an intermolecular bonded existing in proteins, fatty acids, carbohydrates and lignin devices **(Alpert et al., 2012; Reddy et al., 2012).** It is completely known that *MO* seeds are containing a big proportion of proteins **(Gallão et al, 2006),** consequently this area may contains the contribution of N-H stretching which represents amide function **(Araújo et al., 2010; Araújo et al., 2013).** The second peak located about 2924 cm^{-1} corresponds to the asymmetric stretching of C-H bond, whilst the juxtaposes peak positioned approximately at 2853 cm^{-1} represents an asymmetric stretching of CH_2 functional group **(Alpert et al., 2012).**

The peaks located in 1746 cm^{-1} and 1652 cm^{-1}, are respectively corresponding to C=O stretching. This function is attributed to the carbonyl amides located in protein section **(Mistry, 2009; Araújo et al., 2013).** This special disposition of functional groups could be the result of the heterogeneous structure of raw *MO-DS* and *MO-NDS* seeds cake powder.

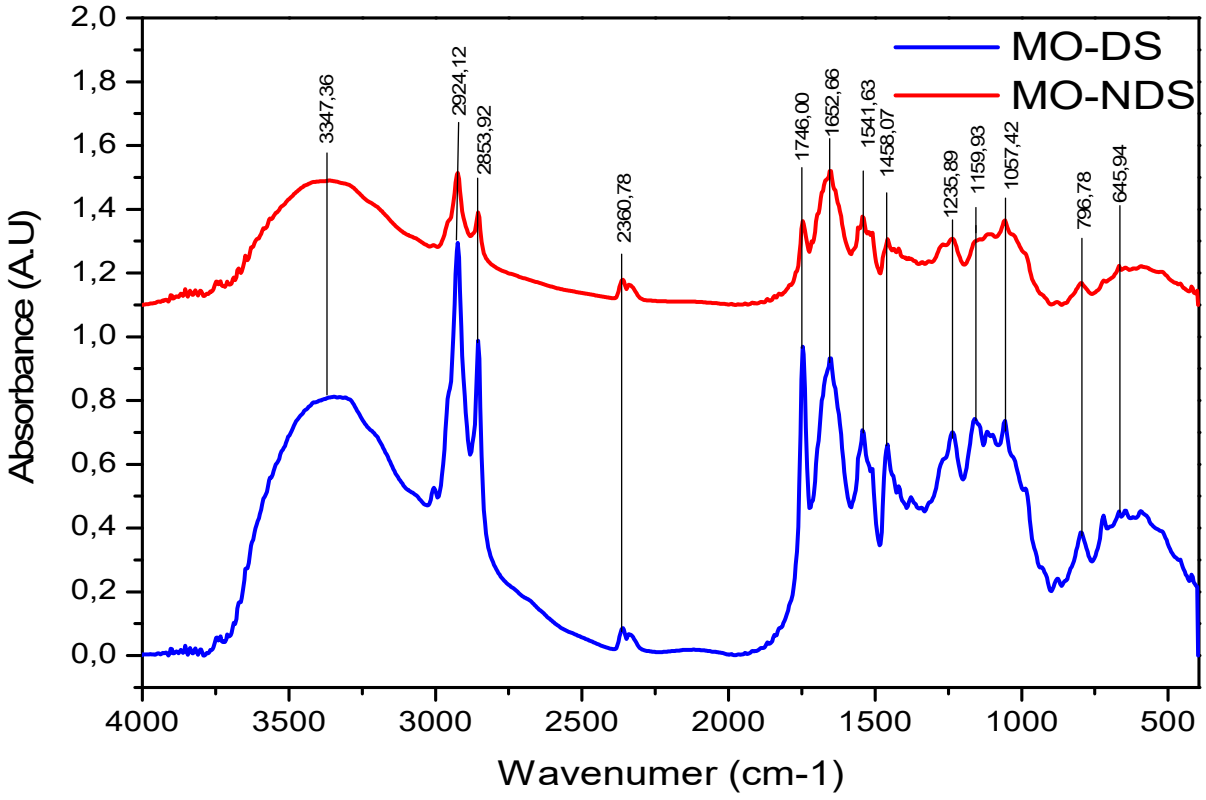

Figure 23. FT-IR analysis of *MO-DS* and *MO-NDS* seeds cake powder.

The observed peak at 1541 cm^{-1} is attributed to CN stretching coupled to NH bending of the peptide group **(Schulz & Baranska, 2007; Reddy et al., 2010; Reddy et al., 2011)** which is also due to the high contents of protein in both *MO* seeds cake powders. The 1235 cm^{-1} peak is another representative confirmation for the high protein content of both types of cake powder. It represents the amide III group **(Mistry, 2009).** Additionally, phenols can be well recognized by IR spectroscopy in this area **(Mistry, 2009; Schulz & Baranska, 2007)**, the 1235 cm^{-1} peak is attributed to the presence of phenyl group. Bands at 1458 and 1541 cm^{-1} areas are attributed to aromatic functional group represented by the C=C connection. This kind of group was also represented in *MO* bark **(Reddy et al., 2011).** The finger print area of 1000–1200 cm^{-1} had put on view the main skeleton cellulose peaks, especially for the *MO-NDS* powder **(Araújo et al., 2013).**

Structural studies on *MO* barks and leaves reveal similarity in functional groups obtained in this characterization for the *MO-DS* and *MO-NDS* **(Reddy et al., 2010; Reddy et al., 2011; Reddy et al., 2012).**

According to the obtained results both *MO* seeds cake powders can be classified as lignocellulosic material due to the presence of cellulosic functions. This was demonstrated by **Araújo et al (2013)**, who have successfully shown that the *MO* seeds are mainly made up of cellulose, hemicellulose and lignin. This structural positioning agrees also well with the proposed cyto-chemical analysis obtained by **Gallão (2006)** that revealed the presence of pectin, cellulose and hemicelluloses in *MO* seeds cells walls. It is also important to note that many functional groups as Hydroxyl, carbonyl and amine groups have been proposed to be responsible for metal binding and uptake by using plant biomass through adsorption, coordination, chelation, complexation and/ or ion exchange **(Volesky, 1999).** It is then very possible that these functional groups may represent the most important elements in conducting the bio-coagulation of both *MO* seeds cake powders.

2.2.Elemental analysis

2.2.1. X-ray fluorescence analysis

The aim of the XRF-mineral analysis is to identify the micro-elemental composition of both *MO* seeds cake powders **(Figure 23).** The obtained results showed remarkable higher concentration of Calcium (Ca) in the *MO-NDS* powder. However, high concentration of potassium (K) was observed in both preparations. In one hand, Low concentration of Sulfur (S), Iron (Fe) and Chloride (cl) have been determined in the *MO-DS* seeds cake powder. In the other hand, other elements were detected also in low concentrations in the *MO-NDS* seeds cake powder such as Sulfur (S), Iron (Fe) and Silicium (Si). These concentrations were found to be barely below detection limits (BDL). This indicates the edibility and non-toxicity of the *MO-DS* and *MO-NDS* seeds cake powders if used in water treatment **(Ernest et al., 2017)**. The obtained elemental analysis results for the *MO-DS* seeds cake powder was very similar to that obtained by **Zaid & Ghazali (2019).** For this reason, the elemental composition of both *MO* seeds cake powders could be expected to affect their coagulating effectiveness.

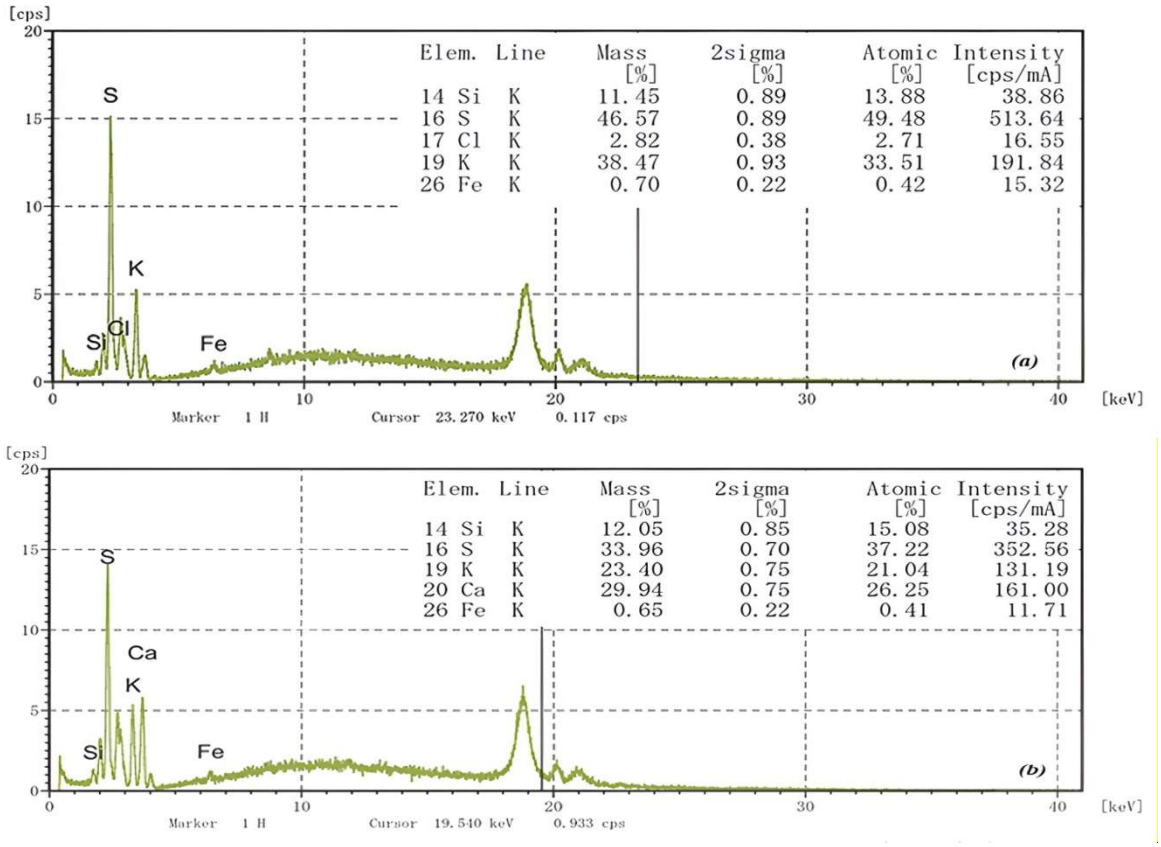

Figure 24. XRF analysis for (a): *MO-DS*, and (b): *MO-NDS* cake powders.

2.2.2. The inductively coupled plasma mass spectrometry analysis (ICP-MS)

This elemental analysis by ICP-MS was performed on the *MO-DS* and *MO-NDS* seeds cake powders to gain information on heavy metals content in the reference materials, since known that the heavy metals content of seeds could vary depending on the elevation, season and soil type **(Melesse et al., 2012).**

Linear calibrations functions (R^2) were limited between 0.9999 and 0,9995 for Cr, Mn, Fe, Ni, Cu, Zn, As, Cd using multi-element pellet standards. The comparative concentrations of the two samples are presented in **Figure 25.** The ICP-MS elemental analysis of both samples revealed high contents of copper (Cu) namely 50, 50 ppb For the *MO-NDS* sample and 21,04 ppb for *MO-DS* , while Ni and Cr have taken the values 64,56 ppb, 52,25 ppb and 50, 50 ppb, 21,04 ppb for *MO-NDS* and *MO-DS*, respectively. Iron (Fe), Manganese (Mn) and Zinc (Zn) have taken very minimal values in both samples. It was identified as well as for the XRF analysis, that these amounts were just below detection limits (bdl). This suggests that the *MO-DS* and *MO-NDS* seeds cake powder are edible and non-toxic when used for water treatment **(Ernest et al., 2017).** Lead (pb) as dangerous heavy metal have taken a very an outstanding

value in the *MO-NDS* sample, this could be due to the soil composition of the ground that grows the *MO* trees. This make the MO-DS seeds cake powder more secure for use in drinking water treatment. The detected values of Pb in *MO-NDS* are also below very minimal allowing its using, especially in drinking water treatment.

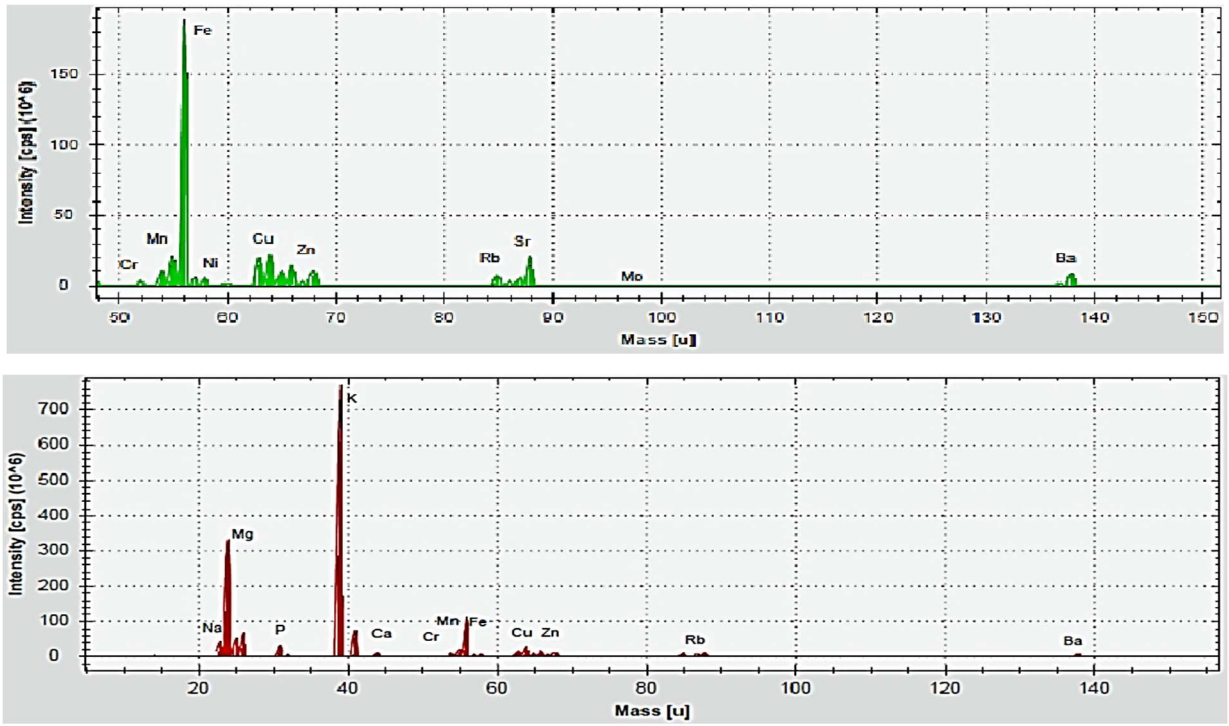

Figure 25. The inductively coupled plasma mass spectrometry analysis for (a): *MO-DS,* and (b): *MO-NDS* seeds cake powders.

Section I

Chapter I

Application in dam water treatment

1. Introduction

In this part of the first section, RSM was already used to remove turbidity using biological material (**Trinh & Kang, 2011).** However, it stills unable to locate the global optimum point and to extrapolate outside of the experimental range. Due to these shortcomings, the ANN are thought to have stronger predictive capacity and are going to popularity **(Amenaghawon & Kazeem, 2020; Kusuma et al., 2021).**

The aim of working on this part is eventually: (i) to assess the effectiveness of dehulled and unhulled *MO* seeds cake powders by figuring out how, and with the goal of valorizing an agricultural waste, the hulling of the seeds impacts the coagulation-flocculation activity on Kissir dam water, (ii) to employ dehulled and unhulled *MO* seeds cake powder extract in the evaluation of turbidity removal for simulated dam water, and to identify the factors that affect the process to yield the best results, (iii) to create a prediction model for the coagulation-flocculation process using *MO* seeds cake powder by RSM and ANN methodologies and to shed light on the relationships between the process variables, and (iv) to assess which model is better able to explain the investigated process. In this part of the first section, the *MO-DS* and *MO-NDS* are named DSCP and USCP, respectively.

2. Modelling and fitting FFD model using RSM

In this part, the treatment effectiveness was assessed by assessing the turbidity, pH, and conductivity of the collected dam water samples treated with DSCP and USCP. The relationship between the factors and the replies was ascertained using FFD. The experimental data findings for the observed, anticipated, and residual values derived as FFD, including runs, are shown in **Table 9**. These outcomes were utilised to establish the ultimate ideal treatment parameters before moving on to the validation phase.

It is clear from the data on **Table 9** that the expected turbidity removal values and the experimental data are very similar. It illustrates that the experimental results, particularly for turbidity removal, suited well to the model utilised thanks to the low residual values. It is clear

from the high degree of agreement between actual and anticipated values that the regression model's response was adequate to reflect the desired optimisation **(Zhang et al., 2013)**.

Guan and Yao (2008) assert that a well-fitted model requires an R^2value of at least 0.80. In this investigation, the R^2 values for turbidity removal, pH, and conductivity fluctuations, respectively, were 0.90, 0.64, and 0.58 **(Table 10).** A high R^2 indicates that the variation can be explained and the data can be effectively fit to the model. This wasn't the case for pH and conductivity changes, but it was for turbidity removal (**Karazhiyan et al., 2011).**

Table 10. Variance analysis for turbidity removal, pH and conductivity variations.

	Source	Coefficient	DF	SS	SM	p-value	Prob > F
Turbidity	Model		15	0.89	0.05		
	Residual		19	0.10	0.005		
	Lack of fit		18	0.09	0.005	<0.0001	0.44
	Pure error		01	0.002	0.002		
	Corrected total		34	0.99			
	R^2	0.90					
	Adj-R^2	0.81					
	CV* (%)	214.28					
	RMSE**	0.07					
	MSE***	0.000049					
	MAE****	0.046					
pH	Model		15	1421.07	94.73		
	Residual		19	814.42	42.86		
	Lack of fit		18	814.36	45.24	0.052	0.02
	Pure error		01	0.055	0.05		
	Corrected total		34	2235.5			
	R^2	0.64					
	Adj-R^2	0.35					
	CV (%)	0.32					
	RMSE	6.54					
	MSE	42.771					
	MAE	0.089					
Conductivity	Model		15	0.49	0.03		
	Residual		19	0.35	0.01		
	Lack of fit		18	0.35	0.01	0.123	0.40
	Pure error		1	0.005	0.005		
	Corrected total		34	0.85			
	R^2	0.58					
	Adj-R^2	0.25					
	CV (%)	7.52					
	RMSE	0.14					
	MSE	0.019					
	MAE	3.652					

**Coefficient of variation, **Root mean squared error, ***Mean squared error, ****Mean*

Table 9. RSM and ANN experimental data for the observed, predicted, and residual values, for dam water treated samples with coagulation-flocculation process

Run	Experimental factors	Turbidity (Y1)					pH (Y1)					Conductivity (Y2)				
		Observed values	RSM Predicted values	RSM Residual	ANN Predicted values	ANN Residual	Observed values	RSM Predicted values	RSM Residual	ANN Predicted values	ANN Residual	Observed values	RSM Predicted values	RSM Residual	ANN Predicted values	ANN Residual
1	−++1	0.40	0.39	0.01	0.42	-0.02	7.85	7.77	0.08	7.76	0.09	178.67	181.90	-3.23	193.68	-15.01
2	−−+1	0.42	0.47	-0.05	0.40	0.02	7.64	7.79	-0.15	7.79	-0.15	192.00	188.06	3.94	191.01	00.99
3	+−−1	0.22	0.23	-0.01	0.20	0.02	7.45	7.51	-0.06	7.56	-0.11	187.67	189.81	-2.14	192.85	-05.18
4	−+−1	0.61	0.56	0.05	0.43	0.18	7.90	7.77	0.13	7.70	0.20	205.33	197.31	8.02	192.83	12.50
5	++−2	0.29	0.28	0.01	0.32	-0.03	7.82	7.90	-0.08	7.68	0.14	212.67	208.45	4.22	191.99	20.68
6	+−+1	0.55	0.53	0.02	0.57	-0.02	7.72	7.64	0.08	7.73	-0.01	193.00	192.56	0.44	192.59	00.41
7	+−−2	0.34	0.36	-0.02	0.32	0.02	7.33	7.43	-0.10	7.46	-0.13	203.33	194.28	9.05	194.70	08.63
8	++−1	0.40	0.36	0.04	0.32	0.08	7.73	7.74	-0.01	7.67	0.06	185.33	188.98	-3.65	195.45	-10.12
9	+−−1	0.23	0.21	0.02	0.23	0.00	7.66	7.60	0.06	7.61	0.05	197.00	194.15	2.85	193.08	03.92
10	++−−1	0.32	0.41	-0.09	0.34	-0.02	7.51	7.59	-0.08	7.67	-0.16	184.33	184.65	-0.32	192.52	-08.19
11	−−−+1	0.20	0.21	-0.01	0.25	-0.05	7.72	7.70	0.02	7.66	0.06	193.33	194.31	-0.98	192.52	00.81
12	+−+−2	0.80	0.86	-0.06	0.89	-0.09	7.73	7.68	0.05	7.66	0.07	195.00	194.87	0.13	192.31	02.69
13	++++1	0.30	0.30	0.00	0.31	-0.01	7.74	7.72	0.02	7.74	0.00	183.33	182.90	0.43	195.83	-12.50
14	+−++2	1.03	0.81	0.22	0.81	0.22	7.65	7.82	-0.17	7.71	-0.06	193.67	203.70	-10.03	192.89	00.78
15	−−−+2	0.35	0.24	0.11	0.27	0.08	7.62	7.54	0.08	7.60	0.02	195.00	196.95	-1.95	194.49	00.51
16	0 0 0 0 1	0.37	0.38	-0.01	0.42	-0.05	7.80	7.71	0.09	7.73	0.07	196.00	190.31	5.69	192.80	03.20
17	−−++2	0.66	0.71	-0.05	0.69	-0.03	7.77	7.75	0.02	7.78	-0.01	195.00	188.53	6.47	191.99	03.01
18	−+−−2	0.53	0.51	0.02	0.43	0.10	7.78	7.66	0.12	7.70	0.08	205.00	199.62	5.38	192.78	12.22
19	−−−−2	0.27	0.31	-0.04	0.25	0.02	7.41	7.49	-0.08	7.54	-0.13	190.67	192.78	-2.11	192.31	-01.64
20	−−−−1	0.21	0.21	0.00	0.17	0.04	7.63	7.75	-0.12	7.62	0.01	190.00	197.81	-7.81	193.38	-03.38
21	−−+−2	0.71	0.74	-0.03	0.72	-0.01	7.80	7.74	0.06	7.75	0.05	185.67	187.53	-1.86	192.22	-06.55
22	−++−1	0.30	0.39	-0.09	0.36	-0.06	7.72	7.80	-0.08	7.79	-0.07	183.33	188.56	-5.23	193.68	-10.35
23	0 0 0 0 2	0.50	0.49	0.01	0.61	-0.11	7.85	7.72	0.13	7.71	0.14	197.00	196.45	0.55	191.94	05.06
24	−+−+1	0.48	0.52	-0.04	0.45	0.03	7.69	7.79	-0.10	7.69	0.00	192.00	193.81	-1.81	193.07	-01.07
25	++−−2	0.41	0.40	0.01	0.40	0.01	7.74	7.65	0.09	7.64	0.10	183.33	196.45	-13.12	193.93	-10.60
26	+++−2	0.54	0.50	0.04	0.53	0.01	7.80	7.79	0.01	7.75	0.05	194.33	191.37	2.96	192.98	01.35
27	+++−1	0.30	0.31	-0.01	0.31	-0.01	7.51	7.61	-0.10	7.75	-0.24	181.67	181.73	-0.06	192.24	-10.57
28	++++2	0.30	0.42	-0.12	0.32	-0.02	8.06	8.00	0.06	7.76	0.30	206.67	200.20	6.47	191.66	15.01
29	−++−2	0.51	0.55	-0.04	0.48	0.03	7.60	7.80	-0.20	7.81	-0.21	188.00	188.70	-0.7	191.09	-03.09
30	0 0 0 0 1	0.43	0.38	0.05	0.42	0.01	7.91	7.71	0.20	7.73	0.18	196.33	190.31	6.02	191.13	05.20
31	+−−+2	0.20	0.27	-0.07	0.28	-0.08	7.70	7.62	0.08	7.54	0.16	206.33	206.28	0.05	191.99	14.34
32	−+−+2	0.39	0.41	-0.02	0.39	0.00	7.60	7.77	-0.17	7.72	-0.12	202.00	203.78	-1.78	193.66	08.34
33	−−+−1	0.51	0.44	0.07	0.45	0.06	7.95	7.88	0.07	7.80	0.15	196.00	194.73	1.27	191.89	04.11
34	+−++1	0.42	0.55	-0.13	0.46	-0.04	7.63	7.69	-0.06	7.74	-0.11	190.33	193.73	-3.4	191.14	-00.81
35	−+++2	0.54	0.48	0.06	0.36	0.18	7.98	7.87	0.11	7.80	0.18	186.00	189.70	-3.7	191.81	-05.81

A high R^2 value, however, does not always signify a successful regression model. Hence, adding a variable to the model will always increase R^2, regardless of whether the additional variable is statistically significant or not. Therefore, it is advisable to use an adj-R^2 to evaluate the model's appropriateness (**Karazhiyan et al., 2011). Table 10** shows that the model's R^2 and adj-R^2 values are statistically different, with the exception of turbidity removal, proving that non-significant components were not taken into account.

For turbidity removal, conductivity, and pH fluctuations, the coefficient of variations (CV) values were discovered to be 214.28, 0.32, and 7.52, respectively. Because CV is a statistic that expresses standard deviation as a percentage of the mean, the smaller values offer higher reproducibility. A CV larger than 10 often denotes considerable variability in the mean value and inadequate development of an efficient response model **(Myers et al., 2009)**. Thus, the turbidity removal responses can be inferred to have a large range of variation between them. Based on these findings, the study will simply monitor the impact of coagulation-flocculation in removing turbidity moving forward.

1.1.Effect of *MO* seeds powders on turbidity removal

To investigate the effectiveness of both *MO* seeds cake powders in turbidity removal and implement a model, the *p*-values were used to evaluate each coefficient's significance. The matching coefficient rises as the p-value falls. If the *p*-value is less than 0.05, then the model terms are deemed significant. This is the case for turbidity removal which was less than 0.0001.

The linear effect of all parameters for turbidity's removal model was significant ($p < 0.05$). Slow mixing had the most adequate and significant impact. From this point on, delayed mixing as an independent component had a significant impact on the eliminated turbidity level. Similar effect was observed with seeds kind parameter. It was the second significant component that had a detrimental impact. The outcome of the analysis of variance reveals that the turbidity removal is mainly influenced by two independent variables as well as certain interactions with additional variables that on their own have no bearing. There are four interactions in this model that have a statistically significant impact on turbidity removal, as shown in **Figure 26,** which displays the second order interaction profile of the investigated components on turbidity removal. From left to right and top to bottom of **Figure 26**, these interactions relate to coagulant dose and fast mixing, fast and slow mixing, fast mixing and seeds kind, and finally slow mixing and seeds kind. This means that while the second order interactions of the components are considerably efficient, the influence of the independent variables on turbidity reduction was not significant for

all factors. This could mean also that the effect of the interactions when changing factors is not the same on the response.

Typically, if a model has a large number of meaningless model terms, model reduction by constricting the parameter ranges may improve the model. One of two things can happen when a model exhibits a "lack of fit": either multiple important terms were omitted from the model, or the model's fitting resulted in unusually large residuals **(Dharma et al., 2016).** In the case of turbidity removal model, the produced residuals are minimal (**Table 9)**. The model description of how the response and the independent variables interact was evaluated in **Table 10**.

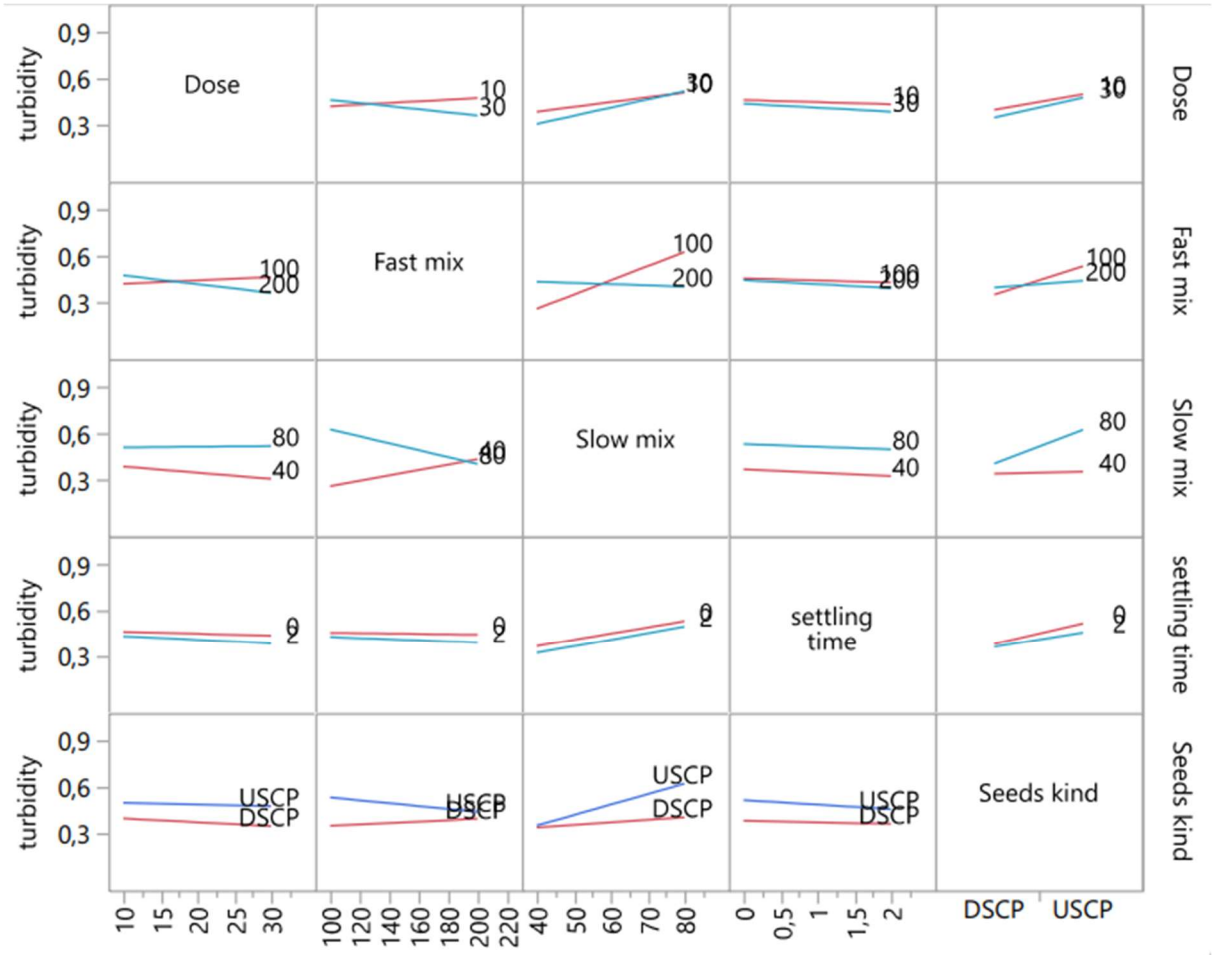

Figure 26. Factors impacting turbidity removal and their interaction profile.

The "lack of fit" in this study was demonstrated by a low *F*-value of 0.44 and a low p-value less than 0.0001, which indicated that the model was significant in comparison to pure error (0.002). The relationship between the dependent and independent variables, as evidenced by the R^2 value, accounts for the dependent variable's variability. The R^2 value for the FFD model is 0.90, which indicates that independent parameters can account for 90% of the variation

in turbidity removal and that the remaining 10% cannot be explained by the model. The adj-$R^2$was 0.81 and the root mean squared error (RMSE) was 0.07. This indicates that the calculated model, as proposed by **Lee et al (2010),** fits the experimental data satisfactorily. The low pure error values displayed by model terms demonstrate that the regression model equation provides a good fit of the experimental data and makes a believable prediction **(Table 10)**. Additionally, other error functions were employed for model accuracy (RMSE= 0.07, MSE = 0.000049, MAE = 0.046). This indicates good accuracy of the model.

1.2.Variables effects on turbidity removal

The Pareto analysis provides crucial data to explain the obtained outcomes (**Haaland, 1989).** This analysis calculates each variable's percentage effect on the response in accordance with the relationship (Eq.11).

$$P_i = \frac{b_i^2}{\sum b_i} \times 100 \ (i \neq 0) \qquad (Eq. 11)$$

Where b_i represents an estimate of the response's major effect of factor i.

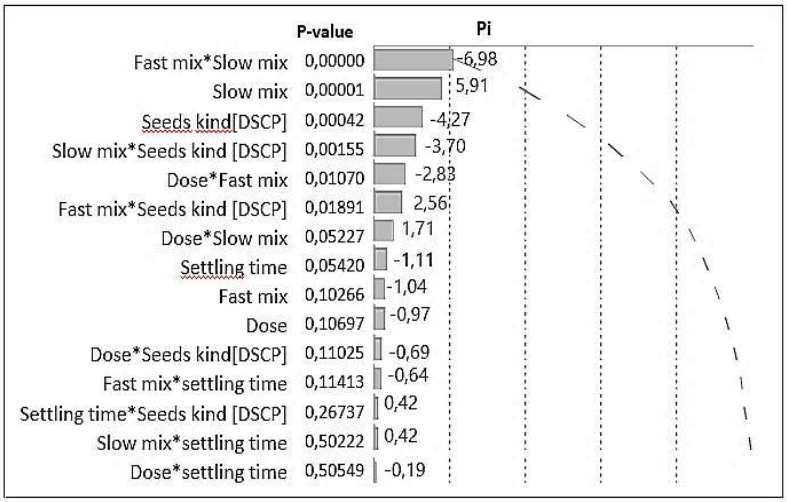

Figure 27. Pareto analysis and a graphical representation of variable effects.

The impact of the examined factors and their interactions on turbidity removal are detailed in **Figure 27**. It demonstrates that by having a negative impact on the examined response, fast and slow mixing interactions with a zero *p*-value represent the interaction that have the greatest bearing. The only significant independent variable that had a beneficial impact on turbidity reduction in the second range is slow mixing, which had a *p*-value of 0.00001. With a similarly significant *p*-value of 0.00042, the DSCP seeds kind negatively impacted the response. Slow

mixing has an adverse impact on the response and interacts with the DSCP seeds kind with a significant *p*-value of 0.00155. With *p*-values of 0.01070 and 0.01891, respectively, the interactions of fast mixing with dosage and DSCP seeds kind were similarly significant, with the former having a negative effect and the latter a positive one. However, the remaining interactions and factors have no statistically significant impact on the response under study. It seems that the only parameters that had a beneficial influence on the response under study were the kind interactions between slow mixing and quick mixing DSCP seeds. Since a positive sign boosts the response while a negative sign reduces it, regression analysis benefits from the influence of parameters on the response (**Öztürk & Sahan, 2015; Yonten et al., 2015)**. The coefficient of the polynomial model was determined considering the obtained results in (Eq.12):

$$Y = 0.43 - 0.014X_1 - 0.015X_2 + 0.088X_3 - 0.016X_4 - 0.060X_5 - 0.042X_1X_2 - 0.103X_2X_3 + 0.038X_2X_5 - 0.055X_3X_5 \quad \text{(Eq.12)}$$

The percentage of significant factor effects and the interactions effect were not particularly high, despite the fact that factor's effects were significant at ($p < 0.05$).

It was balanced between 4.085% and 0.554 %. The percentage of not significant factors and interactions was less than 0.247%. The ratio of 4.085% to 0.554% was balanced. There were less than 0.247% of non-significant variables and interactions.

1.3.Effects of interactive factors on turbidity removal

The ideal coagulation-flocculation conditions are investigated and forecast using the contour and surface response plots **(Onoji et al., 2017).** The general shapes of the 3-D graphs were explicitly identified by different curvatures. This degree of curvature in the FFD model represents the levels of uncertainty associated with each interaction of the process variables. The response surface plots' troughs 3-D plot indicates that the interacting variables' ideal regions were precisely within the design boundary **(Menkiti & Ejimofor, 2016).** There are significant curves in the 3-D plots in **Figures 28(a)** and 2**7(b).** These imply that the interaction of factors was important, which fully matches the outcomes depicted in the pareto graphical **(Figure 27)** of the data.

The related contours in **Figure 28(a)** show how dosage and fast mixing obtained by FFD have an impact on turbidity removal. The reduction of turbidity was shown to be greatly increased when using more powder. Coagulation-flocculation is characterised by fast and slow mixing regimes. Because it helps to cause the production of flocs between the suspended

particles and the coagulant during this mechanism, mixing is crucial **(Shak & Wu, 2014)**. To prevent application accidents such floc breakage, which eventually leads to inadequate turbidity removal, it is crucial for both regimes to determine the ideal mixing speed **(Choong Lek et al., 2018)**.

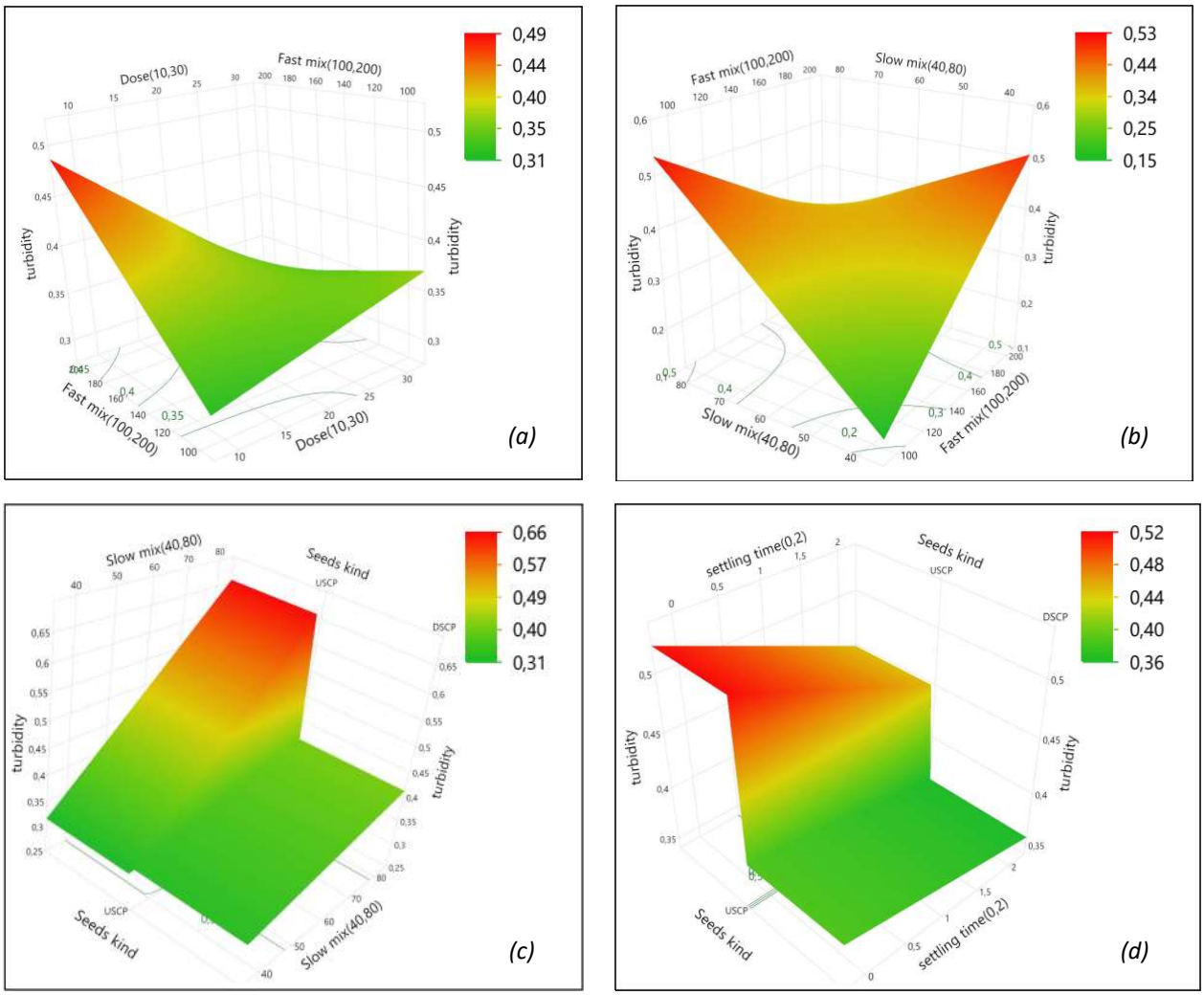

Figure 28. Effect of interactive factors on turbidity removal. ***(a):*** dosage and fast mixing, ***(b):*** fast and slow mixing, ***(c):*** seeds kind and fast mixing, ***(d):*** seeds kind and slow mixing.

The interactions between fast and slow mixing as determined by the FFD model are shown in **Figure 28(b),** along with how they affect the effectiveness of turbidity removal. The semi-concentric contours demonstrate that the interacting pairs of the variables significantly affected the decrease in turbidity in addition to statistically reaching maximum efficiency within an optimal range. It shows that increasing the fast mixing up to 200 rpm, decreased the turbidity removal efficiency. This suggests that slower mixing speeds are more effective at removing turbidity. This may be connected to the necessity of modest mixing speeds to create big flocs with favourable settling qualities **(Kusuma et al., 2021)**. Faster speeds, however, can result in

overmixing, which in turn can shear the flocs too much mechanically and cause them to fragment into smaller pieces. Additionally, vigorous mixing damages the bonds formed during the bridging of the polymer chains, which prevents flocs from forming **(Lee et al., 2012)**. The figure also demonstrates that the slow mix's turbidity reduction decreases with speed over 60 rpm due to inevitable floc disintegration.

The interactive impacts of quick mixing and the type of seeds produced by the FFD model, respectively, on turbidity removal are shown in **Figure 28(c).** According to the response surface plot, turbidity removal is best accomplished when utilising DSCP at all of the measured rapid mixing speeds (100-200 rpm), with a slight drop in turbidity removal efficiency as it approaches high speeds. This might be caused by the simple release of the DSCP protein, which is in charge of coagulation in the case of shelled seeds. The use of USCP under the same conditions of rapid mixing induces low removal of turbidity with slow speeds of stirring. However, increasing the fast mixing rate improves the effectiveness of turbidity removal. This may be the case because the release of useful protein from unshelled seeds needs more energy, implying faster stirring.

Figure 28(d) represents the response surface plot for interactive effects between slow mixing and seeds kind on turbidity removal obtained by FFD model. As seen in the plot, utilising DSCP with all of the tested rapid mixing rates results in an increase in turbidity removal. Utilising USCP at low speeds of slow stirring significantly reduces turbidity. However speeding up slow mixing reduced the effectiveness of removing turbidity. This might be explained by the possibility that increasing stirring rates might help break up the flocs that were created.

2. Modelling and fitting the ANN model

2.1.ANN model architecture

Using the proper weights (w) and biases (b), a prediction model was built by connecting the various layers of the data. **Figure 29** depicts the input-hidden-output interaction's ANN neural architecture. Because the multilayer MFFF network provided the best R^2 and the lowest RMSE value, it was selected as the preferred network architecture. The optimum neural network configuration was obtained as 5-5-5-3 as shown **(Figure 29)**. The outputs of neurons in the input layers serves as inputs to the hidden layers, while the hidden layers' outputs serves as inputs to the output layer, which then produces the desired output **(Menkiti & Ejimofor, 2016)**.

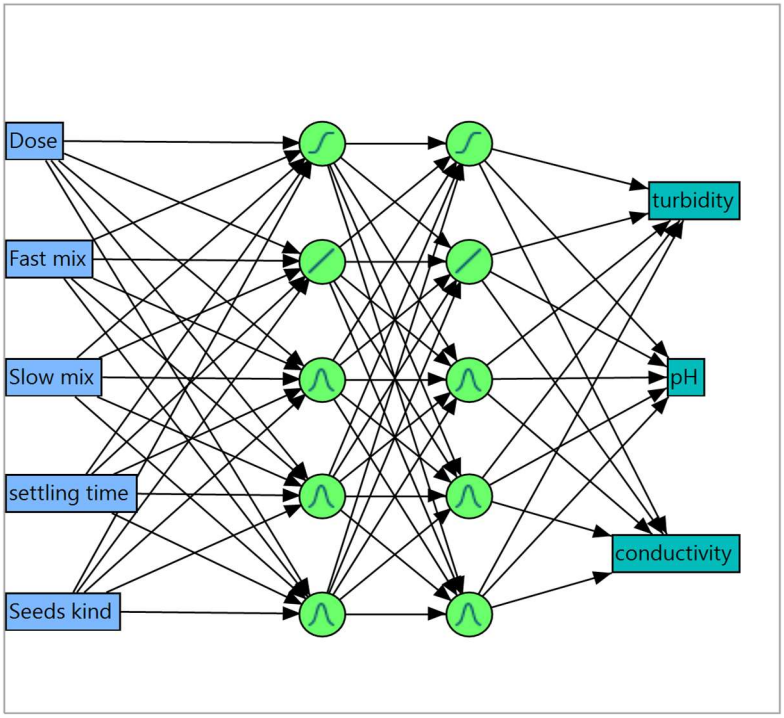

Figure 29. The Artificial Neural Network architecture.

2.2.ANN model fitting

Table 9 provides experimental data for the obtained observed, predicted, and residual values for the ANN model. The acquired data makes it evident that the experimental data, the predicted and the observed values for turbidity removal are very similar. Based on this and on the obtained low residual values, it is shown that the data fit the anticipated model effectively, especially for turbidity removal. Regression analysis could be used to demonstrate this consistency in the results.

The estimation parameters of the derived ANN model for the training, validation, and testing data for turbidity removal, conductivity, and pH fluctuations are shown in **Table 11.** The R^2 values were often significant for removing turbidity but not for pH and conductivity changes. Only turbidity removal was successful in this model investigation. The training, validation, and testing trials revealed that the turbidity model had R^2 values of 0.87, 0.96, and 0.49, respectively. It is clear that the ANN performed exceptionally well at each stage, with the exception of the testing stage, where a decline in R^2 below 0.9 points to a poor model fit at this point. This demonstrates that there isn't enough information to test the network. 15% of the learning option for testing seems insufficient for adequate network testing.

As soon as the error began to increase, network training was halted. In **Table 11**, the values for the Root Mean Square Error (RMSE) are shown. For the training, validation, and testing stages, the RMSE for turbidity reduction was 0.03; 0.12; and 0.14, respectively. This indicates that the neural network has performed well at every stage. The correlation between the target and the anticipated responses is also measured by this metric. The correlation between the target (experimental turbidity removal) and the output (ANN predicted turbidity removal) is frequently associated with the RSME value being less than 3 (**Ejimofor et al., 2021)**. It demonstrates the striking resemblance between the ANN predictions and the actual experimental outcomes, which are shown in **Table 9**. It also shows how accurate and reliable the ANN model's predictions are. The accuracy of the ANN model was also evaluated using error functions (RMSE= 0.03, MSE = 0.0009, MAE = 0.050). These values indicate good accuracy of the obtained model.

Table 11. Estimation parameters of the ANN model for training, validation, and testing data.

	Training			Validation			Testing		
	turbidity	pH	Conductivity	turbidity	pH	Conductivity	turbidity	pH	Conductivity
R^2	0.87	-0.05	0.42	0.96	-0.15	-0.35	0.49	0.04	-0.73
RMSE	0.03	7.08	0.12	0.06	10.57	0.14	0.12	9.76	0.13
Log-likelihood	-33.92	84.42	-17.21	-9.08	18.88	-2.63	8.62	18.48	-3.00
MSE	0.0009	50.12	0.014	0.003	111.72	0.0196	0.0144	95.84	0.016
MAE	0.050	6.01	0.11	0.103	9.22	0.12	0.221	8.54	0.23

2.3. ANN model prediction

The predicted and the obtained experimental values of turbidity removal in the all stages of the ANN modelling are compared in **Figure 30.** A strong connection between the acquired and the experimental data is indicated by the R^2 values achieved in the training and validation stages (0.87 and 0.96, respectively). This illustrates how well the model captured the real link between the elements that were selected.

The path for solution displays the scaled log-likelihood plotted against the number of steps. **Figure 31** shows the path for solution plot. It indicates which of our models is the most effective using the scaled negative log probability statistic. What is occurring with the validation set is shown by the black line. The grey line depicts what is occurring with the training set, and it is clear that there is a point at which the lowest value is received on the validation set. The red line, displays the ideal network conditions for training and network validation established based on the scaled log-likelihood. It serves as an example of this value. The validation set will remain

unchanged after this point. This is regarded as a great approach to investigate model over- and under-fitting. Here, step number 7 produced the best validation results.

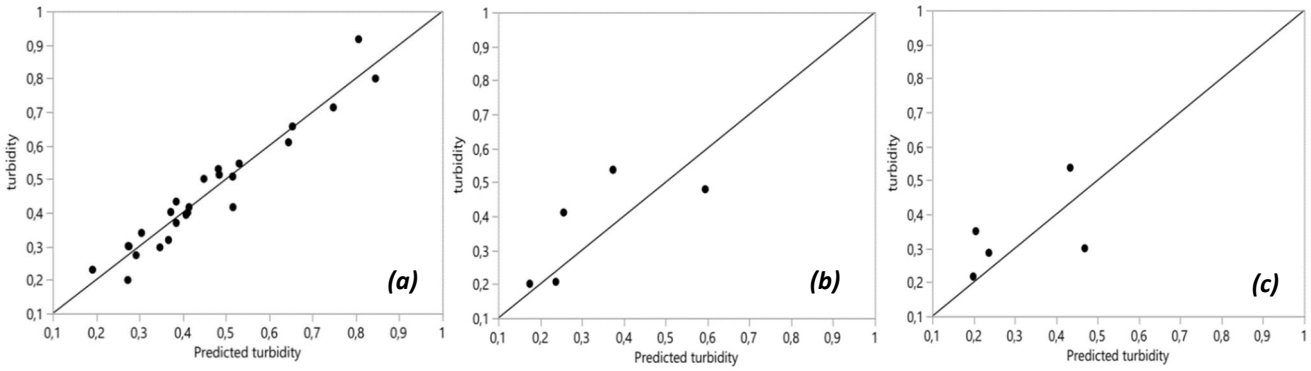

Figure 30. Observed values against expected values in the different stages of the ANN modelling for turbidity removal. *(a): training, (b): validation, (c): testing*.

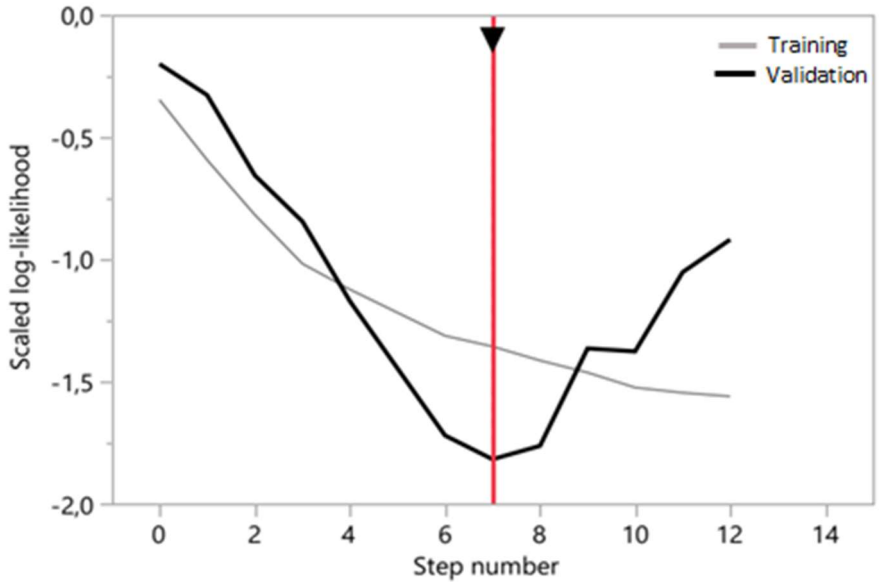

Figure 31: Path for solution plot.

2.4. Effects of input variables on turbidity removal

It was discovered that the ANN response surface plots and those produced by the FFD model were very similar. To determine the impact of the inputs on turbidity removal, the ANN model additionally examined the interactions provided by the FFD model.

The associated contours obtained by the ANN approach are highly similar to those obtained by the FFD model. **Figure 32 (a)** indicates that the influence of dosage and fast mixing on turbidity removal obtained. Higher doses of *MO* seeds powder increase significantly the turbidity removal.

Figures 32(b) shows the interactions between fast and slow mixing obtained by the ANN model and its impact on turbidity removal efficiency. It demonstrates that lowering the rapid mixing speed to 200 rpm reduces the effectiveness of turbidity reduction. This means that slower mixing speeds work better for removing turbidity. This may be related as indicated by **Kusuma et al (2021)** that the requirement of moderate mixing speeds to produce large flocs with good settling properties. The figure also demonstrates how increasing the slow mixing's speed above 60 rpm causes the final floc breakdown to occur at a lower rate, which in turn results in less turbidity removal.

Figure 32(c) demonstrates the obtained interactive effects between fast mixing and seeds kind ANN model on turbidity removal. With all tested rapid mixing speeds (100-200 rpm), turbidity removal is best accomplished when utilising DSCP, with a slight drop in turbidity removal effectiveness as it approaches high speeds. This is probably due to the simple release of the protein responsible of coagulation in the case of DSCP. However, the use of USCP under the same conditions of rapid mixing induces low removal of turbidity with slow speeds of stirring. In contrast, increasing fast mixing could increase turbidity removal efficiency.

Figure 32(d) represents the response surface plot for the obtained interactive effects of slow mixing and seeds kind by ANN model, on turbidity removal. The plot shows that employing DSCP with all of the evaluated rapid mixing rates results in an increase in turbidity removal, as well as for the FFD model plot. While raising the rate of slow mixing had decreased the efficiency of removing turbidity, using USCP at low speeds of slow stirring significantly reduces turbidity. Increasing the stirring speed may help break the created flocs, which could help to explain this.

3. Comparison of FFD and ANN performance

The performance of the RSM and ANN models was evaluated in order to determine which model would be more useful for simulating the turbidity removal process. The ideal conditions are shown in **Table 12**, and the optimal turbidity reduction percentage was computed in the experimental field and in the anticipated data using FFD and ANN. When these settings were used, the experimental field's percentage of turbidity removal was 90.42%, although the FFD and ANN data acquired indicated removal percentages of 90.71 and 92.33%, respectively. The results of turbidity removal obtained experimentally were quite similar to those obtained using both FFD and ANN models. The results obtained by **Gideon and Clinton (2010),** who reported that turbidity removal effectiveness was in the range of 94% or higher, when the coagulant dose

is above 5ml per 1000ml sample volume, are aggregated with the FFD results. These outcomes are also quite similar to those reported by **Gidde et al (2012),** who discovered that shelled mixed *MO* coagulant could remove 76.45% of turbidity at an ideal dosage of 70 mg/L, while dosages of 120 mg/L and 240 mg/L could do the same for 92.33% and 97.7% of turbidity, respectively.

Table 12. FFD and ANN optimal coagulation-flocculation parameters and their efficiency on turbidity removal.

Coagulant dosage (ml)	Fast mixing (rpm)	Slow mixing (rpm)	Settling time (min)	Seeds kind	Turbidity removal efficiency FFD (%)	Turbidity removal efficiency ANN (%)	Experimental Turbidity removal efficiency (%)
10	150	60	60	DSCP	90.71	92.33	90.42

In terms of modelling the turbidity reduction process, both models showed significant modelling capabilities. However, the ANN model definitely outperformed the RSM model as seen by the significantly higher R^2 and modified R^2 values, which signify a better model fit. The ANN model performs better, as evidenced by the error function (RMSE= 0.03, MSE = 0.0009, MAE = 0.050) used to compare the accuracy of the two models.

Since the ANN predictions were more precise than the actual experimental values, the results given in Table 1 also reflect this circumstance. According to **Kusuma et al (2021),** the ANN model deserves to be used since it provides a more accurate depiction of the actual coagulation-flocculation conditions. This shows that in the context of the current study, the ANN model was successful in reproducing the actual experimental settings and in making predictions that were remarkably similar to those of the actual experiments. The model's anticipated removal efficiencies, as shown in **Table 12,** closely matched those of the actual experiment, proving the model's validity.

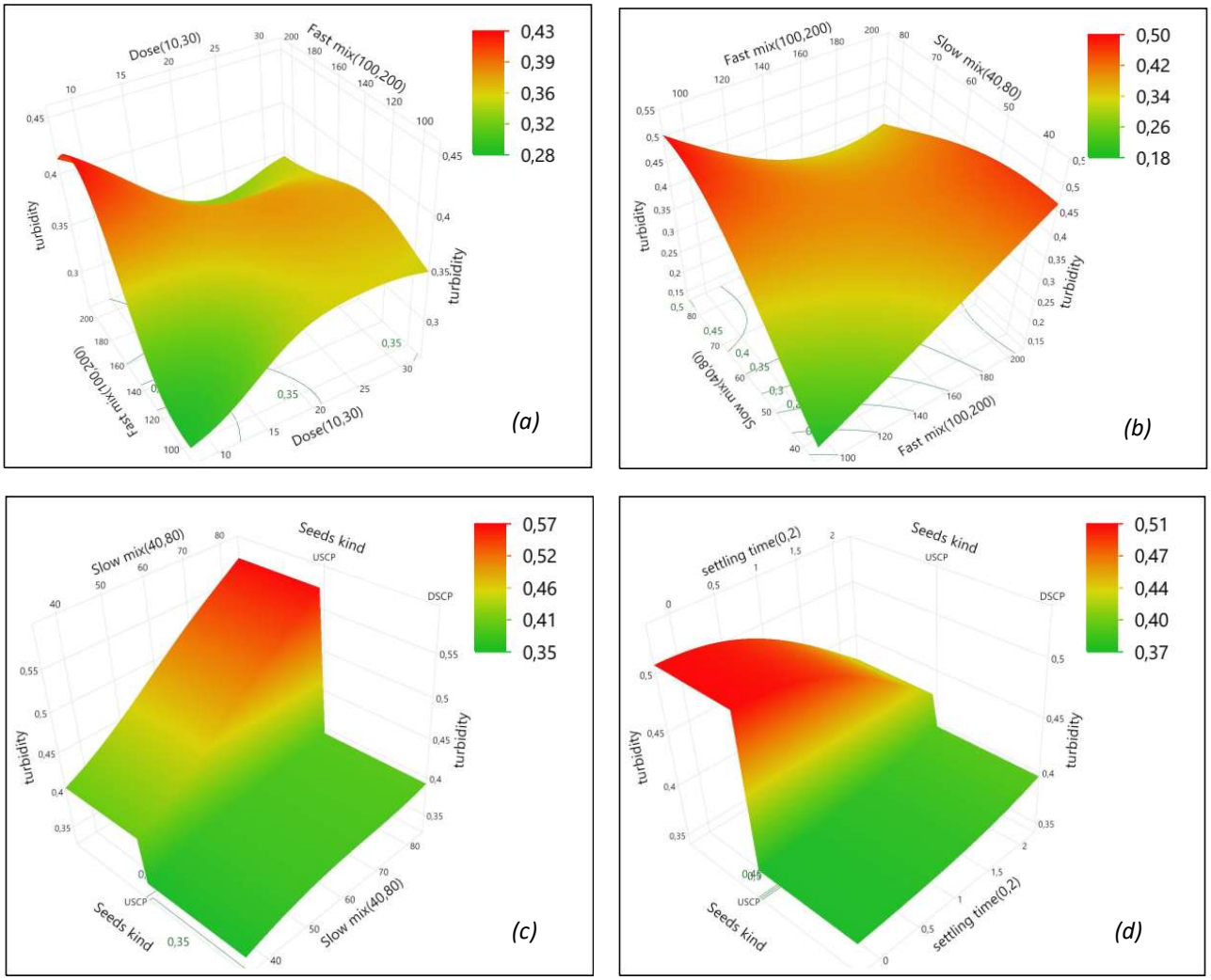

Figure 32: The input effects on turbidity removal. ***(a):*** dosage and fast mixing, ***(b):*** fast and slow mixing, ***(c):*** seeds kind and fast mixing, ***(d):*** seeds kind and slow mixing.

Chapter II

Application in wastewater treatment

1. Introduction

In part B of the first section; the obtained results during the experimental work are presented and discussed in details. The coagulation-flocculation parameters applied with *MO-DS* and *MO-NDS* powders were optimized using the RSM and ANN approaches. In this section validation for generalization on other responses using the obtained optimal values were recovered. This work's first focus is solely on recovering a natural waste in order to safeguard the environment. This might be considered a breakthrough in the field of valorization because it has been found that the treatment and valorization of natural waste has financial benefits due to its low cost of operation, ease of use, and low energy requirements.

The purpose of this work is to (i) investigate whether dehulled and unhulled *MO* seeds can be used to achieve the field's highlighted objectives by utilising seeds waste in wastewater treatment, (ii) implement mathematical models that explain the ideal conditions of the coagulation-flocculation process, and (iii) investigate the generalizability of the resulting models on other parameters on a stationary scale.

2. The application of RSM

2.1.Preliminary trials

The preliminary study shows the results of the single-factor experiments carried out for preliminary optimisation. The results are expressed as TSS content. The tests performed under optimal conditions have the lowest TSS content. The obtained results are illustrated in **Figure 33** showing the TSS content in the inlet (IW) and outlet waters (OW) of the Sidi Ali Lebhar WWTP treated with *MO-DS* and *MO-NDS* seeds cake powder solutions.

The comparison of the obtained concentrations of TSS shows a better efficiency when using *MO-DS*, compared to *MO-NDS.* This could be due to the higher protein content of the *MO-DS* seeds cake powder compared to the *MO-DS* seeds cake powder. According to **Gassenschmidt et al (1995),** this protein is the essential element to ensure a good coagulation-flocculation targeting the suspended pollutants in water. The TSS values in this first stage are

within the margin of acceptability, which does not exceed 35mg/l for treated water at the inlet and the outlet of the WWTP with both preparations of *MO* seeds cake powder.

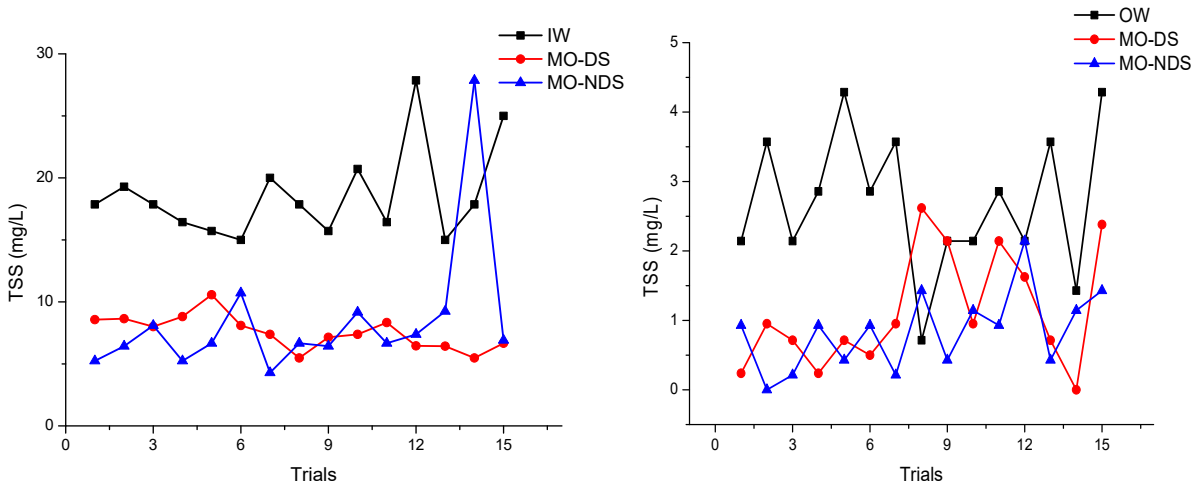

Figure 33. Response to the treatment measured by TSS content

(a): *MO-DS* and *MO-NDS* powders at the IW and ***(b):*** *MO-DS* and *MO-NDS* powder at the OW.

Through the preliminary results for TSS removal, the utilized factors in the rest of the study were set. **Table 13** shows the range of parameter set values at the end of the preliminary tests.

Table 13. Factors and levels for BBD (in coded and uncoded levels) at IW and OW.

	Symbols	**IW**			**OW**		
Level		-1	0	+1	-1	0	+1
Dose (ml)	X1	70	80	90	60	70	80
Fast mixing (rpm)	X2	100	150	200	100	150	200
Low mixing (rpm	X3	20	40	60	20	40	60

2.2.Box-Benken design set up

2.2.1. Modelling and fitting the model using RSM

RSM was used to determine the link between variables and response. **Tables 14** and **15** show the findings of BBD experimental data for the observed, predicted, and residual values obtained after water treatment in the IW and OW, respectively including runs. It is very clear from both tables that the predicted response values are nearly identical to the experimental data. The low values of residuals, demonstrated in **Tables 14** and **15** show that the experimental data fitted well to the model. At this stage, the high agreement between the real and the predicted

values demonstrated that the regression model's response was sufficient to reflect the desired optimization **(Zhang et al., 2013).**

Figure 34 represents the scattering of the experimental and predicted plots for TSS removal in the IW and OW of the WWTP. From various available response models representing the interactions of the variable factors, the most acceptable model was chosen.

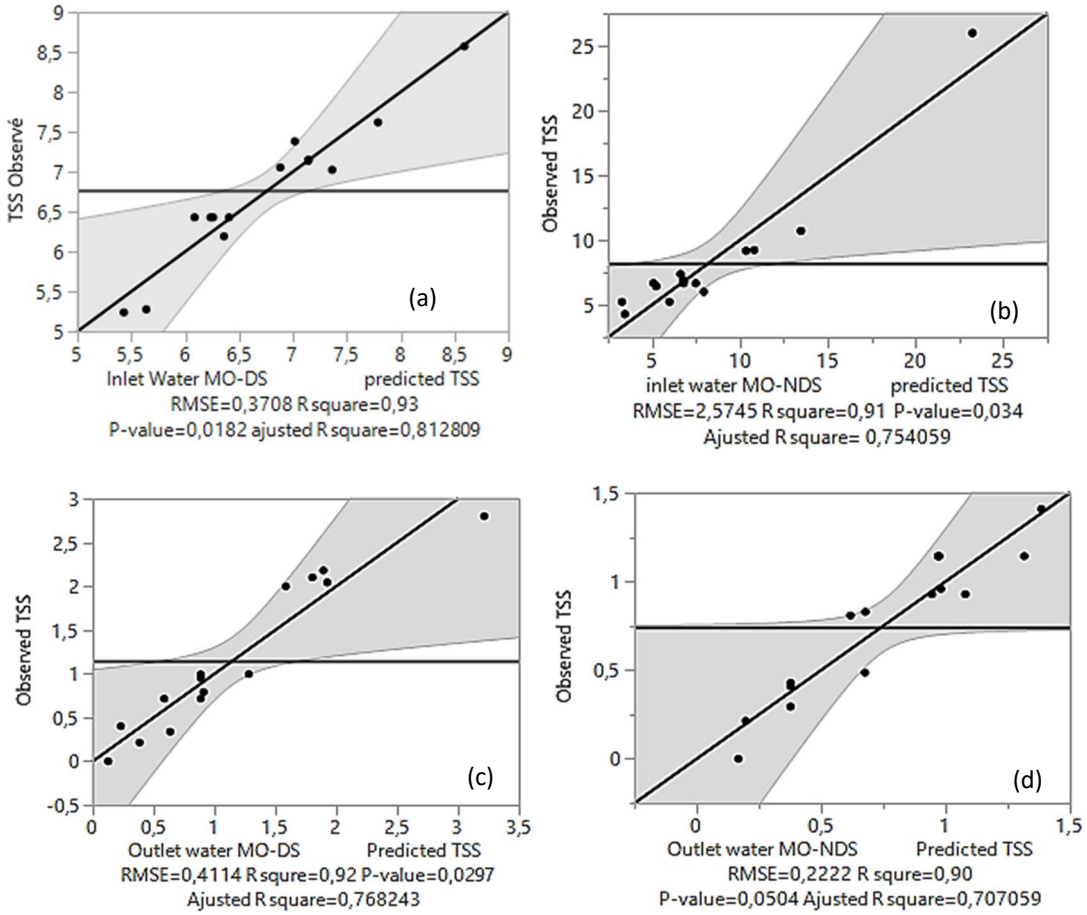

Figure 34. Experimental VS predicted values for suspended solids.

(a) IW-MO-DS treatment, (b) IW-MO-NDS treatment, (c) OW-MO-DS treatment, (d) OW-MO-NDS treatment.

Table 14 The experimental data for observed, predicted and residuals, for the RSM and ANN models, at the IW.

Run	Experimental factors	***MO-DS***					***MO-NDS***				
		Observed TSS	RSM Predicted TSS	ANN predicted TSS	RSM Residual	ANN residual	Observed TSS	RSM predicted TSS	ANN predicted TSS	RSM Residual	ANN residual
1	+ − 0	8.57	8.63	8.22	-0.060	-00.56	05.24	03.06	05.51	2.17	1.15
2	0 + −	6.43	6.23	6.37	-0.194	-00.13	06.01	08.18	06.22	2.17	-0.99
3	− − 0	6.43	6.34	6.64	-0.089	-01.63	06.90	06.79	06.36	-0.11	-0.35
4	0 − +	7.02	7.69	7.22	0.670	-00.80	05.24	05.99	06.13	0.76	0.30
5	0 + +	5.24	5.40	5.16	0.164	00.75	06.67	04.85	06.17	-1.81	0.73
6	0 0 0	7.14	7.14	7.49	0.000	02.22	10.71	13.94	10.64	3.23	0.07
7	+ 0 +	7.38	7.13	7.82	-0.253	19.18	04.29	03.23	26.02	-1.05	-0.02
8	− 0 −	5.28	5.73	5.03	0.453	02.13	06.67	07.72	09.30	1.05	-0.14
9	0 0 0	7.14	7.14	7.30	0.000	00.51	06.43	05.01	06.17	-1.42	0.64
10	+ + 0	6.19	6.28	6.38	0.090	01.00	09.17	10.58	07.81	1.41	-0.42
11	0 − −	6.43	6.23	6.37	-0.194	00.30	06.81	06.79	06.16	-0.02	0.51
12	+ 0 −	7.62	7.72	7.41	0.104	-01.18	07.38	06.62	05.34	-0.76	-0.10
13	− + 0	6.43	6.37	6.25	-0.059	-00.96	09.24	11.05	04.91	1.81	-0.62
14	− 0 +	7.05	6.92	7.18	-0.134	-00.51	25.99	24.63	06.17	-1.37	0.49
15	0 0 0	7.14	7.14	7.22	0.000	02.01	06.67	06.79	09.97	0.13	-0.73

Table 15 The experimental data for observed, predicted and residuals, for the RSM and ANN models, at the OW.

Run	Experimental factors	***MO-DS***					***MO-NDS***				
		Observed TSS	RSM Predicted TSS	ANN predicted TSS	RSM Residual	ANN residual	Observed TSS	RSM predicted TSS	ANN predicted TSS	RSM Residual	ANN residual
1	+ − 0	0.338	0.690	2.25	-0.352	-01.91	0.829	0.723	01.13	0.106	-00.30
2	0 + −	0.792	1.095	0.73	0.303	00.05	0	0.196	0.196	0.196	-0.196
3	− − 0	0.994	1.167	0.73	0.173	00.25	0.294	0.357	0.723	0.063	-00.42
4	0 − +	2.100	1.929	0.15	-0.171	01.94	0.485	0.705	01.43	0.220	-00.94
5	0 + +	0.714	0.873	1.06	0.159	-00.35	0.809	0.652	00.22	-0.157	00.58
6	0 0 0	0.400	0.190	1.81	-0.210	-01.40	0.929	0.920	01.01	-0.009	-00.07
7	+ 0 +	0.952	0.873	0.02	-0.079	00.92	0.214	0.223	01.34	0.009	-01.13
8	− 0 −	2.800	3.216	2.84	0.416	-00.03	1.409	1.348	00.65	-0.061	00.75
9	0 0 0	1.999	1.548	1.92	-0.451	00.08	0.409	0.357	00.36	-0.052	00.05
10	+ + 0	0.992	0.873	0.73	-0.119	00.25	1.143	0.946	00.92	-0.197	00.22
11	0 − −	2.049	2.001	0.81	-0.048	01.23	0.959	1.009	00.95	0.050	00.01
12	+ 0 −	0.214	0.524	0.38	0.310	-00.17	0.929	1.134	00.36	0.205	00.57
13	− + 0	0.714	0.573	2.27	-0.141	-01.55	0.429	0.357	00.71	-0.072	-00.27
14	− 0 +	0	0.143	1.15	0.143	-01.15	1.143	1.143	01.14	0	0.001
15	0 0 0	2.181	1.928	0.22	-0.253	01.95	1.143	1.143	00.36	0	00.78

Table 16 and **17** illustrate the estimated regression coefficients for the quadratic polynomial models and the analysis of variance **(ANOVA)** for the experimental results and the results of test of significance for every coefficient of regression for the IW and the OW, respectively. It is claimed at last, that for each model and depending on the type of the utilized seeds cake powder, the significant interactions change. The model's quality was assessed using statistical indices such as R^2, adj-R^2, *p*-value, estimated coefficient, degree of freedom (Df), standard error, sum of squares, Root Mean Squared Error (RMSE), Mean Squared Error (MSE), Mean Absolute Error (MAE) and Mean Absolute Percent Error (MAPE). It was reported by **Karazhiyan et al (2011)** that the models failed to reflect the data in the experimental domain when points were not included in the regression, as evidenced by a significant lack of fit. The **ANOVA** test showed that lack of fit was not significant for all response surface models at a 95% confidence level, which indicates that both models reflected the data adequately**.**

Table 16 Estimated regression coefficients for the quadratic polynomial model and the analysis of variance (ANOVA) for the experimental results at the IW.

	IW									
	MO-DS					**MO-NDS**				
	Estimated coefficient	**Sum of Squares**	**Df**	**Standard error**	***p*-value**	**Estimated coefficient**	**Sum of Squares**	**Df**	**Standard error**	***p*-value**
Intercept	7.143			0.214		6.794			1.486	
Linear										
X1	0.572	2.616	1	0.131	0.007	-2.596	53.926	1	0.910	0.036
X2	-0.521	2.170	1	0.131	0.011	-2.283	41.687	1	0.910	0.054
X3	0.118	0.111	1	0.131	0.409	0.270	0.582	1	0.910	0.779
Interaction										
X1X2	-0.595	1.417	1	0.185	0.024	6.024	145.144	1	1.287	0.005
X1X3	-0.504	1.016	1	0.185	0.042	-1.165	5.424	1	1.287	0.407
X2X3	-0.446	0.797	1	0.185	0.061	-1.161	5.389	1	1.287	0.409
quadratic										
$X1^2$	0.157	0.091	1	0.193	0.452	2.845	29.892	1	1.340	0.087
$X2^2$	-0.395	0.577	1	0.193	0.096	2.694	26.804	1	1.340	0.101
$X3^2$	-0.468	0.808	1	0.193	0.060	-2.851	30.014	1	1.340	0.086
Lack of fit		0.687	3				33.112	3		
Pure error		0.000	2				0.029	2		
R^2			0.93					0.91		
adj-R^2			0.81					0.75		
RMSE			0.37					2.57		
MSE			0.13					6.60		
MAE			0.16					1.28		
MAPE			2.56					17.73		

For the IW-*MO-DS* model, the *p*-value of X_1, X_2, X_1X_2 , X_1X_3 was significant at 95% confidence level ($p < 0.05$). The mathematical equation for TSS removal related to this model, including significant and non-significant terms is given by (Eq.13):

$$y_{Iw-MO-DS} = 7{,}143 + 0{,}572\,X_1 - 0{,}521X_2 + 0{,}118X_3 - 0{,}595X_1X_2 - 0{,}504X_1X_3 - 0{,}446X_2X_3 + 0{,}157X_1^2 - 0{,}395X_2^2 - 0{,}468X_3^2 \quad \text{(Eq.13)}$$

For the IW- *MO-NDS* model, only the *p*-value of X_1 and X_1X_2 interaction was significant at the same confidence level ($p < 0.05$). The mathematical equation for TSS removal in the IW-*MO-NDS* model, including significant and non-significant terms is given by (Eq.14):

$$y_{Iw-MO-NDS} = 6{,}794 - 2{,}596X_1 - 2{,}283X_2 + 0{,}270X_3 + 6{,}024X_1X_2 - 1{,}165X_1X_3 - 1{,}161X_2X_3 + 2{,}845X_1^2 + 2{,}694X_2^2 - 2{,}851X_3^2 \quad \text{(Eq.14)}$$

On the other hand, **Table 17** represents the estimated coefficients of regression for the quadratic polynomial model and the analysis of variance **(ANOVA)** for the experimental results of the OW.

Table 17 Estimated regression coefficients for the quadratic polynomial model and the analysis of variance (ANOVA) for the experimental results at the OW.

	OW									
	MO-DS					**MO-NDS**				
	Estimated coefficient	**Sum of Squares**	**Df**	**Standard error**	***p*-value**	**Estimated coefficient**	**Sum of Squares**	**Df**	**Standard error**	***p*-value**
Intercept	0.886			0.238		0.377			0.128	
Linear										
X1	0.369	1.088	1	0.145	0.052	-2.596	0.106	1	0.079	0.203
X2	-0.139	0.154	1	0.145	0.383	-2.283	0.059	1	0.079	0.324
X3	0.445	1.587	1	0.145	0.028	0.270	0.665	1	0.079	0.014
Interaction										
X1X2	-0.530	1.125	1	0.206	0.050	6.024	0.054	1	0.111	0.345
X1X3	1.046	4.380	1	0.206	0.004	-1.165	0.327	1	0.111	0.050
X2X3	0.184	0.136	1	0.206	0.412	-1.161	0.375	1	0.111	0.040
quadratic										
$X1^2$	-0.024	0.002	1	0.214	0.914	2.845	0.123	1	0.116	0.175
$X2^2$	0.025	0.002	1	0.214	0.910	2.694	0.152	1	0.116	0.139
$X3^2$	0.492	0.892	1	0.214	0.070	-2.851	0.326	1	0.116	0.050
Lack of fit		0.801	3				0.236	3		
Pure error		0.045	2				0.010	2		
R^2			0.92					0.90		
adj-R^2			0.77					0.70		
RMSE			0.41					0.22		
MSE			0.16					0.04		
MAE			1.17					0.74		
MAPE			106.02					92.96		

For the OW-*MO-DS* model, the *p*-value was clearly significant only for X_3. The X_1X_2 and X_1X_3 interactions were highly significant at a 95% confidence level ($p < 0.05$). The mathematical equation for TSS removal related to the model is given by (Eq.15):

$$y_{Ow-MO-DS} = 0{,}886 + 0{,}369\,X_1 - 0{,}139\,X_2 + 0{,}445X_3 - 0{,}530X_1X_2 + 1{,}046X_1X_3 + 0{,}184X_2X_3 - 0{,}024\,X_1^2 + 0{,}025X_2^2 + 0{,}492X_3^2 \quad \text{(Eq.15)}$$

Whereas, for the OW-*MO-NDS* model, results showed a significant *p*- value for X_3, X_1X_3, X_2X_3 and X_3^2 at the same confidence level ($p < 0.05$). The mathematical equation for TSS removal in the outlet water *MO-NDS* model is given in (Eq.16):

$$y_{ow-MO-NDS} = 0{,}377 - 2{,}596X_1 - 2{,}283X_3 + 0{,}270\,X_3 + 6{,}024X_1X_2 - 1{,}165\,X_1X_3 - 1{,}161\,X_2X_3 + 2{,}845X_1^2 + 2{,}694X_2^2 + 2{,}851X_3^2 \quad \text{(Eq.16)}$$

It is claimed at last, that for each model and depending on the type of starting wastewater treated and the type of cake powder used, the significant interactions change.

As it was reported by **Guan and Yao (2008),** the value of R^2 should be at least 0.80 for a good-fitted model. This is useful for understanding the model's variability and obtaining a well-fitted model. It is clearly shown in **Figure 34,** representing experimental and predicted plots for TSS, that the coefficient of determination is greater than or equal to 0.90 for each model, at the rates of 0.93, 0.91, 0.92, 0.90 for the IW-*MO-DS,* IW- *MO-NDS*, OW-*MO-DS* and OW-*MO-NDS,* respectively. This indicates that the models are well-fitting, with the independent factors accounting for more than 90% of the dependent variable's sample variance and the independent factors accounting for only 10% of the total variation models.

Karazhiyan et al (2011) have reported that the models failed to reflect the data in the experimental domain when points were not included in the regression, as evidenced by a significant lack of fit. The **ANOVA** showed that lack of fit was not significant for all response surface models at a 95% confidence level, which indicates that all the models reflected the data adequately. For a solid statistical model the adjusted R^2 should be close to calculated R^2 (**Zhang et al., 2013).** This was the case for all models, especially for the *MO-DS* coagulant model **(Table 16** and **17)**

Other than regression and mathematical models for both coagulants, the comparison between the obtained models was also designed using several error functions. The *IW-MO-DS* model presented lower error values (MSE = 0.13, RMSE = 0.37, MAE = 0.16 and MAPE = 2.56) compared to *IW-MO-NDS* model (MSE = 6.60, RMSE = 2.57, MAE = 1.28 and MAPE = 17.73). This indicates that the *IW-MO-DS* model has better accuracy. However, the *OW-MO-DS* model presented better performance (MSE = 0.16, RMSE = 0.41, MAE = 1.17 and

MAPE = 106.02) than the *OW-MO-NDS* model (MSE = 0.04, RMSE = 0.22, MAE = 0.74 and MAPE = 92.96).

Given that the lower MAE value, the better the model predicted. However, the relationship between MAE values and how good a model performs depends on the data. Regarding the MAPE values, indicating the sum of the individual absolute forecast errors, divided by the actual values for each period. It's an accuracy measure based on the relative percentage of errors. The closer the MAPE value is to zero, the better the predictions is. This was the case only for the *IW-MO-DS* treatment. It is then the better performed model.

1.1.1. Analysis of the response surface model

The interactive effects of the independent variables and their mutual interactions on the TSS removal efficiency can also be observed on the three-dimensional response surface profiles of multiple non-linear regression models. Only significant interactions obtained by the model were presented on the plots.

Coagulation-flocculation is characterised by fast and slow mixing regimes. Because it helps to induce the production of flocs between the suspended particles and the coagulant during this mechanism, mixing speed determination is crucial **(Shak &Wu, 2014). Figure 34(b)** and **Figure 35(b')** show the effect of slow mixing and *MO-DS* and *MO-NDS* dosage, respectively on TSS removal. The Figures show that increasing the speed of the slow mix above 60 rpm contributes to the decrease in TSS removal by eventual floc breakdown.

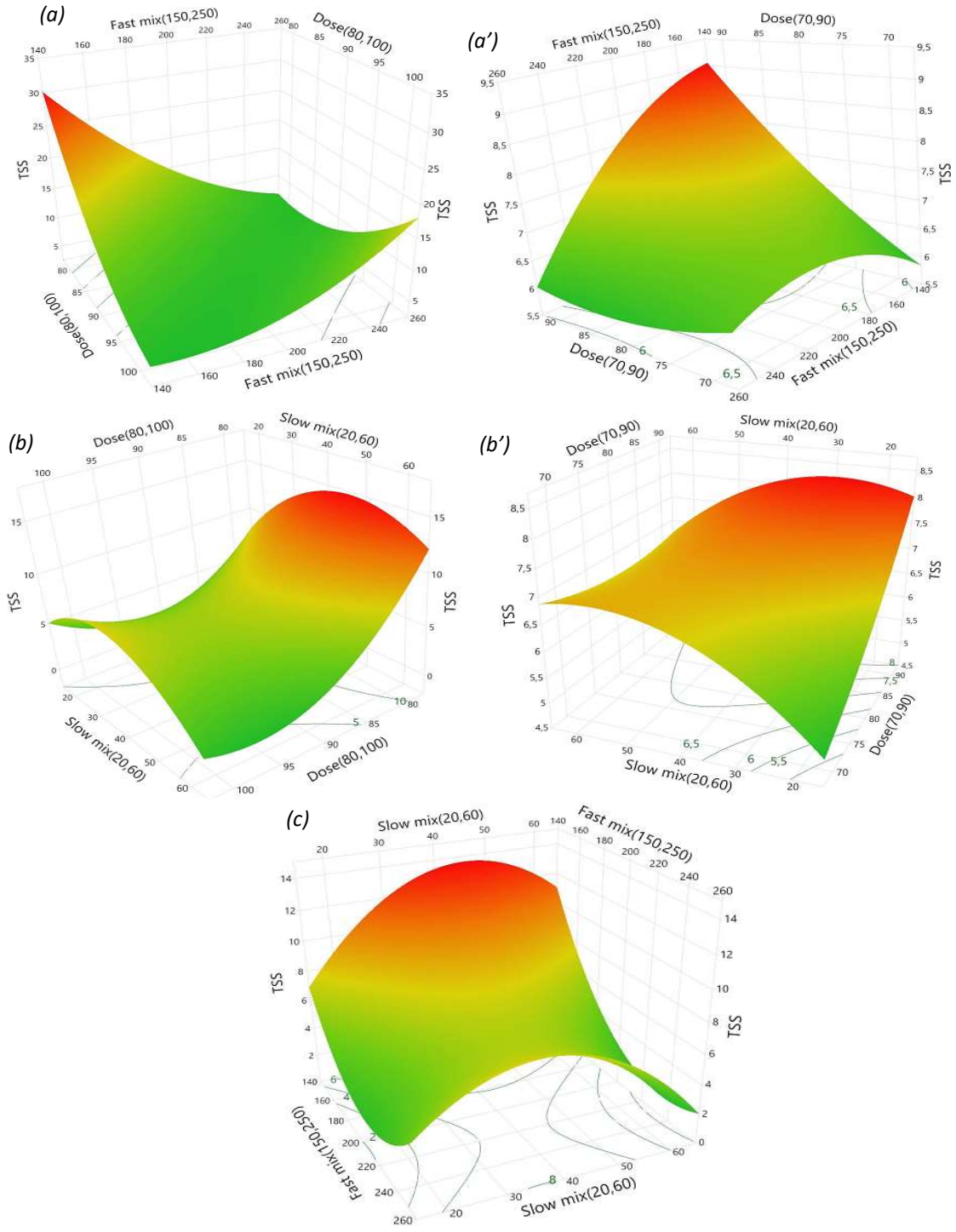

Figure 35. RSM interactive effects of operational parameters on the TSS removal at the IW.

(a): MO-NDS dosage and fast mixing, *(b): MO-NDS* dosage and slow mixing, *(c):* fast and slow mixing in *MO-NDS* treatment, *(a'): MO-DS* dosage and fast mixing, *(b'): MO-DS* dosage and slow mixing.

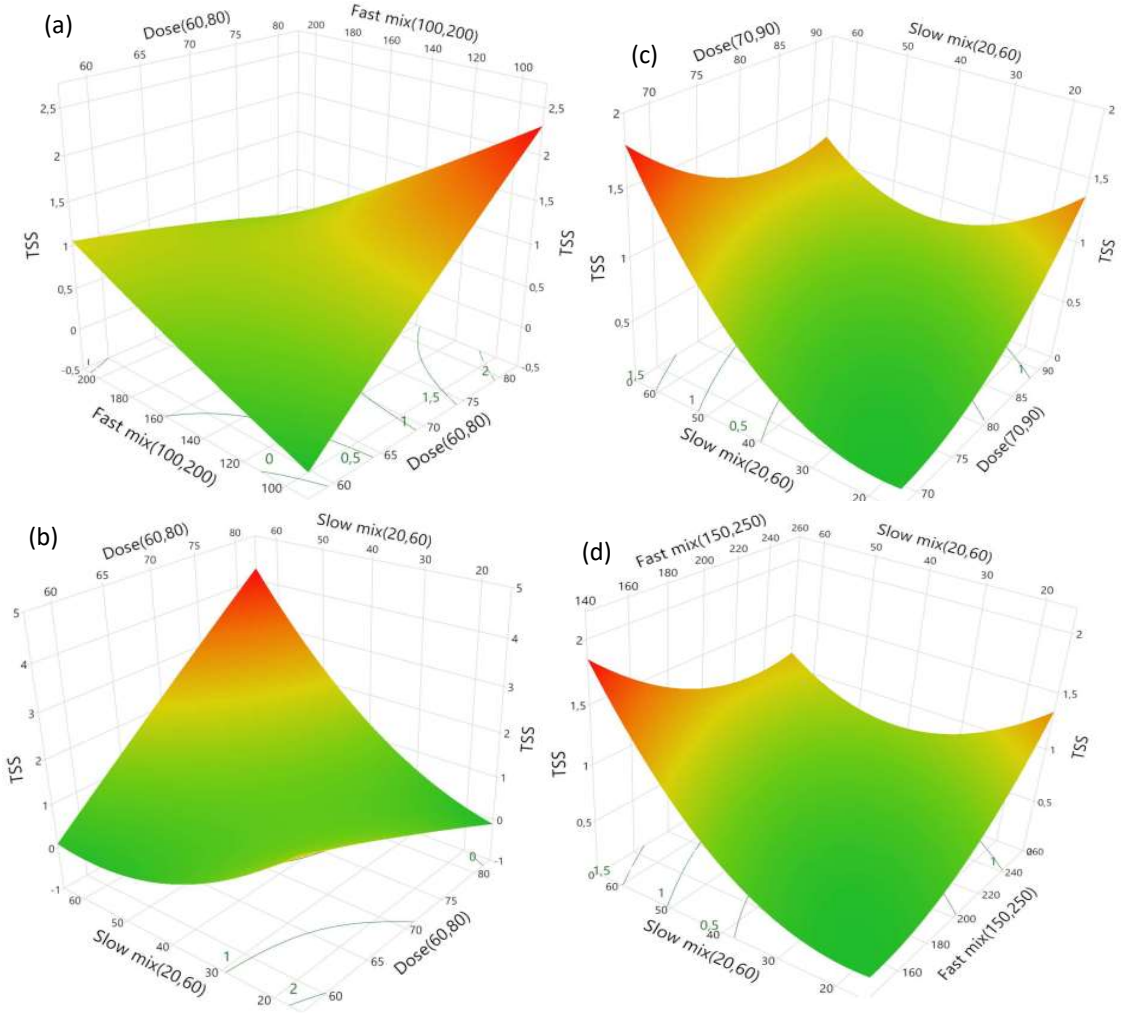

Figure 36. RSM interactive effects of the operational parameters on TSS removal at the OW.

(a): MO-DS dosage and fast mixing, *(b): MO-DS* dosage and slow mixing, *(c): MO-NDS* dosage and slow mixing, *(d):* fast and slow mixing in *MO-NDS* treatment.

Figure 35(a) and **Figure 35(a')** illustrate the effect of fast mixing and both coagulants dosage on TSS removal. This reveals that increasing the *MO* seeds cake powder dosage could reduce TSS removal. However, decreasing fast mixing and *MO* seeds cake powder dosage under the optimal values could increase TSS removal. TSS removal is widely decreased by decreasing dosage and fast mix, while decreasing fast mixing and increasing dosage could in contrast increase TSS removal. These findings are consistent with those obtained in the preliminary investigation whereby, according to the type of preparation of *MO* seeds, increasing or decreasing the *MO* seeds cake powder dosage combined with a well-determined fast and slow agitation could lead to a good TSS removal (in the range). The interaction between fast and slow mixing as shown in **Figure 35(c)** demonstrates that the combination of different ranges of fast

and slow mixing give a good process performance. It illustrates that speeds not exceeding 200 rpm performed well in reducing the TSS content, especially when combined with slow mixing in the vicinity of 40rpm. The same observations were detected on the OW plots with its specific optimal conditions **(Figure 36).**

2. The application of the ANN design

2.1.ANN models architecture

The various data layers are connected with the appropriate biases and weights to create a prediction model. **Figure 37** depicts the ANN neural network for the interaction between input and hidden output. The optimum neural network configuration was obtained as 3-5-5-1. The experimental data for the observed, predicted, and residual values obtained with the ANN model at the IW and the OW, are illustrated in **Table 14** and **15.** The collected data clearly show that the experimental results, as well as the predicted and actual values for TSS elimination, are highly close. The results fit the expected model well, especially for TSS removal and in the BBD model, as evidenced by the low residual values.

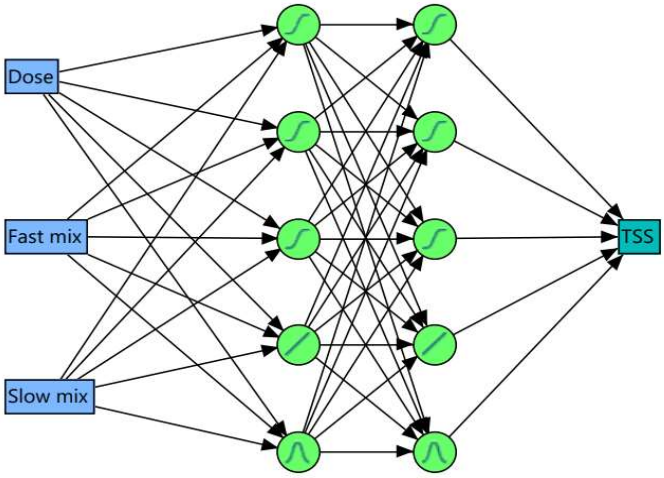

Figure 37. The ANN architecture.

2.2. ANN models analysis

Table 18 represents the estimation parameters of the obtained ANN model for training and validation data set for TSS removal at the inlet and the outlet of the plant. At each level (training and validation), the network system's accuracy was evaluated using the R^2 values. TSS removal was found to have a R^2 value of 0.99 and 0.96 for *MO-DS* and *MO-NDS*, respectively in training and 0.86 and 0.84 for *MO-DS* and *MO-NDS*, respectively in validation trials. However, at the outlet of the plant the obtained models had a coefficient of regression R^2 of 0.99 and 0.96 for

MO-DS and *MO-NDS*, respectively in training and 0.96 and 0.80 for *MO-DS* and *MO-NDS,* respectively in validation trials.

Table 18. Estimation parameters of the ANN model for training and validation data.

	IW				OW			
	MO-DS		***MO-NDS***		***MO-DS***		***MO-NDS***	
	Training	**Validation**	**Training**	**Validation**	**Training**	**Validation**	**Training**	**Validation**
R^2	0.99	0.86	0.96	0.84	0.99	0.96	0.96	0.80
RMSE	0.054	0.19	1.09	0.78	0.05	0.145	0.08	0.05
MSE	0.0029	0.036	1.19	0.61	0.0025	0.021	0.0064	0.0025
Log-likelihood	-17.94	-0.71	16.61	4.71	-15.46	-2.023	-12 .06	-6.09
SSE	0.035	0.108	13.22	2.47	0.038	0.085	0.07	0.01
MAE	0.03		0.48		1.14		0.76	
MAPE	2.99		7.08		143.14		137.30	

The correlation between the target and the anticipated responses is also measured by RMSE, and other several error functions for *MO-DS* (RMSE= 0.054, MSE=0.0029, SSE= 0.035) and *MO-NDS* (RMSE= 1.09, MSE=1.19, SSE= 13.22) at the training stage. The same functions were calculated at the validation stage for *MO-DS* (RMSE= 0.19, MSE=0.036, SSE= 0.108) and *MO-NDS* (RMSE= 0.78, MSE=0.61, SSE= 2.47). When the RMSE value is less than 3, this indicates how well the experimental outcomes match the predictions made by the ANN method (**Ejimofor et al., 2021**). This shows strong network performance throughout the neural network's lifecycle. It also shows how accurate and reliable the ANN model's predictions are. The low value of SSE for the *MO-DS* model indicates a better fitting model. The accuracy of both models was also assessed using other error functions (MAE= 0.03 and MAPE= 2.99) for *MO-DS* coagulant, and (MAE= 0.48 and MAPE= 7.08) for *MO-NDS* coagulant. The lower the MAPE the better the model is able to forecast values. This is the case of the *MO-DS* model which presented the lower MAPE.

At the outlet of the WWTP, low values of error function were recorded at the training stage in the case of the *MO-DS* treatment (RMSE= 0.05, MSE=0.0025, SSE= 0.038) and *MO-NDS* treatment (RMSE= 0.08, MSE=0.0064, SSE= 0.07). At the validation stage, the studied error functions have also been minimised (RMSE= 0.141, MSE=0.021, SSE= 0.085) for the *MO-DS* treatment and (RMSE= 0.05, MSE=0.0025, SSE= 0.01) for the *MO-NDS* treatment. The obtained RMSE values were less than 3 for all models; this indicates how closely the experimental results fit the ANN's predictions. The accuracy of the obtained models was also evaluated using the other error functions (MAE= 1.14 and MAPE= 143.14) for the *MO-DS*

coagulant, and (MAE= 0.76 and MAPE= 137.30) for the *MO-NDS* coagulant. The studied statistical parameters indicate good accuracy for all models.

The log-likelihood values give an indication of the best model using the scaled negative log probability statistic. It is a measure of goodness of fit for any model. Higher the value is, better is the model. The actual log-likelihood value for a given model is mostly meaningless, but it is useful for comparing two or more models**.** On the basis of log-likelihood estimation, it looks like the *IW-MO-NDS* represents the better model for TSS removal.

2.3.ANN models prediction

Figure 38 shows the path to solution plot for the *MO-DS* and *MO-NDS* models. It displays the scaled log-likelihood plotted against the number of steps.

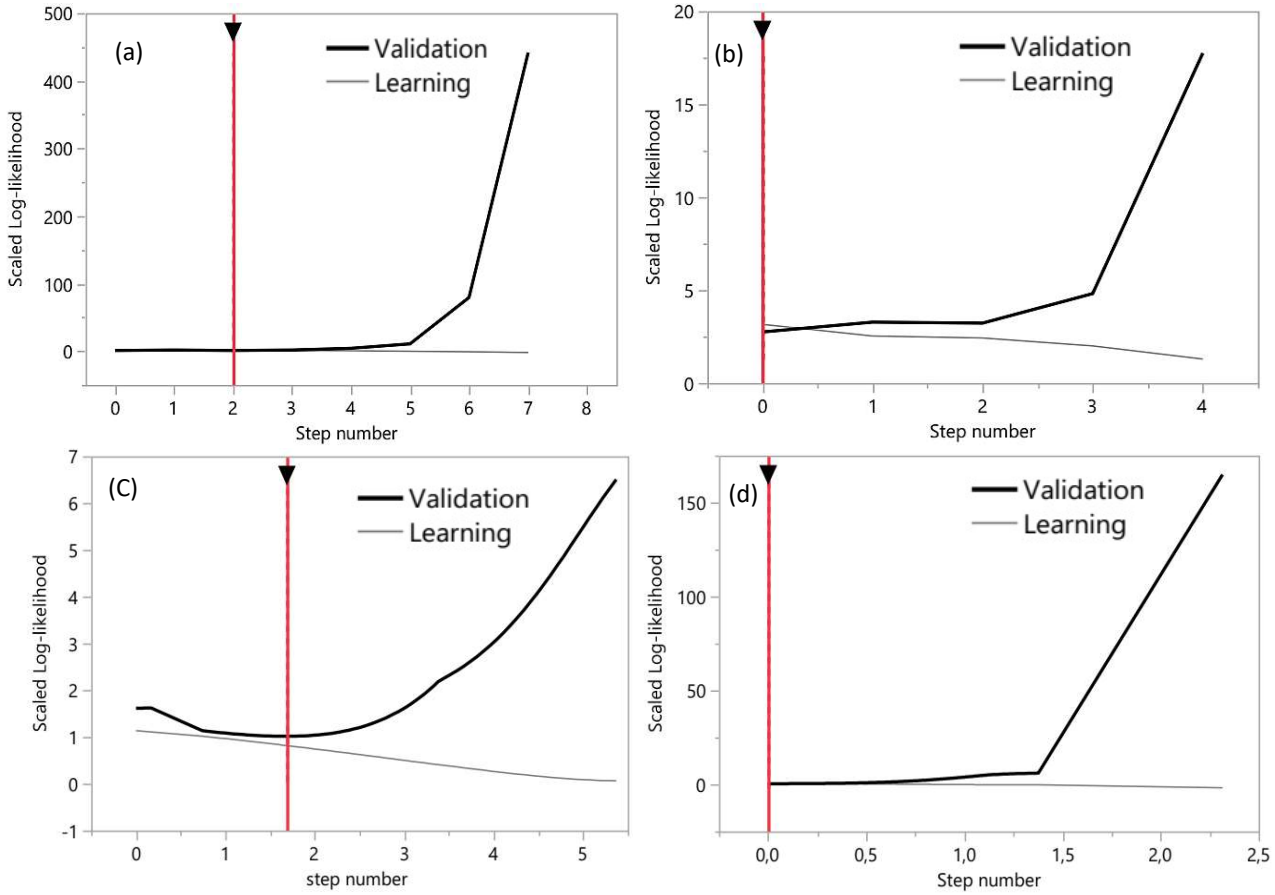

Figure 38. ANN path for solution.

(a): IW-*MO-DS,* (b): *IW*-MO-NDS, (c): *OW*-MO-NDS, and (d): *OW-MO-NDS* models

Using the scaled negative log probability statistic, it indicates which of our models is the most effective. It represents a great approach to investigate model over- or under-fitting. The optimal network settings based on the scaled log-likelihood for training and validation were

defined. It was obtained at the step 2 for the *MO-DS* model and just at the beginning at the step 0 for the *MO-NDS* model. After these values, no changes will be observed on the validation set.

Figure 39 and **40** compare the predicted and the experimental values of TSS removal in all stages of the ANN method. A strong connection between the acquired and the experimental data is indicated by the obtained R^2 in the training and validation stages for *MO-DS* and *MO-NDS* treatments. This shows that the model was successful in reflecting the real relationship between the items that were selected.

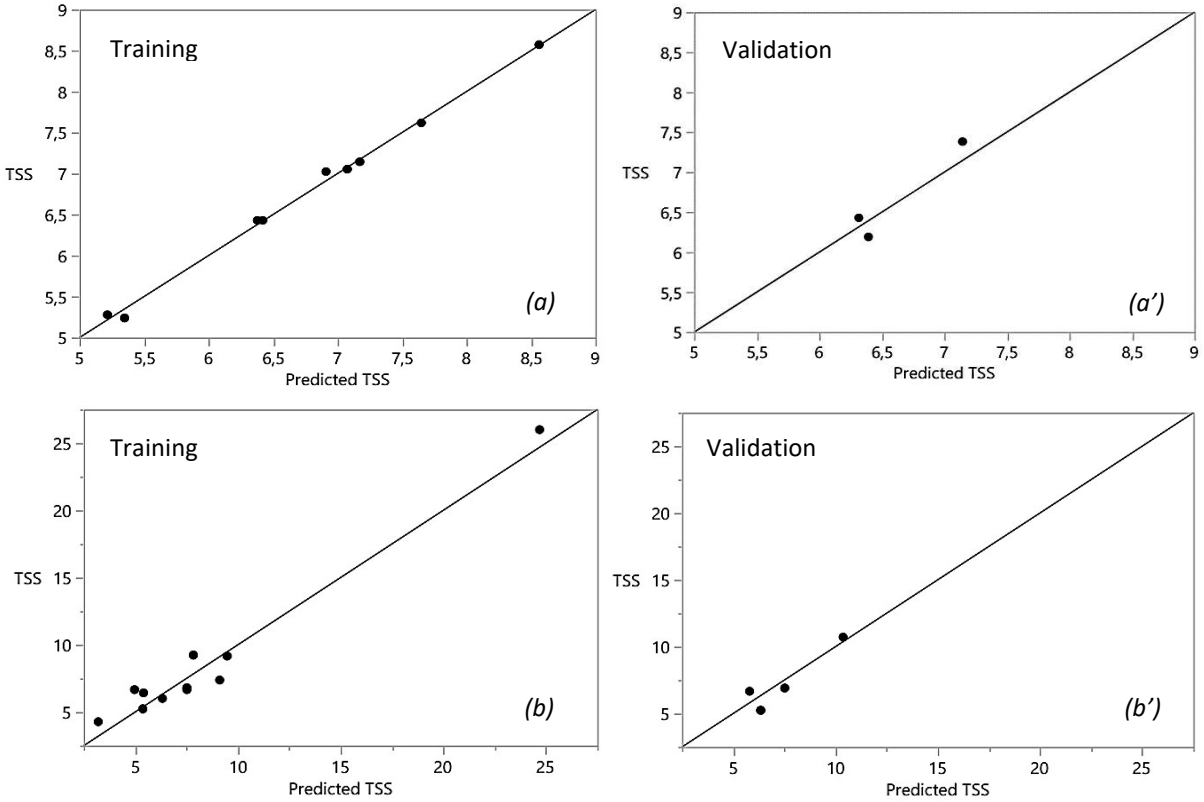

Figure 39. Predicted and the experimental TSS in the training and validation stages at the IW. **(a) (a'):** *MO-DS* model, **(b) (b'):** *MO-NDS* model.

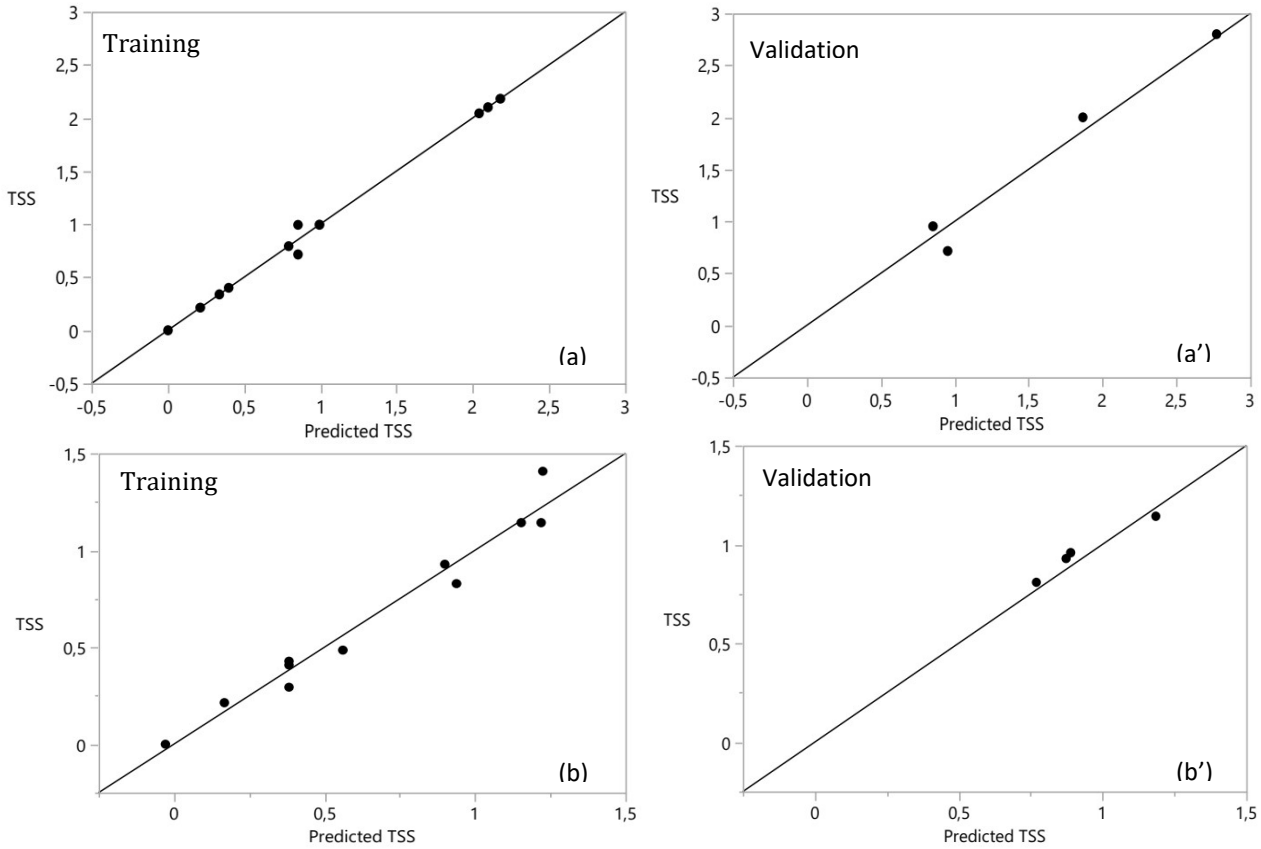

Figure 40. Predicted and the experimental TSS in the training and validation stages at OW.

(a) (a'): *MO-DS* model, **(b) (b'):** *MO-NDS* model.

2.4. Analysis of Response surface plots for the ANN models

The obtained interactions by the BBD model were also studied by the ANN model to identify the effect of the inputs on TSS removal **(Figure 41)** and **(Figure 42).** It was observed that the interactive effects on TSS removal plots obtained by the ANN models were very similar to those obtained by the RSM model, with supplementary curvatures explaining the ability of ANN method to extrapolate outside of the experimental range to find the global optimal point. Through this, it can be concluded that decreasing the *MO* seeds cake powder dosage combined with a well-determined fast and slow agitation could lead to a good TSS removal (in the range).

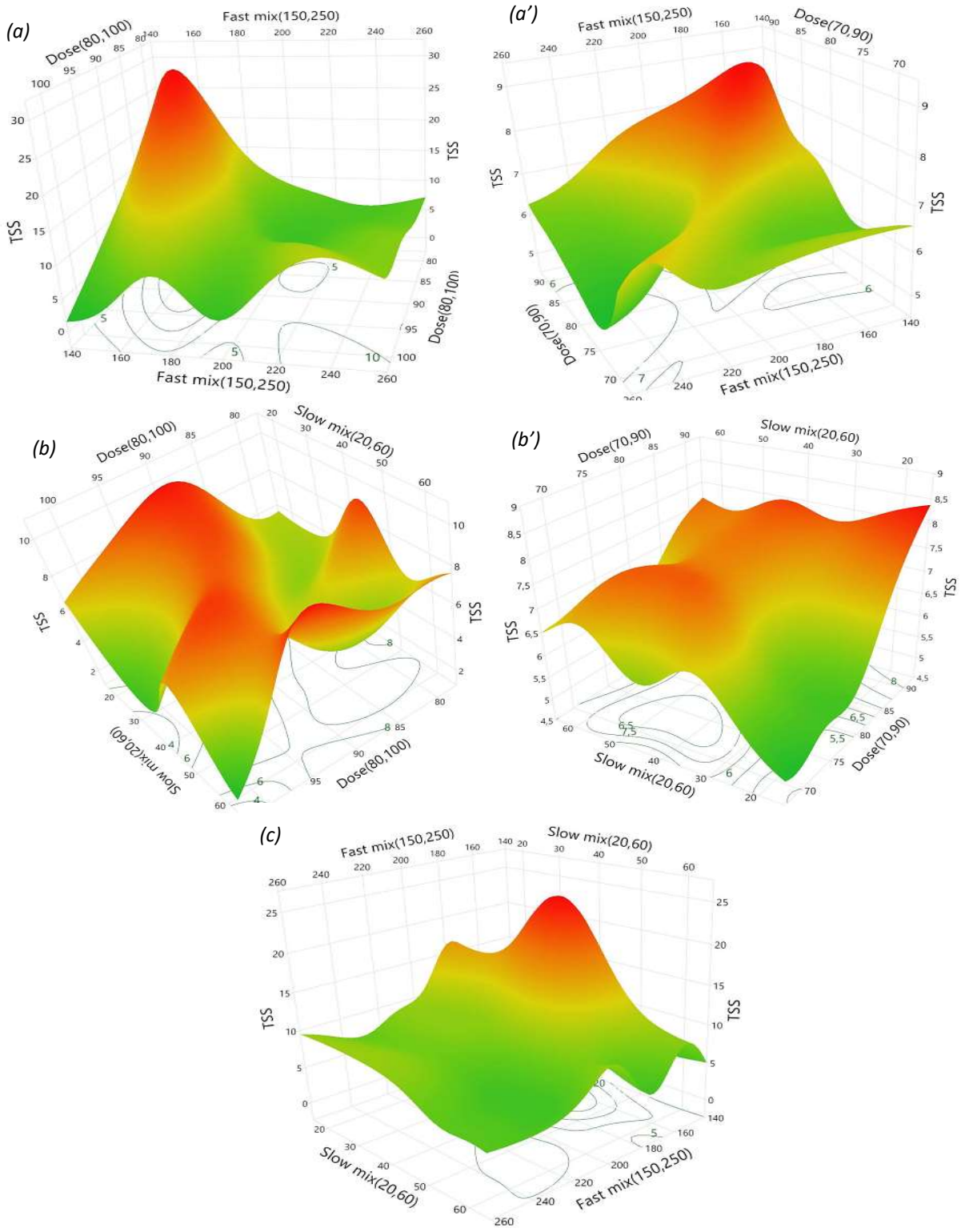

Figure 41: ANN interactive effects of both *MO* seeds cake powder on TSS removal at the IW. *(a): MO-NDS* dosage and fast mixing, *(b): MO-NDS* dosage and slow mixing, *(c):* fast and slow mixing in *MO-NDS* treatment, *(a'): MO-DS* dosage and fast mixing, *(b'): MO-DS* dosage and slow mixing

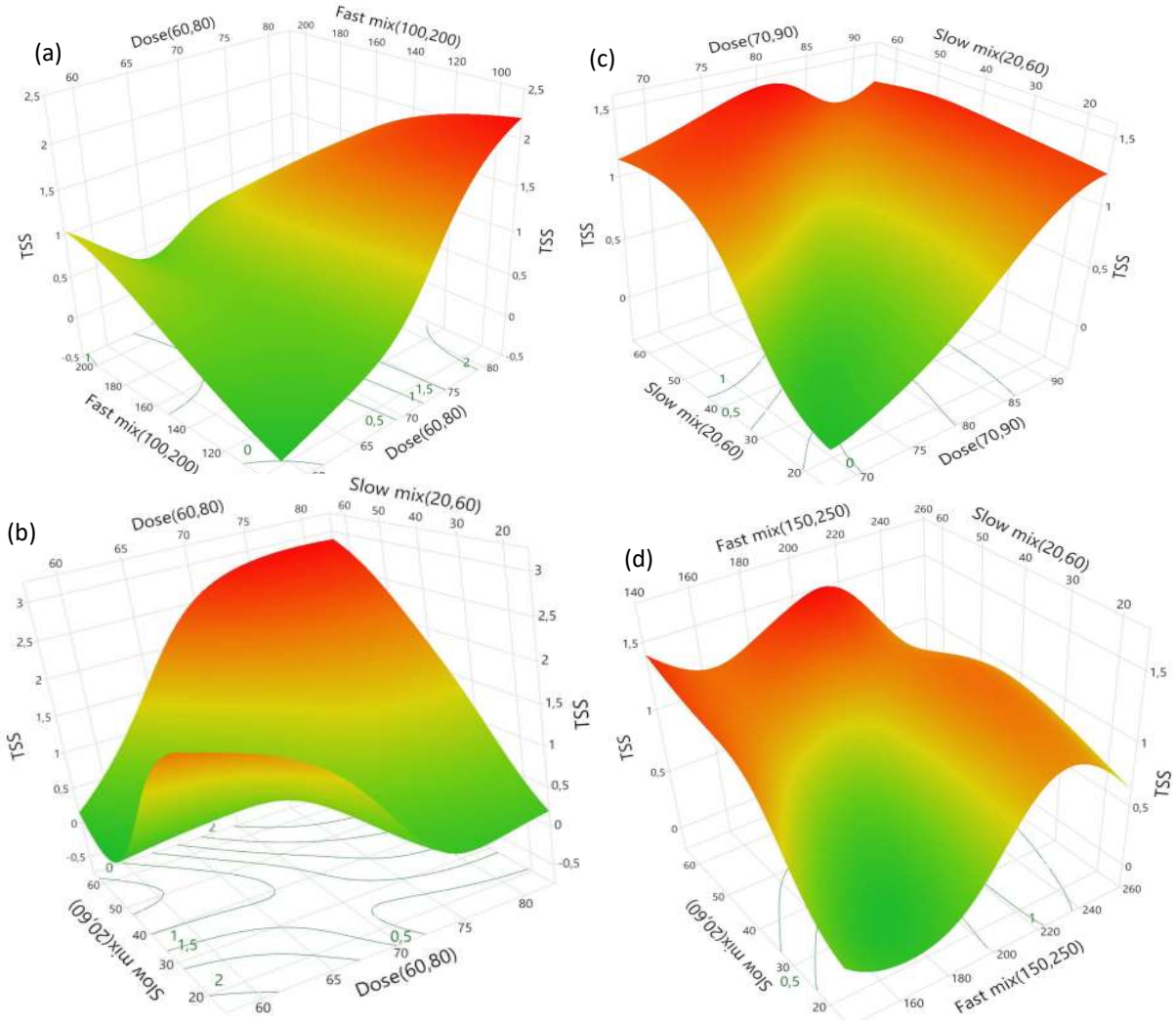

Figure 42. ANN interactive effects of both *MO* seeds cake powder on TSS removal at the OW.

(a): MO-DS dosage and fast mixing, *(b): MO-DS* dosage and slow mixing, *(c): MO-NDS* dosage and slow mixing, *(d):* fast and slow mixing in *MO-NDS* treatment.

3. Comparison of RSM and ANN models

Based on the results for R^2, MAE, MAPE, RMSE and MSE, and the relative error the accuracy of both RSM and ANN models was evaluated. According to the values of R^2 for the *MO-DS* treatment (0.93 and 0.99) and *MO-NDS* treatment (0.90 and 0.96) at the IW, and the *MO-DS* treatment (0.92 and 0.99) and the *MO-NDS* treatment (0.90 and 0.96) at the OW, the findings demonstrate that both optimisation strategies provided accurate forecasts. However, ANN performed better, especially at the IW with lower values of MAE (0.03, 0.48) and MAPE (2.99%, 7.08%) in the case of *IW-MO-DS* and *IW-MO-NDS* models, respectively. However MAPE values in the OW models were more than 100% which indicate that the error is greater than the actual value. However concerning the other error functions, both *OW-MO-DS* and *OW-MO-NDS* models illustrate good performance.

At the end, the optimal values for each model were selected. For the *IW-MO-DS*, it was found that the 80 ml dose stirred at a fast speed of 200 rpm and a slow speed of 40 rpm after that gave the best coagulant efficiency. As for the *IW-MO-NDS*, it appears that an increase of coagulant dosage to 90 ml was necessary to have good performance of the model. In the *MO-DS* treated outlet water, the 70 ml coagulant dose performed best when used with a fast speed of 150 rpm followed by a slow speed of 40 rpm. The *MO-NDS* coagulant has been used as 80 ml dosage under fast agitation conditions of 200 rpm and slow agitation of 40 rpm. The optimal obtained conditions are well illustrated in **Table 19**.

Table 19. The optimal Jar test conditions obtained at the IW and OW.

	RSM			ANN		
	Dose (ml)	**Fast mixing (rpm)**	**Low mixing (rpm)**	**Dose (ml)**	**Fast mixing (rpm)**	**Low mixing (rpm)**
Inlet water *MO-DS*	80	200	40	80	200	40
Inlet water *MO-NDS*	90	200	40	90	200	40
Outlet water *MO-DS*	70	150	40	70	150	40
Outlet water *MO-NDS*	80	200	40	80	200	40

4. Experimental validation for generalization

In the validation for generalization the obtained optimal parameters of coagulation-flocculation by RSM and ANN were performed again under the same conditions, but this time looking for other responses (other than TSS).

4.1.TSS removal

As illustrated in **table 14** and **15**, and according to the RSM and ANN models, the predicted suspended solids removal results were very close to the observed results. The obtained TSS values at the validation for generalization tests carried out under the same conditions were in the same range and nearly equal to the RSM and ANN values as exposed in **Figure 43**, TSS has been reduced to 6.67 and 7.81 in the IW treated with *MO-DS* and *MO-NDS*, respectively. In the OW, TSS removal could reach 1.71 and 1.88 with *MO-DS* and *MO-NDS* treatment, respectively. It seems clear from the plot, that TSS removal was more effective with *MO-DS* in the inlet water, while in the outlet water the difference in efficiency between the two treatments was not significant. The *MO-DS* coagulant used in the IW treatment has better coagulation ability to reduce TSS compared to other treatments. It was able to reduce the TSS by 73.76% in the IW treated by *MO-DS*. This value corresponds well to that obtained by **Bhatia et al (2007).** These results were lower than those obtained by **Al-Jadabi et al (2021),** who found that TSS

removal with *MO* extract had reached 95.5%. The difference in the TSS elimination rates could be due to the difference in the starting dose of the coagulant. The *IW-MO-NDS*, *OW-MO-DS* and *OW-MO-NDS* had a removal rate of 69.26, 39.13 and 33.11%, respectively. The obtained values are a function of the pollutant load and the nature of the discharges at the treatment plant in the sampling day.

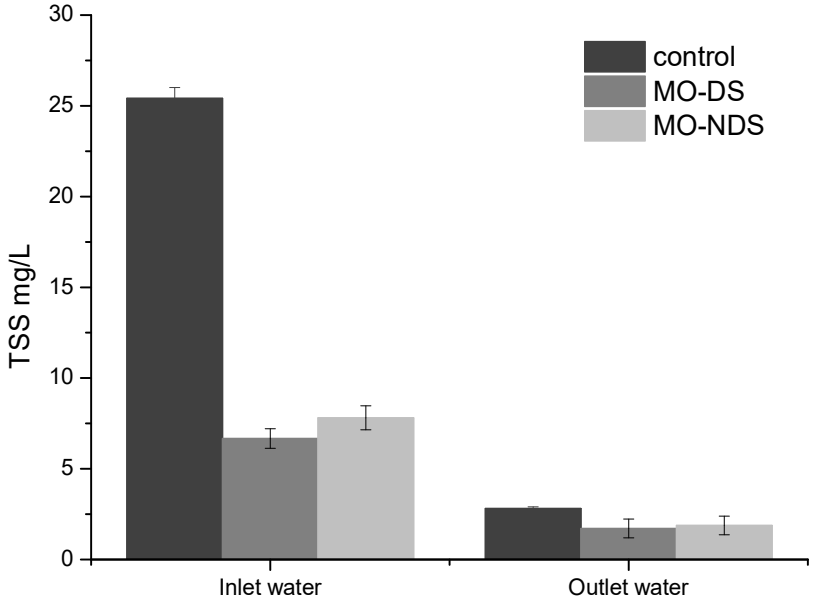

Figure 43. Suspended solids removal by *MO-DS* and *MO-NDS* in the IW and OW.

4.2.Turbidity removal

Suspended materials, including organic and inorganic particles, generate turbidity in water. Sand, sludge, rock fragments, and dissolved metals are examples of inorganic materials. In coagulation process, the cationic protein from *MO* seeds cake powder could be spread to every area of the liquid, and it could then interact with the negatively charged particles to produce scattered turbidity. Such interactions disrupt the force that holds the particles in place, allowing it to attach to small particles and produce precipitates (**Hendrawati et al., 2016).** Turbidity removal in validation tests revealed, as shown in **Figure 44** that *MO-DS* coagulant had a better capacity to remove turbidity in the IW. The *MO-DS* coagulant was able to reduce turbidity by 95.56%. The *MO-NDS* coagulant has low effectiveness compared to the *MO-DS* coagulant by reducing water turbidity to 89.42% at the IW. These findings were completely consistent with earlier research findings, which demonstrated that turbidity in water samples was reduced after treatment with *MO* seeds cake (**Ghebremichael et al., 2005; Sotheeswaran et al., 2011; Hendrawati et al., 2016; Shan et al., 2017; Merwad, 2018).**

Adelodun et al (2020) reported that turbidity removal with *MO* extract could be maximal and reach 94.44%, but decreased upon reaching a dose of 150 mg/L. They also reported that the cause of the additional decrease in turbidity removal could be due to the absence of opposite charged colloidal particles needed by *MO* biomass excess to react with, which have been thoroughly neutralised and precipitated with the ideal biomass dosage. **Al-Jadabi et al (2021)** have reported that *MO* cake powder effectiveness in turbidity removal can be as high as 97.5%, which supports these findings.

On the other hand, the *MO-DS* and *MO-NDS* coagulants had reversal of roles in the OW, with a reduction rate of 50.93 and 63.66%, respectively. This could be due to the decrease in the amount of protein contained in the *MO* seeds cake powder, especially in *MO-NDS.* It could also be due, as per **Muyibi & Okuofu (1995),** to the fact that turbidity removal was found to increase with increasing initial turbidity. At last, it seems like that the *MO-NDS* coagulant is more effective in low turbidity water.

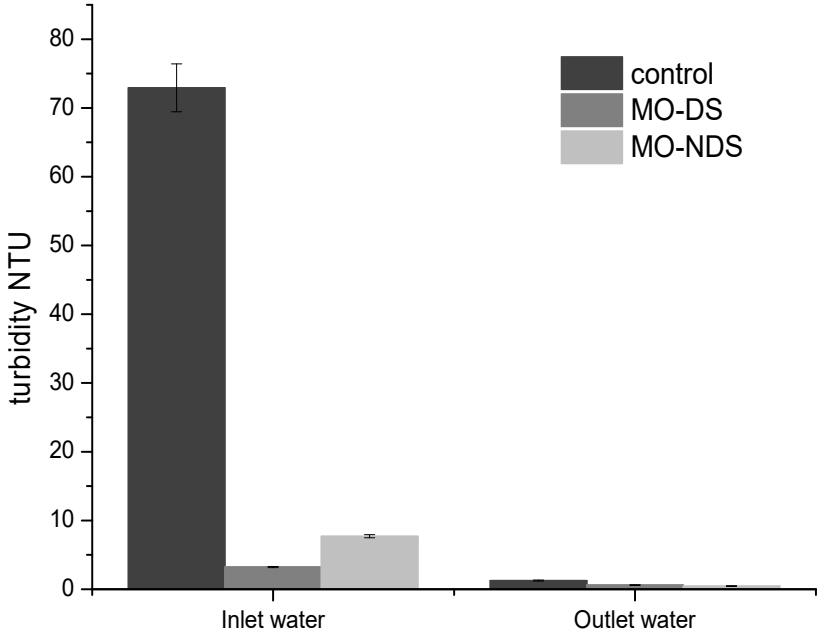

Figure 44. Turbidity removal by *MO-DS* and *MO-NDS* in the IW and OW.

4.3.Biochemical oxygen demand removal

Figure 45 illustrates that BOD removal was affected by both *MO* coagulants. In the IW, the *MO-NDS* coagulant was more effective than *MO-DS* coagulant. Its reduction rate was 5.16 and 9.92% with *MO-DS* and *MO-NDS* coagulants, respectively. This implies that the use of any preparation of *MO* seeds cake powder has an impact on BOD. These results were very similar to those demonstrated by **Shan et al (2017)** and **Merwad (2018),** even though the starting dose of the used coagulant was not the same, especially for *MO-NDS* coagulant. The optimal dose

obtained may not be effective enough to remove BOD. This was represented in the work carried out by **Adelodun et al (2020),** which found that the rate of BOD removal increased with increasing *MO* seeds cake powder dosage. On the other hand, the outlet water was considered as low polluted water. The addition of both coagulants had increased BOD by 93.51 and 55.15% with *MO-DS* and *MO-NDS* coagulants, respectively. It seems like that the *MO* seeds cake powder is more effective in the inlet water for BOD removal.

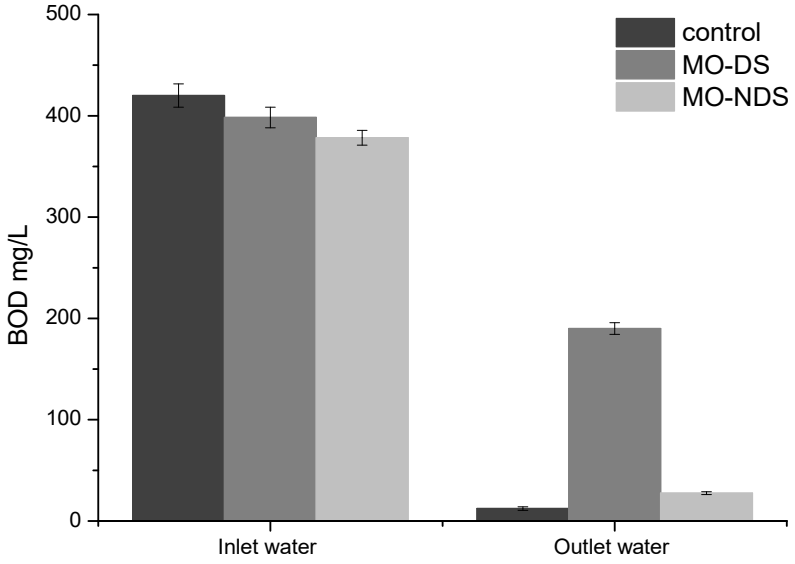

Figure 45. BOD removal by *MO-DS* and *MO-NDS* in the IW and OW.

4.4.Chemical oxygen demand removal (COD)

As illustrated in **Figure 46**, COD values have increased after treatment in the IW and the OW with both preparations of *MO* seeds cake powders. This could be due to the residual content of *MO* seeds oil which has not been completely removed as described by **Shan et al (2017). Adelodun et al (2020)** have also reported that COD removal can be increased by increasing the *MO* seeds cake powder dosage. According to **Baptista et al (2017)** and **Eman et al (2014),** this was explained by the drawbacks of using the *MO* seeds as a coagulant. After all, the release of organic matter from the seed into the wastewater treatment system frequently results in a greater need for chemical oxygen. **Desta & Bote (2021)** have reported that it is possible to remove COD using the *MO* seeds cake powder by increasing the *MO* seeds cake powder dosage. The increase of *MO* seeds cake powder dosage could increase other water quality parameters, especially turbidity. It may have then an opposite effect on water clarity. This could be due to the presence of more positive ions. **Arnoldsson et al (2008)** reported that the COD value rises due to the remaining organic materials in the *MO* seeds cake powder. **Hendrawati et al (2016)** have claimed that when the coagulant dosage is exceeded, the water samples are subject to an increase

in turbidity because the surplus coagulants no longer interact with the oppositely charged colloidal particles after most of them have undergone adequate neutralisation and precipitation. From the plot, it seems clear that the *MO-DS* contributes to COD increasing more than *MO-NDS* in both types of the treated wastewater.

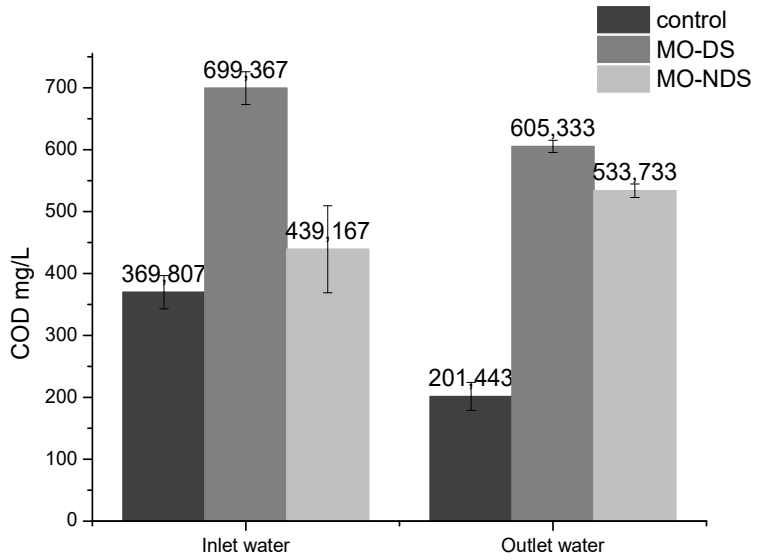

Figure 46. COD removal by *MO-DS* and *MO-NDS* in the inlet and outlet wastewater

4.5.Nitrates (NO_3^-) removal

From the data presented in **Figure 47**, results showed that the samples treated at the IW and the OW with both *MO-DS* and *MO-NDS* powders showed a clear increase in NO_3^- compared to the raw sample. Higher values of NO_3^- were recorded in the OW samples compared to those collected in the IW. We have recorded a value of 3.1, 3.71, 3.68 mg/L for control, *MO-DS* and *MO-NDS* samples collected in the IW, respectively. This corresponds to an increase of 14.84 and 14.30% in the IW samples treated with *MO-DS* and *MO-NDS,* respectively. On the other hand, OW samples have resulted in 0.85, 3.66 and 3.45 mg/L for control, *MO-DS* and *MO-NDS* samples, respectively. The rate of increase reached 76.87 and 75.46% respectively, in these treated samples. This increase would be due to the degradation of the organic matter by the bacteria previously present in the samples. These findings do not agree with those reduced by **Sotheeswaran et al (2011)** and **Merwad (2018).** However, **Kilingo et al (2022)** have found that coagulation-flocculation using the *MO* seeds cake powder had a very low effectiveness in NO_3^- elimination. It is even increased NO_3^- from 0.29 to 2.52 mg/L, which agrees perfectly with our findings. As well as experimental results by **Singh & Patidar (2020),** the NO_3^- rose following the coagulation process due to the ions present in the *MO* proteins.

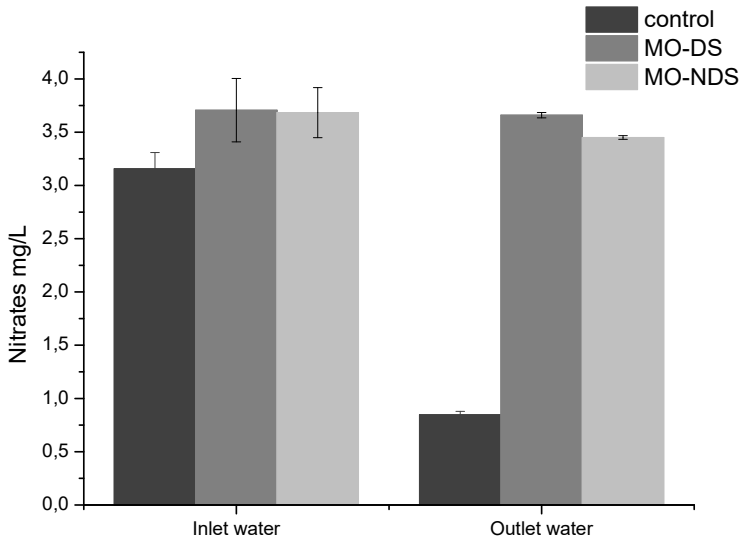

Figure 47. Nitrates removal by *MO-DS* and *MO-NDS* in the inlet and outlet wastewater

4.6.Nitrites (NO_2^-) removal

In contrast to NO_3^-, a significant decrease in NO_2^- rate was noted in the treated samples in the IW and the OW, with both *MO* seeds cake powder preparations. Results presented in **Figure 48** show that the rate of NO_2^- decreased in the range of 47.61 and 41.90 % in the IW with the *MO-DS* and *MO-NDS* coagulant, respectively. While, in the OW the NO_2^- reduction was in the range of 47.47 and 43.44% for the *MO-DS* and *MO-NDS* treatments. The conclusions reached by **Kilingo et al (2022)** using the *MO* seeds cake powder in coagulation-flocculation process as a pre-treatment and **Garde et al (2017)** using the *MO* seeds extract to treat coffee fermentation water were entirely supported by these findings.

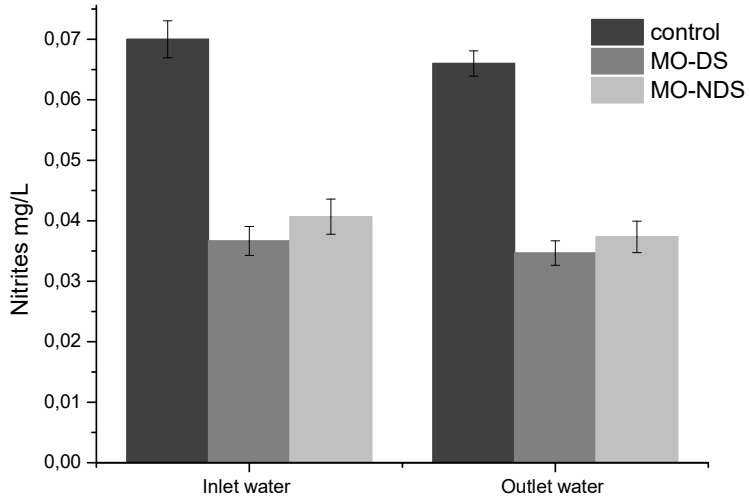

Figure 48. Nitrites removal by *MO-DS* and *MO-NDS* in the inlet and outlet wastewater

4.7.Phosphorus (PO_4^{-3}) removal

The PO_4^{-3} in the treated wastewater using both *MO* seeds cake powder preparations was almost entirely removed **(Figure 49).** In the treated IW with *MO-SD* and *MO-NSD* coagulant, the reduction of $PO_4^{-3}$was in the range of 95.03 and 94.40%, respectively. In the OW this reduction has reached 96.37 and 96.84% with the same preparations, respectively. These findings totally agreed with what concluded by **Subha et al (2015),** using *MO* seeds as an activated adsorbent**,** it has exceeded the values observed by **Kilingo et al (2022),** who used a saline solution of *MO* seeds powder in the coagulation coupled with the VFCW (Vertical Flow Constructed Wetland) system and found that removal efficiencies for PO_4^{-3} was ranging from 42 to 99.9% and from 41 to 89%, recorded in the autumn and winter, respectively.

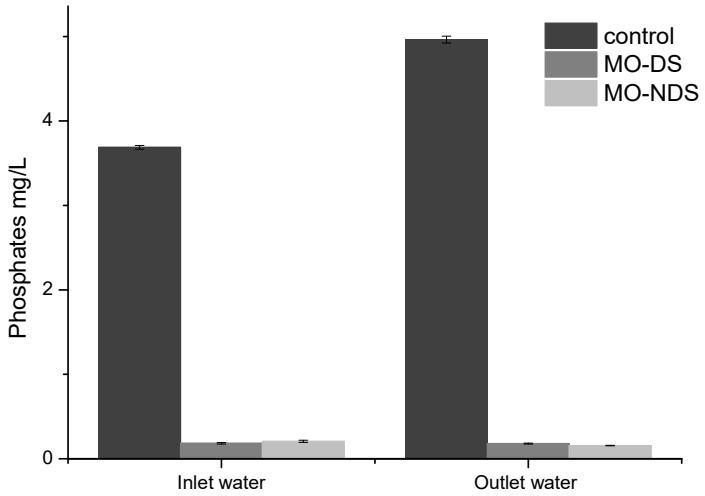

Figure 49. Phosphorus removal by *MO-DS* and *MO-NDS* in the inlet and outlet wastewater

4.8.Heavy metals removal

The *MO* seeds cake solution acts as a natural adsorbent to remove heavy metals from water samples. The *MO-DS* and *MO-NDS* coagulants have been used to remove Pb, Cd, Zn. **Table 20** shows that the addition of coagulants can reduce the level of Cd, *Z*n and Pb in wastewater significantly. It seems clear from **Table 20** that Cd was detected in the IW and the OW at the range of 0.106 and 0.022 mg/L. However, in the *MO-DS* and *MO-NDS* water treatments, it was completely not detectable (below detection limit: b.d.l). This could be due to the high effectiveness of both preparations of *MO* seeds cake powder to remove Cd. The result was consistent with what **Hendrawati et al (2016)** have demonstrated, with a range of Cd removal that exceeds 99%. This was also reported by **Meneghel et al (2013),** which found that *MO* seeds

extract could remove more than 90% of Cd. However, only 60% of Cd could be eliminated using MSE (Moringa Saline Extract), according to **Nand et al (2012).**

In terms of Zn, it was only detectable in the IW in the range of 0.9329 mg/L. It was also completely not detectable in treated wastewater with both *MO* seeds cake preparations. It seems clear that *MO* seeds cake powder coagulant make that Zn level decrease to below detection limit.

Table 20. Heavy metals removal by *MO-DS* and *MO-NDS* in the IW and OW.

	Inlet water (mg/L)			Outlet water (mg/L)		
	Raw	MO-DS	MO-NDS	Raw	MO-DS	MO-NDS
Zn	0.9392	b.d.l*	b.d.l	b.d.l	b.d.l	b.d.l
Cd	0.1060	b.d.l	b.d.l	b.d.l	b.d.l	b.d.l
Pb	1.959	0,066	0.034	0.583	0.018	0.013

**b.d.l.: below detection limit.*

Regarding Pb level, it has been reduced in the IW to 96.63 and 98.25% with *MO-DS* and *MO-NDS,* respectively. In the OW, the reduction rate was in the range of 96.97 and 97.75%, with the *MO-DS* and *MO-NDS* treatments, respectively. The percentage of the removed Pb in our study is higher than the one in the study carried out by **Merwad (2018),** with a removal rate of 70%, **Sotheeswaran et al (2011)** determining a removal rate of 80% and **Sajidu et al (2005)** with a rate removal ranging between 70.86 to 89.40%.

This study established that the rate of heavy metals in the wastewater may be decreased by both types of coagulant. According to **Hendrawati et al (2016),** the use of the *MO* seeds cake to ensure the precipitation of colloidal materials, including heavy metals could take place through changes in the properties of these materials either with or without oxidation-reduction reactions. This precipitation could also take place, resulting from the oxidation reaction. The *Moringa* amphoteric protein may bind to the oppositely charged metal ions binding, causing the metal ions to precipitate, and lowering levels of these metals. The alkaline pH generated by the addition of *MO* seeds powder is due to the release of O-H groups that could allow the positively charged metal ions to precipitate as insoluble metal hydroxides. This was supported by the fact that precipitation induced by chemical coagulant is only improved in alkaline water, especially when pH is above 10.5.

Section II

MO Seed husk valorization

1. Introduction

In this section, the *MO* seed husks were characterized. Based on that, the decision of the cellulosic crystalline NPs synthesis has been adopted. After that, the adsorption process using the obtained material from *MO* seeds waste was studied. The obtained biomaterial was characterised in order to identify its behaviour during the adsorption process.

2. Characterisation of synthesised biomaterials

2.1.Structural characterization

2.1.1. FTIR analysis

The infrared spectra of the raw synthesis matrix and the synthesised material are shown in **Figure 50**.

The FTIR of *MO* seed husk powder was carried out to study the structural changes that occur in the material after chemical treatment and to approve that the resultant product is pure cellulose. From the infrared spectra corresponding to the obtained material with the indicated preparation, we noticed a similarity in the wavelength of appearance of the functional groups, with a change in the intensity of the peaks corresponding to these functional groups (**Figure 50**). The greatest similarity lies between the spectra of the *MO* seeds waste and those of the synthetized NPs. The examination of the obtained spectra reveals the following absorption bands:

- A broad absorption band observed between 3600-3300 cm-1 with a maximum around 3400 cm-1. This band is characteristic of the hydrogen elongation vibration of the hydroxyl groups (OH) (from carboxyls, phenols or alcohols) and water absorbed by the analysed materials. This indicates the reflectance of hydrophilic property in the analysed materials **(Singh et al., 2017).** The observed bands at 2900 cm-1 in the *MO* seed waste spectrum are attributed to the asymmetric and symmetric valence vibration of the $-CH_3$ group **(Nuruddin et al., 2011).**
- The observed bands at 1700 cm-1 and 1600 cm-1 are caused by the elongation vibration of C=O in the ketone, aldehyde, lactone, carbonyl and aromatic ring groups

and especially to ester linkages and acetyl groups (1732 cm-1) in hemicellulose and lignin present in the *MO* seeds husks **(Kumar et al., 2014).** This indicates also the formation of carbonyl-containing groups in raw material. These bands are very numerous in the *MO* seed waste spectra. However, they are very limited in the NPs spectra and not referred to the lignin and hemicellulose vibrations, due to the chemical elimination of hemicellulosic material during the bleaching step, giving thus purified cellulose **(Mohamed et al., 2015).**

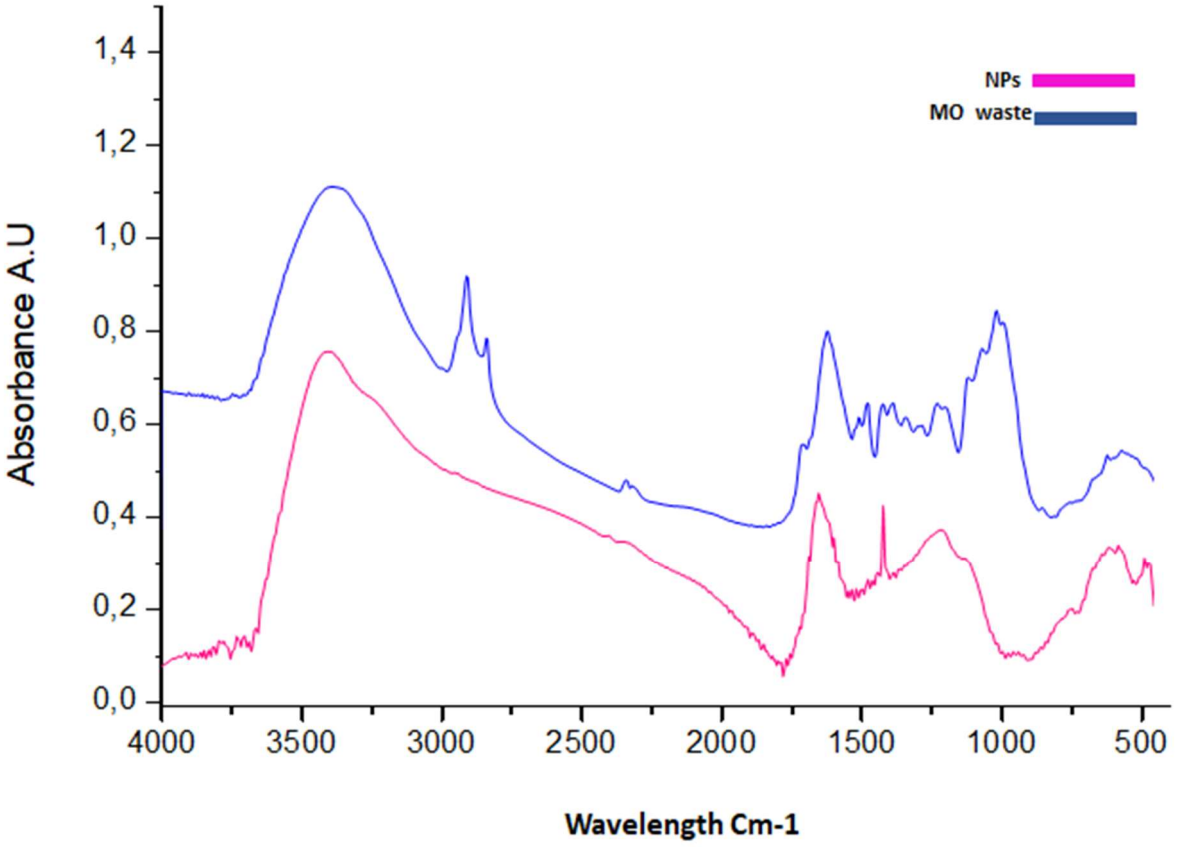

Figure 50. FTIR analysis for the *MO* seed waste, and the prepared *MO* seed waste NPs.

- The observed bands at the area from 1470 to 1370 cm-1 represent a domain formed by an overlap of absorption bands attributable to hydroxyl function grouping each other on the surfaces. It is also attributed to the vibrations in the plane of the C─H bond in several $C = C - H$ type structures. The *MO* seed waste structure is very rich in this type of grouping. Only one such grouping was noted in the case of NPs material.
- The observed bands between 1000-500 cm-1 are due to the out-of-plane deformation of C─H in differently substituted aromatic cycles.

- The hydroxyl group of the phenolic function and the carboxylic function give the surface of the materials an acidic character, while the carbonyl function gives the surface of the materials a basic character.

2.1.2. Scanning Electron microscope (SEM) analysis

The surface morphology of the prepared *MO* seed husk nanoparticles has been studied using a scanning electron microscope (SEM), as shown in **Figure 51.**

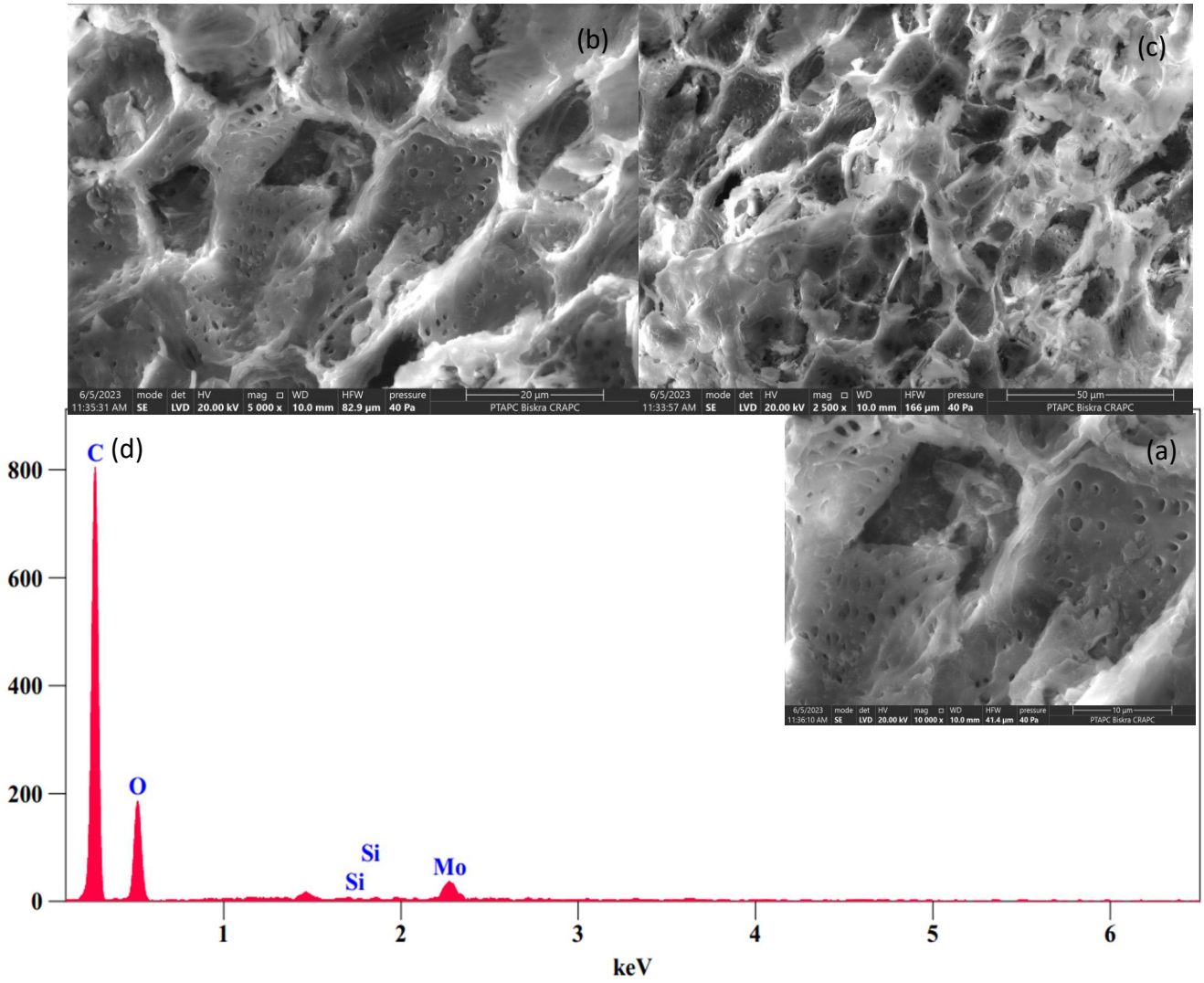

Figure 51. The analysis of *MO* seed husk NPs using Scanning electron microscope (SEM) at (a): 10 µm magnification, (b): 20 µm magnification, (c): 50 µm magnification, and (d) Energy dispersive X-ray spectra (EDX) analysis.

The obtained images show a spherical structure of the outer surface with agglomerated concavities in the depth. The swelling of cellulose was observed marked by cavities surrounded by whitish walls as evident in **Figure 51(a).** The whitish structures are obtained after bleaching stage. This indicates that almost the obtained material is in basis a pure cellulosic material. This

notifies the removal of non-cellulosic materials such as lignin, hemicelluloses, pectin, and other impurities from cucumber peels, upon successive chemical pre-treatments (**Prasanna & Mitra, 2020).** In other words, the acquired individual cellulose microfibers have bundles of cellulose nanocrystals joined by crystalline and amorphous regions along the microfibers. This is explained by the fact that the -1,4-glucopyranose linkage has been broken and the cellulose's amorphous regions have been destroyed during the sulfuric acid hydrolysis for the cellulose nanocrystals **(Melikoglu et al., 2019).** After that cellulose's micro-sized fibres were transformed into individual nano-sized crystals, resulting in a significant size reduction **(Naduparambath et al., 2018).** The different compartments of the obtained cellulose nanocrystals are covered with pores scattered over their surface, giving thus a homogeneous and porous structure, which explains its adsorbent character.

The SEM analysis was coupled to the Energy dispersive X-ray spectra (EDX) analysis. The obtained composition shown in **Figure 51(b),** illustrates that the particles obtained present a very high degree of purity with traces of Molybdenum and silinium of less than 0.2% by weight. The primary components of EDX spectra are carbon and oxygen, which are related to the usual composition of cellulose (**Krishnan & Ramesh, 2013; Kian et al., 2017).** The increase of carbon contents in NPs is relative to confirm the sorption character of the obtained material (**Hamadeen et al., 2021).**

2.2.Physico-chemical characterization

The physical characteristics (porosity, total pore volume, moisture content and apparent and real densities) of the adsorbent material tested were measured. The results of the physical characterisation are shown in **Table 21.** It illustrates the physical characterization of the obtained material.

Table 21. Physical characterization of the obtained NPs.

Physical character	**NPs**
Apparent mass ($\boldsymbol{\rho}$**a**)	277.77 mg /ml
Real mass ($\boldsymbol{\rho r}$)	4.03×10^2 mg /ml
Porosity ($\boldsymbol{\varepsilon}$%)	126.3 %
pH$_{PZC}$	6.5

Generally, the physical characteristics of the adsorbent depend on the material and the method of preparation. It seems that the sulfuric acid impregnation in the NPs preparation has conferred grate porosity to the obtained material (126.3 %). The real mass of the obtained

material is almost double the apparent mass, which gives the material good adsorption characteristics.

Only one chemical characterization parameter was studied. The pHpzc is very important parameter for characterising adsorbents, as it gives the surface charge of an adsorbent as a function of pH solution in which it is found. The pHpzc is a good indicator of the chemical and electronic properties of surface functional groups. It depends on the origin of the precursor and the type of modification envisaged. The acquired adsorbent is therefore acidic, which confirms the obtained infrared results.

3. Application in the adsorption

In order to determine the residual concentrations of our adsorbate (MB) by UV-visible the preparation of series of standard solutions of MB with a concentration does not exceed 100mg/l. The absorbance of each standard was measured in order to produce the calibration curve of MB. The curve has R^2 of 0.9954. The calibration curve is given by the equation below:

$$y = 0.1775x + 0.0379 \qquad (\text{Eq. } 17)$$

3.1.The effect of adsorbent dose

This is a crucial parameter to establish the ability of an adsorbent to reduce a specified concentration of MB solution. In order to identify the optimal dose of the bio-sorption used in MB removal, 100 ml of MB solution at initial concentration of 20mg/l was brought into contact with different masses of the studied bio-sorbent. The contact surface between an adsorbent and the solution plays a decisive role in the adsorption phenomenon. The adsorption capacity of a solid and the time required to reach equilibrium are also linked to this parameter. The effect of the suspension on the quantity of the adsorbed MB by the adsorbent was studied using the material concentration ranging from 15 to 110 mg / 250 ml. The results are expressed as the total adsorption amount (qt) of MB obtained as a function of time (min).

The obtained results are presented in **Figure 51.** The results show that the total adsorption amount increases as the dose of the adsorbent used increases. The ideal concentration for better absorption was obtained at the concentration of 110mg/250ml. This can be explained by the fact that increasing the dose of the adsorbent increases the number of sites available for dye fixation, which in turn favours discolouration (**Kifuani et al., 2018)**. The total adsorption amount remains constant after 90min for all adsorbent concentrations. As it was reported by **Hamadeen et al**

(2021), higher concentrations of adsorbents could lead to the movement of dye to the energetic adsorption sites. Thus, the adsorption capacity could be reduced.

It is important to note that in the first stage, the adsorption is rapid. Then, this step is followed by spreading with saturation stage. This means that in the first stage, there is external transfer of MB molecules to the surface. This change in the quantity of MB adsorbed is attributed to the phenomenon of adsorption. This phenomenon can be explained by the fact that the driving force increases as the concentration increases, facilitating therefore, and the flow of solutes from the solution to the studied material.

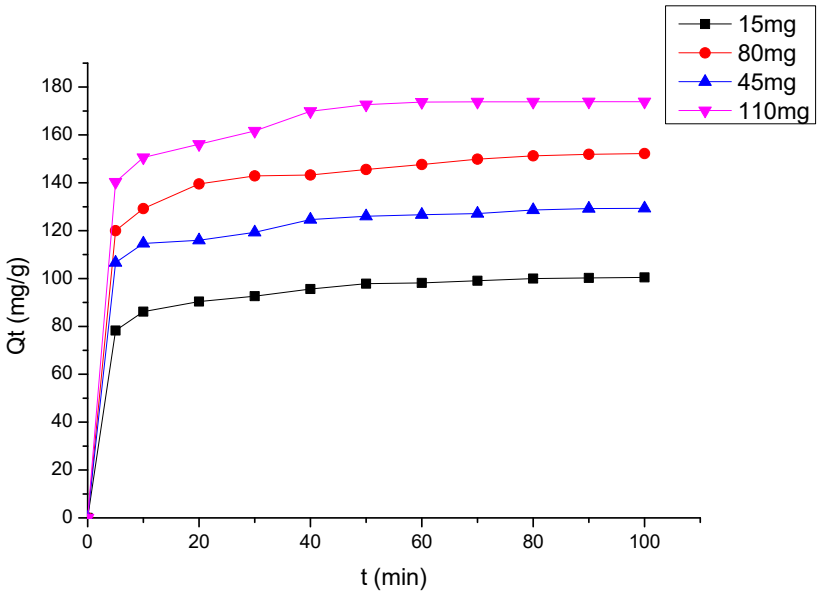

Figure 52. The adsorbent dose effect on the MB adsorption.

The second stage can be attributed to diffusion of molecules within the porous structure (micro-pores) of the adsorbent. Beyond this stage, a saturation zone is observed due to an almost constant quantity of MB adsorbed by the adsorbent sites. Because of this, adsorption process depends on the accessibility of the organic molecules to the micro-porosities **(Dias et al., 2007).**

3.2.The effect of pH

The adsorption of MB in aqueous solution on the surface of a solid depends not only on the porosity but also on the surface area of the adsorbent and the degree of dissociation of the surface charge of the solid. This last factor is related to the pH of the medium. The adsorption of MB on the tested adsorbent was studied as a function of pH of solution. The experiments were carried out with an MB concentration of 20 mg/L, a suspension of 110 mg/250 ml at room temperature. The studied pH ranges were over 7 and 11.

Figure 53 shows the total adsorption amount (qt) of MB obtained as a function of time in different ranges of pH solution. A decrease in the reduced concentration as a function of adsorption time, at different ranges of pH was observed. The obtained curves show better adsorption of MB when the pH increases over 7. The MB adsorption remains constant after 90 min, in all cases. Before that and at high pH values, the concentration of MB is much higher than that in other pH ranges. These findings are similar to those obtained by **Hamadeen et al (2021).**

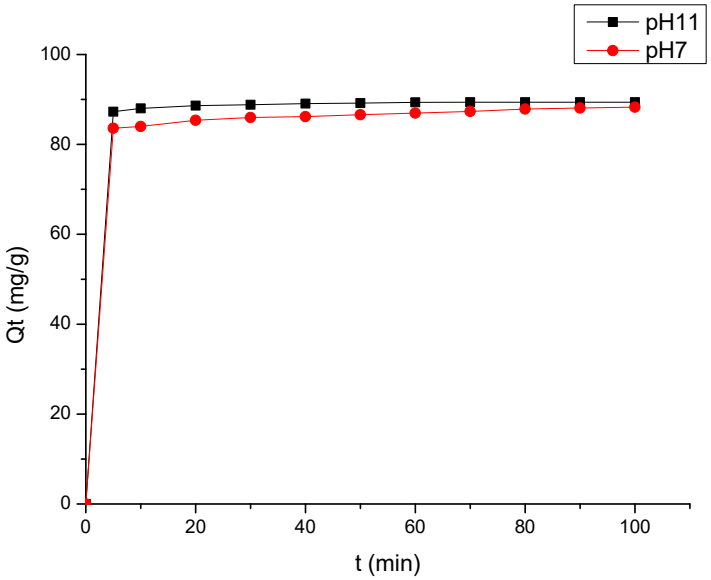

Figure 53. The effect of pH on MB adsorption.

The obtained results in the determination of pH at zero charge indicate that, below the pHpzc of the used material, the charge of samples treated with NPs is positive. Beyond that point, the charge is negative. The obtained pHpzc of NP is 6.5, this means that the charge on these adsorbents is negative at pHs< pHpzc, and that they undergo electrostatically attractive interactions with organic cations. As a result, MB adsorption is further enhanced. This is explained by the fact that, as the pH decreases, the number of negatively charged sites decreases and the number of positively charged sites increases **(Tahir & Rauf, 2006; Tsai et al., 2007; Weng & Pan, 2007).**

3.3.Effect of initial concentration of MB

As it allows us to know the ideal concentration at which MB could be absorbed from aqueous medium, this is one of the crucial parameters to be calculated. From the evaluation of the adsorbent concentration giving maximum yield, it is useful to study the variations in this

adsorption yield for the same quantity of adsorbent at variable beginning concentrations (C_0) of MB mentioned. This is shown in **Figure 54.**

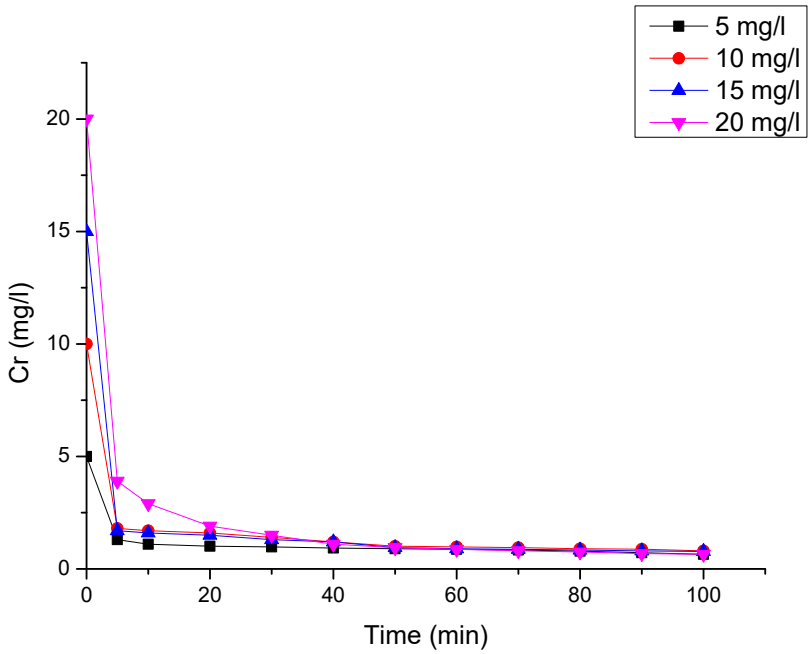

Figure 54. The effect of the beginning concentration of MB solution.

The obtained curves show that the residual concentration of MB after adsorption decreases with time (the adsorbed quantity by the support increases with time) until it reaches an approximately constant value at the same equilibrium time whatever the initial concentration of MB. It is clear that more the MB solution is concentrated, lower its adsorption rate is. This means that any increase in the initial concentration of MB requires the right choice of adsorbent mass to avoid any loss of efficiency during the treatment. The equilibrium is obtained when the available pore volume of the adsorbent had been occupied. The interaction between the adsorbent and the subsequent dye is reduced as a result.

4. Study of the adsorption kinetics

The evolution of the quantity of the adsorbate fixed by the solid as a function of time describes the kinetics of the adsorption process. The adsorption kinetics enabled us to determine the type of kinetic model chosen for the studied adsorption.

In order to determine the mechanism limiting the kinetics of the adsorption process, correlations between the quantities adsorbed and time were established. Several kinetic models were used to interpret the experimental data, providing essential information for the use of these

adsorbents in the adsorption field. To this end, the pseudo-first and pseudo-second order kinetic models were tested. The results of the experiments are shown below. The various constants of these models and their correlation coefficients were determined **(Table 22)**. It can be deduced that the adsorption process fitted well into pseudo first-order as the R^2 value (0.969) obtained is higher compared to that of the pseudo second-order.

Table 22. Parameters of pseudo-first-order and Pseudo second-order kinetic models for adsorption of MB onto NPs.

Pseudo first-order			**Pseudo second-order**
R^2	0,969	R^2	0,827
K_1 (min^{-1})	0,2661	K_2/g ($g.mg.min^{-1}$)	0,595
Standard error	0,00321	Standard error	0,00195

The high correlation coefficients obtained using both models, 0,969 for pseudo first-order and 0,827 for the pseudo second-order, and the small standard error obtained for both models, allow us to conclude that the kinetics can follow both models, with better representation using the pseudo first-order model.

The low apparent speed of concentrated solutions could be explained by the occupation of the active sites by MB molecules during the adsorption phase. In this way, the electrostatic forces become weak to attraction of new molecules. More the MB solution concentrated is, lower its adsorption rate is. These results confirm those obtained at previous section (effect of initial concentration).

In order to describe the interaction between the adsorbate and the surface of the adsorbent, the establishment of adsorption isotherms as models represents an important stage in the study of adsorption. This will be dealt with in subsequent work.

General conclusion

General Conclusion

The main objective of this dissertation was to develop an efficient, waste-free water treatment system using different materials obtained from the *MO* seeds, all applied in a number of physicochemical water and wastewater treatment processes. The *MO* seeds cake powder has been used as a bio-coagulant to prepare different extracts used in the coagulation-flocculation process. The *MO* seed extract was prepared using the dehulled and hulled *MO* seed cake powders to valorise the peel of the *MO* seeds often discarded without being recycled.

Giving that turbidity is considered as an important parameter used in water quality monitoring. It is typically considered to be a sign of how easily water can be filtered. For this, a minimum turbidity value for drinking water has been set. The suspended materials in water mostly arise from land erosion, the dissolution of minerals, the decay of vegetation, and it often entails this minerals (especially heavy metals) while sedimentation. These metals are ultimately much more concentrated in the sediment silt. This sediment always has an impact on the siltation of the dam's reservoir and consequently reduces its available useful volume, which translates into a decrease in the levels of services provided by the reservoir. Also, Water with high levels of turbidity is typically characterized by the presence of germs that can induce major symptoms. For this, the necessity to remove as many suspended solids as possible results from the population's uncertainty regarding the safety of the excessively turbid water for ingestion. For this, the prepared *MO* seeds extracts were applied in dam water treatment and wastewater purification taking turbidity and suspended solids as reference elements to be eliminated.

The jar-test was used to develop optimal conditions (type of coagulant, coagulant dose, fast mixing, slow mixing, and settling), for water and wastewater treatment using the obtained bio-coagulants. Mathematical methods were to enhance optimisation performance, VIZ, the RSM and ANN methods.

In dam water treatment using *MO-DS* and *MO-NDS* coagulants, the FFD was adopted as a powerful RSM design. However for the ANN model the MFFF method was applied. Through this, the coagulation-flocculation investigated factors had a noticeable impact on turbidity. The developed turbidity removal models (FFD and ANN) had an $R^2$of 0.90, adj-R^2 of 0.81, and a low

RMSE of 0.07 for the FFD model, which fit the experimental data well. For the ANN model, an $R^2$of 0.96 and RMSE of 0.06 were found. For the dam water treatment using both preparations of the *MO* seeds cake powder, the dehulled *MO* seed cake powder was found to be effective at the dose of 10ml, used at fast mixing rate of 150 rpm for 3 min and 60rpm for 30 min for slow agitation, when allowed to settle for 60min. turbidity removal performance has reached 90.42, 90.71, and 92.33%, using the experimental and the predicted data for FFD and ANN models, respectively. By using the *MO* seeds engaged in the coagulation-flocculation process, it has been demonstrated that both models are effective at removing turbidity, with better performance of the ANN model.

In wastewater treatment, the effectiveness of both *MO* seeds cake preparations was tested this time around TSS removal. The RSM and ANN methods have been also used to evaluate the effectiveness of dehulled and unhulled *MO* seeds cake powders in coagulation-flocculation process at the inlet and the outlet of the plant. The BBD was the chosen design for RSM application. The influence of each input parameter and how it interacts with other parameters has been depicted in RSM and ANN models, which also displays the response's trend. The resulting experimental findings fitted well with the obtained BBD and ANN models. High accuracy of all models was demonstrated at the outl---+--et and the inlet of the plant. Better accuracy was performed using the *MO-DS* coagulant model with an R^2 of 0.93 and 0.99 for RSM and ANN models, respectively as well as a very low MAE (0.03), MAPE (2.99) for the ANN model giving it better accuracy. All models have been tested for an eventual generalization. At this stage, TSS removal has been restored for both types of coagulants (*MO-DS* and *MO-NDS,* respectively), with a range of 95.56 and 89.42 % in the inlet water and 50.93 and 63.66 % in the outlet water. Other physicochemical parameters have been also tested. Turbidity, as it comes from suspended solids, its elimination rate has followed that of TSS with a slight elimination of BOD in the inlet water, while in the outlet water an increase was noticed. However, both kinds of coagulant had contributed to increase COD and NO_3^-, at the inlet and the outlet of the plant. Regarding NO_2^-, PO_4^{-3} and heavy metals, excellent efficiency performance has been noted with *MO-DS* and *MO-NDS* in any type of water. This effectiveness varied between 47.61 and 41.90 % in the inlet water, and between 47.47 and 43.44% for *MO-DS* and *MO-NDS* treatments in the outlet water in NO_2^- case. In PO_4^{-3} case, it was up to 95.03 and 94.40% in the inlet water and 96.37 and 96.84% in the outlet water treated with *MO-DS* and *MO-NDS,* respectively. Heavy metals removal was most successful by attending values bdl, in Zn and Cd case and extremely low values in Pb case.

It is then preferable to optimise a more effective dose to reduce these last parameters considered to be water pollution parameters.

At the end, the models' further validation using the additional experimental data obtained shows that they are very reliable for use within the specified range of parameters. Through which we were able to objectively evaluate the effectiveness of both *MO* seeds cake powders in certain physico-chemical parameters in Sid Ali Lebhar WWTP.

MO seed husks are waste products that are generally discarded without any economic value. In this dissertation, this waste was valorised to be used in water treatment. As the *MO* seed husks were found to be cellulose-rich, this waste was covered for nano-cellulosic crystalline particles (CNC) synthesis. The obtained NPs were found to have a grate homogenous porous structure, with a large specific surface area, giving it a high adsorption capacity. The obtained NPs had a porosity of 126.3%, with a higher apparent density.

The adsorption capacity of the obtained adsorbent was tested against one of the most widely used textile dyes (MB). The obtained results allow us to conclude that:

- The synthetized adsorbent was characterized by high real mass ($4.03x10^2$ mg /ml) compared to the apparent mass (277.77 mg /ml), which gives it more adsorptive capacity;
- The synthetized adsorbent was to have a high porosity (126.3%), which explains its adsorptive character;
- The adsorption process was to be affected by, the initial concentration of MB solution, the adsorbent dosage and the pH of the solution;
- The adsorption of MB using the synthetized NPs is better in a basic medium;
- The kinetic adsorption fitted well to both pseudo first order model and pseudo second order model with better performance of the first one

Finally, the whole study leads to applicable perspectives to the different studied systems to improve their efficiency:

- In the dam water coagulation-flocculation process study, as the protection of the environment and therefore of human health is a major concern, and in view of the conclusive results, It would be ideal to progressively take these trials up to the station level;

- As the coagulation-flocculation process using *MO* seeds cake powder in wastewater treatment was effective on a regional scale, why not go further and try to apply the model on a large scale. The model was effective for TSS removal. It was also effective when applied for the removal of heavy metals, nitrites and phosphorus, but not for BOD, COD and nitrates. It is then preferable to optimise a more effective dose to reduce these last parameters considered to be water pollution parameters;
- The determination of suitable adsorption isotherms for the obtained NPs. These are important tools for describing the interaction between the adsorbate and the adsorbent, and understand the behaviour of NPs towards the adsorbate;
- The application of the adsorption using the *MO* seed husks NPs could be effective on other pollution parameters and other dyes. For this, extending the range of uses for nanotechnology in the field of water purification by testing on other pollutants such as trace metals, COD…could provide a good research area;
- The quest for these treatment methods is essential if we want to protect our world, for this the application of nanotechnology by covering agricultural wastes represent an excellent outcome to treat water and wastewater.

Refrences

Refrences

Abderrezak, N., & Alim, A. (2020). Moringa Oleifera: Propriétés bioactives et utilisations.

Abdulkarim, S. M., Long, K., Lai, O. M., Muhammad, S. K. S., & Ghazali, H. M. (2005). Some physico-chemical properties of Moringa oleifera seed oil extracted using solvent and aqueous enzymatic methods. *Food chemistry*, *93*(2), 253-263. https://doi.org/10.1016/j.foodchem.2004.09.023

Abiyu, A., Yan, D., Girma, A., Song, X., & Wang, H. (2018). Wastewater treatment potential of Moringa stenopetala over Moringa olifera as a natural coagulant, antimicrobial agent and heavy metal removals. *Cogent Environmental Science*, *4*(1), 1433507. https://doi.org/10.1080/23311843.2018.1433507

Adamowski, J., & Sun, K. (2010). Development of a coupled wavelet transform and neural network method for flow forecasting of non-perennial rivers in semi-arid watersheds. *Journal of Hydrology*, *390*(1-2), 85-91.http://doi.org/10.1016/j.jhydrol.2010.06.033

Adelodun, B., Ogunshina, M. S., Ajibade, F. O., Abdulkadir, T. S., Bakare, H. O., & Choi, K. S. (2020). Kinetic and Prediction Modeling Studies of Organic Pollutants Removal from Municipal Wastewater using Moringa oleifera Biomass as a Coagulant. *Water, 12(7), 2052.* doi:10.3390/w12072052.

Adelodun, B., Ajibade, F. O., Ogunshina, M. S., & Choi, K. (2019). Dosage and settling time course optimization of Moringa oleifera in municipal wastewater treatment using response surface methodology. *Desalin. Water Treat*, *167***,** 45-56. doi: 10.5004/dwt.2019.24616

Agoyi, E. E., Assogbadjo, A. E., Gouwakinnou, G., Okou, F. A., & Sinsin, B. (2014). Ethnobotanical Assessment of Moringa oleifera Lam. in Southern Benin (West Africa). *Ethnobotany Research and Applications*, *12*, 551-560.doi: 10.17348/era.12.0.551-560.

Ahmed, M. J., & Dhedan, S. K. (2012). Equilibrium isotherms and kinetics modeling of methylene blue adsorption on agricultural wastes-based activated carbons. *Fluid phase equilibria*, *317*, 9-14. https://doi.org/10.1016/j.fluid.2011.12.026

Ahmadi, S., Banach, A., Mostafapour, F. K., & Balarak, D. (2017). Study survey of cupric oxide nanoparticles in removal efficiency of ciprofloxacin antibiotic from aqueous solution: adsorption isotherm study. *Desalin Water Treat*, *89*(89), 297-303. doi: 10.5004/dwt.2017.21362

Ajao, V., Bruning, H., Rijnaarts, H., & Temmink, H. (2018). Natural flocculants from fresh and saline wastewater: Comparative properties and flocculation performances. *Chemical Engineering Journal*, *349*, 622-632. doi: 10.1016/j.cej.2018.05.123. https://doi.org/10.1016/j.cej.2018.05.123

Alam, M., Alam, M., Hakim, M., Huq, A. O., & Moktadir, S. G. (2014). Development of fiber enriched herbal biscuits: a preliminary study on sensory evaluation and chemical composition. *Int J Nutr Food Sci*, *3*, 246-50. doi: 10.11648/j.ijnfs.20140304.13

Alcamo, J., Flörke, M., Märker, M. (2007). Future long-term changes in global water resources driven by socio-economic and climatic changes. *Hydrological Sciences Journal*, *52*(2), 247-275. doi:10.1623/hysj.52.2.247

Alenazi, M., Hashim, KS., Hassan, AA., Muradov, M., Kot, P., & Abdulhadi, B. (2020). Turbidity removal using natural coagulants derived from the seeds of strychnos potatorum: Statistical and experimental approach. *IOP Conference Series: Materials Science and Engineering*, *888*(1). https://doi.org/10.1088/1757-899X/888/1/012064

Al-Ghouti, M. A., & Da'ana, D. A. (2020). Guidelines for the use and interpretation of adsorption isotherm models: A review. *Journal of hazardous materials*, *393*, 122383. https://doi.org/10.1016/j.jhazmat.2020.122383

Al-Jadabi,N., Laaouan,M., Mabrouki,J., Fattah,G., El Hajjaji.,S. (2021). Comparative study of the coagulation efficacy of Moringa Oleifera seeds extracts to alum for domestic wastewater treatment of Ain Aouda City, Morocco. *E3S Web of Conferences* , Volume 314 https://doi.org/10.1051/e3sconf/202131408003.

Alpert, N. L., Keiser, W. E., & Szymanski, H. A. (2012). *IR: theory and practice of infrared spectroscopy*. Springer Science & Business Media.

Amenaghawon, N.A., & Kazeem, J.O. (2020). Evaluation of response surface methodology, artificial neural network and adaptive neurons fuzzy inference system for modelling and optimizing oxalic acid production from pineapple waste. FUW Trends Sci. Technol. J. 5, 255–263. e-ISSN: 24085162; p-ISSN: 20485170.

Amran, A. H., Zaidi, N. S., Muda, K., & Loan, L. W. (2018). Effectiveness of natural coagulant in coagulation process: a review. *International Journal of Engineering & Technology*, *7*(3.9), 34-37.

Anctil, F., Perrin, C., & Andréassian, V. (2004). Impact of the length of observed records on the performance of ANN and of conceptual parsimonious rainfall-runoff forecasting models. *Environmental Modelling & Software*, *19*(4), 357-368.http://doi.org/10.1016/s1364-8152(03)00135-x

Ang, T. H., Kiatkittipong, K., Kiatkittipong, W., Chua, S. C., Lim, J. W., Show, P. L., ... & Ho, Y. C. (2020). Insight on extraction and characterisation of biopolymers as the green coagulants for microalgae harvesting. *Water*, *12*(5), 1388.doi: 10.3390/W12051388.

Anwar, F., & Bhanger, M. I. (2003). Analytical characterization of Moringa oleifera seed oil grown in temperate regions of Pakistan. *Journal of Agricultural and food Chemistry*, *51*(22), 6558-6563. https://doi.org/10.1021/jf0209894

Anwar, F., Latif, S., Ashraf, M., & Gilani, A. H. (2007). *Moringa oleifera*: a food plant with multiple medicinal uses. *Phytotherapy Research: An International Journal Devoted to Pharmacological and Toxicological Evaluation of Natural Product Derivatives*, *21*(1), 17-25. **https://doi.org/10.1002/ptr.2023**

Araujo, C. S., Alves, V. N., Rezende, H. C., Almeida, I. L., de Assuncao, R. M., Tarley, C. R., ... & Coelho, N. M. M. (2010). Characterization and use of Moringa oleifera seeds as biosorbent for removing metal ions from aqueous effluents. *Water Science and Technology*, *62*(9), 2198-2203. https://doi.org/10.2166/wst.2010.419

Araújo, C. S., Carvalho, D. C., Rezende, H. C., Almeida, I. L., Coelho, L. M., Coelho, N. M., ... & Alves, V. N. (2013). Bioremediation of waters contaminated with heavy metals using Moringa oleifera seeds as biosorbent. *Applied bioremediation-active and passive approaches*, *23*, 227-255.

Arise, A. K., Arise, R. O., Sanusi, M. O., Esan, O. T., & Oyeyinka, S. A. (2014). Effect of Moringa oleifera flower fortification on the nutritional quality and sensory properties of weaning food. *Croatian journal of food science and technology*, *6*(2), 65-71. https://hrcak.srce.hr/131735

Arnell, NW. (2004). Climate change and global water resources: SRES emissions and socio-economic scenarios. *Global Environmental Change, 14(1), 31–52.* doi:10.1016/j.gloenvcha.2003.10.006

Ayerza, R. (2012). Seed and oil yields of Moringa oleifera variety Periyakalum-1 introduced for oil production in four ecosystems of South America. *Industrial Crops & Products*, *36*(1), 70-73.doi: 10.1016/j.indcrop.2011.08.008.

Babu, B. R., Parande, A. K., Raghu, S., & Kumar, T. P. (2007). Cotton textile processing: waste generation and effluent treatment. *Journal of cotton science*.

Baptista, A. T. A., Coldebella, P. F., Cardines, P. H. F., Gomes, R. G., Vieira, M. F., Bergamasco, R., & Vieira, A. M. S. (2015). Coagulation–flocculation process with ultrafiltered saline extract of Moringa oleifera for the treatment of surface water. *Chemical Engineering Journal*, *276*, 166-173.doi: 10.1016/j.cej.2015.04.045.

Baptista, A. T. A., Silva, M. O., Gomes, R. G., Bergamasco, R., Vieira, M. F., & Vieira, A. M. S. (2017). Protein fractionation of seeds of Moringa oleifera lam and its application in superficial water treatment. *Separation and Purification Technology*, *180*, 114-124. https://doi.org/10.1016/j.seppur.2017.02.040

Babayeju, A. A. B. C., Gbadebo, C., Obalowu, M., Otunola, G., Nmom, I., Kayode, R., ... & Ojo, F. (2014). Comparison of Organoleptic properties of egusi and efo riro soup blends produced with moringa and spinach leaves. *Food Sci Qual Manag*, *28*, 15-8.

Barrera-Díaz, C. E., Balderas-Hernández, P., & Bilyeu, B. (2018). Electrocoagulation: Fundamentals and prospectives. In *Electrochemical water and wastewater treatment* (pp. 61-76). Butterworth-Heinemann.doi: 10.1016/B978-0-12-813160-2.00003-1.

Behbahaninia, A., Mirbagheri, S. A., Khorasani, N., Nouri, J., & Javid, A. H. (2009). Heavy metal contamination of municipal effluent in soil and plants. *Journal of Food, Agriculture and Environment*, *7*(3-4), 851-856.

Bell, D. A., Towler, B. F., & Fan, M. (2010). *Coal gasification and its applications*. William Andrew.

Benalia, A., Derbal, K., Panico, A., & Pirozzi, F. (2018). Use of acorn leaves as a natural coagulant in a drinking water treatment plant. *Water*, *11*(1), 57. https://doi.org/10.3390/w11010057

Bender, M. (1958). The colloidal state. *American Scientist*, *46*(4), 368-387. https://www.jstor.org/stable/27827200

Bhattacharya, A., Tiwari, P., Sahu, P. K., & Kumar, S. (2018). A review of the phytochemical and pharmacological characteristics of Moringa oleifera. *Journal of pharmacy & bioallied sciences*, *10*(4), 181. doi: 10.4103/JPBS.JPBS_126_18

Bhateria, R. and Jain, D. (2016). Water quality assessment of lake water: a review', *Sustainable Water Resources Management*, 2(2), pp. 161–173. doi: 10.1007/s40899-015-0014-7.

Bhatia, S., Othman, Z., & Ahmad, A. L. (2006). Palm oil mill effluent pretreatment using Moringa oleifera seeds as an environmentally friendly coagulant: laboratory and pilot plant studies. *Journal of Chemical Technology & Biotechnology: International Research in Process, Environmental & Clean Technology*, *81*(12), 1852-1858. **https://doi.org/10.1002/jctb.1619**

Bhatia, S., Othman, Z., & Ahmad, A. L. (2017). Coagulation–flocculation process for POME treatment using Moringa oleifera seeds extract: optimization studies. *Chemical Engineering Journal*, *133*(1-3), 205-212. doi:10.1016/j.cej.2007.01.034.

Bichi, M. H. (2013). A review of the applications of Moringa oleifera seeds extract in water treatment. *Civil and Environmental Research*, *3*(8), 1-10.

Bidima, I. M. (2016). Production et transformation du moringa. *CTA ISF Pro-Agro series*.

Biswas, W. (2008). Life cycle assessment of biodiesel production from Moringa oleifera oilseeds. Staff Publications- Conference Papers. Paris: Moringanews, Moringa and Plant Resources Network; 1–9.

Bolón-Canedo, V. and Alonso-Betanzos, A. (2018). 'Basic concepts', *Intelligent Systems Reference Library*, 147, pp. 1–11. doi: 10.1007/978-3-319-90080-3_1.

Biswas, S. K., Chowdhury, A., Das, J., Roy, A., & Hosen, S. Z. (2012). Pharmacological potentials of Moringa oleifera Lam.: a review. *International Journal of Pharmaceutical Sciences and Research*, *3*(2), 305.

Boelee, E., Geerling, G., van der Zaan, B., Blauw, A., & Vethaak, A. D. (2019). Water and health: From environmental pressures to integrated responses. *Acta tropica*, *193*, 217-226.doi: 10.1016/j.actatropica.2019.03.011.

Bondy, S. C., Campbell, A. (2018). Water quality and brain function. *International Journal of Environmental Research and Public Health*, *15*(1). https://doi.org/10.3390/ijerph15010002

Borthakur, A., & Singh, P. (2020). Sustainability Science—below and above the Ground as per the United Nation's Sustainable Development Goals. In *Climate Change and Soil Interactions* (pp. 453-471). Elsevier.doi: 10.1016/b978-0-12-818032-7.00017-5.

Boulal, A., Atabani, A. E., Mohammed, M. N., Khelafi, M., Uguz, G., Shobana, S., ... & Kumar, G. (2019). Integrated valorization of Moringa oleifera and waste Phoenix dactylifera L. dates as potential feedstocks for biofuels production from Algerian Sahara: An experimental perspective. *Biocatalysis and Agricultural Biotechnology*, *20*, 101234.

Boulaadjoul, S., Zemmouri, H., Bendjama, Z., & Drouiche, N. (2018). A novel use of Moringa oleifera seed powder in enhancing the primary treatment of paper mill effluent. *Chemosphere*, *206*, 142-149. doi: 10.1016/j.chemosphere.2018.04.123.

Bratby, J. (2016). *Coagulation and flocculation in water and wastewater treatment*. IWA publishing.

Brilhante, R. S. N., Sales, J. A., Pereira, V. S., Castelo, D. D. S. C. M., de Aguiar Cordeiro, R., de Souza Sampaio, C. M., ... & Rocha, M. F. G. (2017). Research advances on the multiple uses of Moringa oleifera: A sustainable alternative for socially neglected population. *Asian Pacific journal of tropical medicine*, *10*(7), 621-630. https://doi.org/10.1016/j.apjtm.2017.07.002

Budevska, B. O., Sum, S. T., & Jones, T. J. (2003). Application of multivariate curve resolution for analysis of FT-IR microspectroscopic images of in situ plant tissue. *Applied spectroscopy*, *57*(2), 124-131.

Buenaño, B., Vera, E., & Aldás, M. B. (2019). Study of coagulating/flocculating characteristics of organic polymers extracted from biowaste for water treatment. *Ingeniería e Investigación*, *39*(1), 24-35. doi:10.15446/ing.investig.v39n1.69703

Bulut, Y., Gözübenli, N., & Aydın, H. (2007). Equilibrium and kinetics studies for adsorption of direct blue 71 from aqueous solution by wheat shells. *Journal of hazardous materials*, *144*(1-2), 300-306. https://doi.org/10.1016/j.jhazmat.2006.10.027

Camacho, F. P., Sousa, V. S., Bergamasco, R., & Teixeira, M. R. (2017). The use of Moringa oleifera as a natural coagulant in surface water treatment. *Chemical Engineering Journal*, *313*, 226-237. https://doi.org/10.1016/j.cej.2016.12.031

Carmen, Z., & Daniela, S. (2012). *Textile organic dyes-characteristics, polluting effects and separation/elimination procedures from industrial effluents-a critical overview* (Vol. 3, pp. 55-86). Rijeka: IntechOpen.

Chatsungnoen, T., & Chisti, Y. (2019). Flocculation and electroflocculation for algal biomass recovery. In *Biofuels from Algae* (pp. 257-286). Elsevier. https://doi.org/10.1016/B978-0-444-64192-2.00011-1

Cheremisinoff, N. P. (1997). *Biotechnology for waste and wastewater treatment*. Elsevier.P44.

Chinma, C. E., Abu, J. O., & Akoma, S. N. (2014). Effect of germinated tigernut and moringa flour blends on the quality of wheat-based bread. *Journal of food processing and preservation*, *38*(2), 721-727. **https://doi.org/10.1111/jfpp.12023**

Chong, M. F. (2012). Direct flocculation process for wastewater treatment. *Advances in water treatment and pollution prevention*, 201-230. https://doi.org/10.1007/978-94-007-4204-8

Choong Lek, B. L., Peter, A. P., Qi Chong, K. H., Ragu, P., Sethu, V., Selvarajoo, A., & Arumugasamy, S. K. (2018). *Treatment of palm oil mill effluent (POME) using chickpea (Cicer arietinum) as a natural coagulant and flocculant: Evaluation, process optimization and characterization of chickpea powder. Journal of Environmental Chemical Engineering.* doi:10.1016/j.jece.2018.09.038

Choy, S. Y., Prasad, K. M. N., Wu, T. Y., Raghunandan, M. E., & Ramanan, R. N. (2014). Utilization of plant-based natural coagulants as future alternatives towards sustainable water clarification. *Journal of environmental sciences*, *26*(11), 2178-2189. https://doi.org/10.1016/j.jes.2014.09.024

Chukwuebuka, E. (2015). Moringa oleifera "the mother's best friend". *International Journal of Nutrition and Food Sciences*, *4*(6), 624-630. doi: 10.11648/j.ijnfs.20150406.14

Crotty, P. A. (2004). *Selection and definition of performance indicators for water and wastewater utilities*. American Water Works Association.

Ćurko, J., Matošić, M., Crnek, V., Stulić, V., & Mijatović, I. (2016). Adsorption characteristics of different adsorbents and iron (III) salt for removing As (V) from water. *Food Technology and Biotechnology*, *54*(2), 250-255. doi: 10.17113/FTB.54.02.16.4064

Cusioli, L. F., Bezerra, C. D. O., Quesada, H. B., Alves Baptista, A. T., Nishi, L., Vieira, M. F., & Bergamasco, R. (2021). Modified Moringa oleifera Lam. Seed husks as low-cost biosorbent for atrazine removal. *Environmental technology*, *42*(7), 1092-1103. doi: 10.1080/09593330.2019.1653381.

Daba, M. (2016). Miracle tree: A review on multi-purposes of Moringa oleifera and its implication for climate change mitigation. *J. Earth Sci. Clim. Change*, *7*(4), 1-5. DOI: 10.4172/2157-7617.1000366

Dahiya, S., Kumar, A. N., Sravan, J. S., Chatterjee, S., Sarkar, O., & Mohan, S. V. (2018). Food waste biorefinery: Sustainable strategy for circular bioeconomy. *Bioresource technology*, *248*, 2-12.

Davies-Colley, R. J., & Smith, D. G. (2001). Turbidity suspeni) ed sediment, and water clarity: a review 1. *JAWRA Journal of the American Water Resources Association*, *37*(5), 1085-1101. https://doi.org/10.1111/j.17521688.2001.tb03624.x

Desta, W. M., & Bote, M. E. (2021). Wastewater treatment using a natural coagulant (Moringa oleifera seeds): optimization through response surface methodology. *Heliyon*, *7*(11), 08451. doi:10.1016/j.heliyon.2021.e08451.

Dias, J. M., Alvim-Ferraz, M. C., Almeida, M. F., Rivera-Utrilla, J., & Sánchez-Polo, M. (2007). Waste materials for activated carbon preparation and its use in aqueous-phase treatment: a review. *Journal of environmental management*, *85*(4), 833-846. https://doi.org/10.1016/j.jenvman.2007.07.031

Dongyu, L., Zheng, L., Zhang, H., & Deng, Y. (2018). Coagulation of colloidal particles with ferrate (VI). *Environmental Science: Water Research & Technology*, *4*(5), 701-710.701–710. doi: 10.1039/c8ew00048d.

Dotto, J., Fagundes-Klen, M. R., Veit, M. T., Palacio, S. M., & Bergamasco, R. (2018). Performance of different coagulants in the coagulation/flocculation process of textile wastewater. *Journal of cleaner production*, *208*, 656-665.

Dutta, A. K., Maji, S. K., & Adhikary, B. (2014). γ-Fe2O3 nanoparticles: an easily recoverable effective photo-catalyst for the degradation of rose bengal and methylene blue dyes in the waste-water treatment plant. *Materials Research Bulletin*, *49*, 28-34. https://doi.org/10.1016/j.materresbull.2013.08.024

Eagland, D. (1973). The colloidal state. *Contemporary Physics*, *14*(2), 119-148. https://doi.org/10.1080/00107517308213729

Ejimofor, M. I., Ezemagu, I. G., & Menkiti, M. C. (2021). RSM and ANN-GA modelling of colloidal particles removal from paint wastewater via coagulation method using modified Aguleri montmorillonite clay. *Current Research in Green and Sustainable Chemistry*, *4*, 100164. https://doi.org/10.1016/j.crgsc.2021.100164

Eman, N. A., Tan, C. S., & Makky, E. A. (2014). Impact of Moringa oleifera cake residue application on wastewater treatment: a case study. *Journal of Water Resource and Protection*, *Vol.6 No.7,* doi:10.4236/jwarp.2014.67065.

El-Rahman, K. A., El-Kamash, A. M., El-Sourougy, M. R., & Abdel-Moniem, N. M. (2006). Thermodynamic modeling for the removal of Cs+, Sr 2+, Ca 2+ and Mg 2+ ions from aqueous waste solutions using zeolite A. *Journal of radioanalytical and nuclear chemistry*, *268*(2), 221-230. https://doi.org/10.1007/s10967-006-0157-y

Ernest, E., Onyeka, O., David, N., & Blessing, O. (2017). Effects of pH, dosage, temperature and mixing speed on the efficiency of water melon seed in removing the turbidity and colour of Atabong River, Awka-Ibom State, Nigeria. *International Journal of Advanced Engineering, Management and Science*, *3*(5), 239833. https://dx.doi.org/10.24001/ijaems.3.5.4

Estrella, M. C. P., Jacinto Bias III, V., David, G. Z., & Taup, M. A. (2000). A double-blind, randomized controlled trial on the use of malunggay (Moringa oleifera) for augmentation of the volume ofbreastmilk among non-nursing mothers of preterm infants. *Phillipp J Pediatr*, *49*(1), 3-6.

FAO. (2007), Agriculture et rareté de l'eau: une approche programmatique pour l'efficacité de l'utilisation de l'eau et la productivité agricole. COAG/2007/7, Rome, pp15.

Fatombi, J. K., Jossé, R. G., Wotto, V., Aminou, T., & Coulomb, B. (2007). Paramètres physico-chimiques de l'eau d'Opkara traitée par les graines de Moringa oleifera. *JOURNAL-SOCIETE OUEST AFRICAINE DE CHIMIE*, *23*, 75.

Ferreira, S. C., Bruns, R. E., Ferreira, H. S., Matos, G. D., David, J. M., Brandão, G. C., ... & Dos Santos, W. N. L. (2007). Box-Behnken design: An alternative

for the optimization of analytical methods. *Analytica chimica acta*, *597*(2), 179-186. https://doi.org/10.1016/j.aca.2007.07.011

Foidl, N., Makkar, H. P. S., & Becker, K. (2001). The potential of Moringa Oleifera for agricultural and industrial uses', in *What development potential for Moringa products ?* Dar Es Salaam, Tanzania.

Freeman III, A. M. (2010). Water pollution policy. In *Public policies for environmental protection* (pp. 179-224). Routledge.

Gallão, M. I., Damasceno, L. F., & de Brito, E. S. (2006). Avaliação química e estrutural da semente de moringa. *Revista Ciência Agronômica*, *37*(1), 106-109.

Gao, B. Y., Wang, Y., Yue, Q. Y., Wei, J. C., & Li, Q. (2007). Color removal from simulated dye water and actual textile wastewater using a composite coagulant prepared by ployferric chloride and polydimethyldiallylammonium chloride. *Separation and Purification Technology*, *54*(2), 157-163. https://doi.org/10.1016/j.seppur.2006.08.026

Garde, W. K., Buchberger, S. G., Wendell, D., & Kupferle, M. J. (2017). Application of Moringa Oleifera seed extract to treat coffee fermentation wastewater. *Journal of Hazardous Materials*, *329*, 102-109. doi:10.1016/j.jhazmat.2017.01.00.

Gassenschmidt, U., Jany, K. D., Bernhard, T., & Niebergall, H. (1995). Isolation and characterization of a flocculating protein from Moringa oleifera Lam. *Biochimica et Biophysica Acta (BBA)-General Subjects*, *1243*(3), 477-481. doi : 10.1016/0304-4165(94)00176-x.

Gautam, S., & Saini, G. (2020). Use of natural coagulants for industrial wastewater treatment. *Global Journal of Environmental Science and Management*, *6*(4), 553-578.

Gautam, S., Arora, A. S., Singh, A. K., Ekka, P., Daniel, H., Gokul, B., ... & Lyngdoh, J. F. (2021). Coagulation influencing parameters investigation on textile industry discharge using Strychnos potatorum seed powders. *Environment, Development and Sustainability*, *23*, 5666-5673.

Gerba, C. P., & Pepper, I. L. (2019). Drinking water treatment. In *Environmental and Pollution Science* (pp. 435-454). Academic Press. https://doi.org/10.1016/B978-0-12-814719-1.00024-0

Ghebremichael, K. A., Gunaratna, K. R., Henriksson, H., Brumer, H., Dalhammar, G. (2005). A simple purification and activity assay of the coagulant protein from Moringa oleifera seed. *Water Research*, *39*(11), 2338–2344. https://doi.org/10.1016/j.watres.2005.04.012

Gholami, M., NASERI, S., ALIZADEH, F. M., Mesdaghinia, A. R., Vaezi, F., MAHVI, A., & NADAFI, K. (2001). Dye removal from effluents of textile industries by ISO9888 method and membrane technology.

Giakisikli, G., & Anthemidis, A. N. (2013). Magnetic materials as sorbents for metal/metalloid preconcentration and/or separation. A review. *Analytica chimica acta*, *789*, 1-16. https://doi.org/10.1016/j.aca.2013.04.021

Gideon, S., & Clinton, P.R. (2010). Coagulation efficiency of Moringa oleifera for removal of turbidity and reduction of total coliform as compared to aluminum sulfate. *African journal of agricultural research*, *5*(21), 2939-2944. Microsoft Word - Sarpong and Richardson pdf (academicjournals.org)

Gidde, M.R., Bhalerao, A.R., & Malusare, C.N. (2012). Comparative study of different forms of Moringa oleifera extracts for turbidity removal. *International Journal of Engineering Research and Development*, *2*(1), 14-21. ISSN: 2278-067X.

Gleick, P. H. (2002). *Dirty-water: estimated deaths from water-related diseases 2000-2020* (pp. 1-12). Oakland: Pacific Institute for Studies in Development, Environment, and Security.

Grizzetti, B., Lanzanova, D., Liquete, C., Reynaud, A., & Cardoso, A. C. (2016). Assessing water ecosystem services for water resource management. *Environmental Science & Policy*, *61*, 194-203 doi: 10.1016/j.envsci.2016.04.008.

Guan, X., & Yao, H. (2008). Optimization of Viscozyme L-assisted extraction of oat bran protein using response surface methodology. *Food chemistry*, *106*(1), 345-351. doi:10.1016/j.foodchem.2007.05.041.

Guo, R. (2021). *Cross-border environmental pollution and human health*, *Cross-Border Resource Management*. doi: 10.1016/b978-0-323-91870-1.00010-0.

Guo, X., & Wang, J. (2019). Sorption of antibiotics onto aged microplastics in freshwater and seawater. *Marine Pollution Bulletin*, *149*, 110511. https://doi.org/10.1016/j.marpolbul.2019.110511

Gupta, V. K., Ali, I., Saleh, T. A., Nayak, A., & Agarwal, S. (2012). Chemical treatment technologies for waste-water recycling—an overview. *Rsc Advances*, *2*(16), 6380-6388.

Haaland, P.D. (1989). Experimental Design in Biotechnology (1st ed.). CRC Press. https://doi.org/10.1201/9781003065968

Hamadeen, H. M., Elkhatib, E. A., Badawy, M. E., & Abdelgaleil, S. A. (2021). Novel low cost nanoparticles for enhanced removal of chlorpyrifos from

wastewater: sorption kinetics, and mechanistic studies. *Arabian Journal of Chemistry*, *14*(3), 102981. https://doi.org/10.1016/j.arabjc.2020.102981

Hamed, M. M., Ahmed, I. M., & Metwally, S. S. (2014). Adsorptive removal of methylene blue as organic pollutant by marble dust as eco-friendly sorbent. *Journal of Industrial and Engineering Chemistry*, *20*(4), 2370-2377. https://doi.org/10.1016/j.jiec.2013.10.015

Haseena, M., Malik, M. F., Javed, A., Arshad, S., Asif, N., Zulfiqar, S., & Hanif, J. (2017). Water pollution and human health. *Environmental Risk Assessment and Remediation*, *1*(3).

Halder, J. N., & Islam, M. N. (2015). Water pollution and its impact on the human health. *Journal of environment and human*, *2*(1), 36-46. DOI: 10.15764/EH.2015.01005

Harif, T., Khai, M., & Adin, A. (2012). Electrocoagulation versus chemical coagulation: Coagulation/flocculation mechanisms and resulting floc characteristics. *Water Research*, *46*(10), 3177-3188. https://doi.org/10.1016/j.watres.2012.03.034

Harter, T. (2003). Groundwater quality and groundwater pollution. DOI 10.3733/ucanr.8084

Hekmat, S., Morgan, K., Soltani, M., & Gough, R. (2015). Sensory evaluation of locally-grown fruit purees and inulin fibre on probiotic yogurt in Mwanza, Tanzania and the microbial analysis of probiotic yogurt fortified with Moringa oleifera. *Journal of health, population, and nutrition*, *33*(1), 60.

Hendrawati, Yuliastri, I. R., Nurhasni, Rohaeti, E., Effendi, H., & Darusman, L. K. (2016). The use of Moringa Oleifera Seed Powder as Coagulant to Improve the Quality of Wastewater and Ground Water. *IOP Conference Series: Earth and Environmental Science, 31, 012033.* doi:10.1088/1755-1315/31/1/012033.

Hernandez, J. T., Muriel, A. A., Tabares, J. A., Alcázar, G. P., & Bolaños, A. (2015). Preparation of Fe3O4 nanoparticles and removal of methylene blue through adsorption. In *Journal of Physics: Conference Series* (Vol. 614, No. 1, p. 012007). IOP Publishing. **DOI** 10.1088/1742-6596/614/1/012007

Hinrichsen, D., & Tacio, H. (2002). The coming freshwater crisis is already here. *The linkages between population and water. Washington, DC: Woodrow Wilson International Center for Scholars*, 1-26.

Huang, B. C., He, C. S., Fan, N. S., Jin, R. C., & Yu, H. Q. (2020). Envisaging wastewater-to-energy practices for sustainable urban water pollution control: Current achievements and future prospects. *Renewable and Sustainable Energy Reviews*, *134*, 110134.

Hu, H., & Xu, K. (2020). Physicochemical technologies for HRPs and risk control. In *High-risk pollutants in wastewater* (pp. 169-207). Elsevier. https://doi.org/10.1016/B978-0-12-816448-8.00008-3

Iftekhar, S., Ramasamy, D. L., Srivastava, V., Asif, M. B., & Sillanpää, M. (2018). Understanding the factors affecting the adsorption of Lanthanum using different adsorbents: a critical review. *Chemosphere*, *204*, 413-430.doi: 10.1016/j.chemosphere.2018.04.053.

Igwegbe, C. A., Banach, A., & Ahmadi, S. (2018). Adsorption of reactive blue 19 from aqueous environment on magnesium oxide nanoparticles: kinetic, isotherm and thermodynamic studies. *Pharm Chem J*, *5*, 111-121.

Ihsanullah, I. (2020). MXenes (two-dimensional metal carbides) as emerging nanomaterials for water purification: Progress, challenges and prospects. *Chemical Engineering Journal*, *388*, 124340. https://doi.org/10.1016/j.cej.2020.124340

Inglezakis, V. J., Balsamo, M., & Montagnaro, F. (2020). Liquid–solid mass transfer in adsorption systems—An overlooked resistance?. *Industrial & Engineering Chemistry Research*, *59*(50), 22007-22016.. doi: 10.1021/acs.iecr.0c05032.

Jahn, S. A., Musnad, H. A., & Burgstaller, H. (1986). The tree that purifies water: cultivating multipurpose Moringaceae in the Sudan. *Unasylva*, *38*(152), 23-28. **https://hdl.handle.net/10535/8421**

Jena, P. R., Basu, J. K., & De, S. (2004). A generalized shrinking core model for multicomponent batch adsorption processes. *Chemical Engineering Journal*, *102*(3), 267-275.doi: 10.1016/j.cej.2003.12.006.

Jiang, J. Q. (2015). The role of coagulation in water treatment. *Current Opinion in Chemical Engineering*, *8*, 36-44. https://doi.org/10.1016/j.coche.2015.01.008

Kabore A. (2011). Study of the flocculating power and purifying qualities of Moringa oleifera seeds in the treatment of raw drinking water in sub-Saharan Africa: the case of Burkina Faso water. DEA thesis, University of Ouagadougou, Ouagadougou Burkina Faso, 54 p.(In french).

Kalbar, P. P., Karmakar, S., & Asolekar, S. R. (2016). Life cycle-based decision support tool for selection of wastewater treatment alternatives. *Journal of Cleaner Production*, *117*, 64-72.

Kansal, S. K., & Kumari, A. (2014). Potential of M. oleifera for the treatment of water and wastewater. *Chemical reviews*, *114*(9), 4993-5010. https://doi.org/10.1021/cr400093w

Kapse, G., & Samadder, S. R. (2021). Moringa oleifera seed defatted press cake based biocoagulant for the treatment of coal beneficiation plant effluent. *Journal of Environmental Management*, *296*, 113202.

Karazhiyan, H., Razavi, S. M., & Phillips, G. O. (2011). Extraction optimization of a hydrocolloid extract from cress seed (Lepidium sativum) using response surface methodology. *Food Hydrocolloids*, *25*(5), 915-920. doi:10.1016/j.foodhyd.2010.08.022.

Karim, A. B., Mounir, B., Hachkar, M., Bakasse, M., & Yaacoubi, A. (2010). Élimination du colorant basique «Bleu de Méthylène» en solution aqueuse par l'argile de Safi. *Revue des sciences de l'eau*, *23*(4), 375-388. https://doi.org/10.7202/045099ar

Karim, O., Kayode, R., Oyeyinka, S., & Oyeyinka, A. (2015). Physicochemical properties of stiff dough 'amala'prepared from plantain (Musa Paradisca) flour and Moringa (Moringa oleifera) leaf powder. *Hrana u zdravlju i bolesti: znanstveno-stručni časopis za nutricionizam i dijetetiku*, *4*(1), 48-58. https://hrcak.srce.hr/147064

Karmakar, A., Karmakar, S., & Mukherjee, S. (2010). Properties of various plants and animals feedstocks for biodiesel production. *Bioresource technology*, *101*(19), 7201-7210. https://doi.org/10.1016/j.biortech.2010.04.079

Kecili, R., & Hussain, C. M. (2018). Mechanism of adsorption on nanomaterials. In *Nanomaterials in chromatography* (pp. 89-115). Elsevier. https://doi.org/10.1016/B978-0-12-812792-6.00004-2

Khalafalla, M. M., Abdellatef, E., Dafalla, H. M., Nassrallah, A. A., Aboul-Enein, K. M., Lightfoot, D. A., ... & El-Shemy, H. A. (2010). Active principle from Moringa oleifera Lam leaves effective against two leukemias and a hepatocarcinoma. *African Journal of Biotechnology*, *9*(49), 8467-8471. DOI: 10.5897/AJB10.996

Khataee, A. R., & Kasiri, M. B. (2010). Artificial neural networks modeling of contaminated water treatment processes by homogeneous and heterogeneous nanocatalysis. *Journal of Molecular Catalysis A: Chemical*, *331*(1-2), 86-100. https://doi.org/10.1016/j.molcata.2010.07.016

Khataee, A. R., & Kasiri, M. B. (2011). Modeling of biological water and wastewater treatment processes using artificial neural networks. *CLEAN–Soil, Air, Water*, *39*(8), 742-749. **https://doi.org/10.1002/clen.201000234**

Kian, L. K., Jawaid, M., Ariffin, H., & Alothman, O. Y. (2017). Isolation and characterization of microcrystalline cellulose from roselle fibers. *International Journal of Biological Macromolecules*, *103*, 931-940. https://doi.org/10.1016/j.ijbiomac.2017.05.135

Kifuani, K. M., Mayeko, A. K. K., Vesituluta, P. N., Lopaka, B. I., Bakambo, G. E., Mavinga, B. M., & Lunguya, J. M. (2018). Adsorption d'un colorant basique, Bleu de Méthylène, en solution aqueuse, sur un bioadsorbant issu de déchets agricoles de Cucumeropsis mannii Naudin. *International Journal of Biological and Chemical Sciences*, *12*(1), 558-575.

Kilingo, F. M., Bernard, Z., & Hongbin, C. (2022). Study of domestic wastewater treatment using Moringa oleifera coagulant coupled with vertical flow constructed wetland in Kibera Slum, Kenya. *Environmental Science and Pollution Research*, *29*(24), 36589-36607. https://doi.org/10.1007/s11356-022-18692-3.

Kim, T. H., Lee, Y., Yang, J., Lee, B., Park, C., & Kim, S. (2004). Decolorization of dye solutions by a membrane bioreactor (MBR) using white-rot fungi. *Desalination*, *168*, 287-293. https://doi.org/10.1016/j.desal.2004.07.011

Kitchener, B. G., Wainwright, J., & Parsons, A. J. (2018). A review of the principles of turbidity measurement. *Progress in Physical Geography*, *41*(5), 620-642. https://doi.org/10.1177/0309133317726540

Kleiman, R., Ashley, D. A., & Brown, J. H. (2008). Comparison of two seed oils used in cosmetics, moringa and marula. *Industrial Crops and Products*, *28*(3), 361-364.doi:
10.1016/j.indcrop.2008.04.003.

Kolawole, F. L., Balogun, M. A., Opaleke, D. O., & Amali, H. E. (2013). An evaluation of nutritional and sensory qualities of wheat-moringa cake. *Agrosearch*, *13*(1), 87-94.

Koohestanian, A., Hosseini, M., & Abbasian, Z. (2008). The separation method for removing of colloidal particles from raw water. *American-Eurasian J. Agric. & Environ. Sci*, *4*(2), 266-273.ISSN 1818-6769 Available at: http://idosi.org/aejaes/jaes4(2)/20.pdf

Koshani, R., Tavakolian, M., & van de Ven, T. G. (2020). Cellulose-based dispersants and flocculants. *Journal of Materials Chemistry B*, *8*(46), 10502-10526.10502–10526.
doi: 10.1039/d0tb02021d.

Kosmulski, M. (2001). *Chemical properties of material surfaces* (Vol. 102). CRC press.

Krishnan, V. N., & Ramesh, A. (2013). Synthesis and characterization of cellulose nanofibers from coconut coir fibers. *IOSR J. appl. chem*, *6*, 18-23. https://doi.org/10.9790/57360631823.

Kumari, P., Sharma, P., Srivastava, S., & Srivastava, M. M. (2006). Biosorption studies on shelled Moringa oleifera Lamarck seed powder: removal and recovery

of arsenic from aqueous system. *International Journal of Mineral Processing*, *78*(3), 131-139. https://doi.org/10.1016/j.minpro.2005.10.001

Kumar, A., Negi, Y. S., Choudhary, V., & Bhardwaj, N. K. (2014). Characterization of cellulose nanocrystals produced by acid-hydrolysis from sugarcane bagasse as agro-waste. *Journal of materials physics and chemistry*, *2*(1), 1-8.

Kumar, G., Sivagurunathan, P., Pugazhendhi, A., Thi, N. B. D., Zhen, G., Chandrasekhar, K., & Kadier, A. (2017). A comprehensive overview on light independent fermentative hydrogen production from wastewater feedstock and possible integrative options. *Energy Conversion and Management*, *141*, 390-402. https://doi.org/10.1016/j.enconman.2016.09.087

Kusuma, H. S., Amenaghawon, A. N., Darmokoesoemo, H., Neolaka, Y. A., Widyaningrum, B. A., Anyalewechi, C. L., & Orukpe, P. I. (2021). Evaluation of extract of Ipomoea batatas leaves as a green coagulant–flocculant for turbid water treatment: Parametric modelling and optimization using response surface methodology and artificial neural networks. *Environmental Technology & Innovation*, *24*, 102005. https://doi.org/10.1016/j.eti.2021.102005

Lalas, S., & Tsaknis, J. (2002). Characterization of Moringa oleifera seed oil variety "Periyakulam 1". *Journal of food composition and analysis*, *15*(1), 65-77. https://doi.org/10.1006/jfca.2001.1042

Landrigan, P. J., Stegeman, J. J., Fleming, L. E., Allemand, D., Anderson, D. M., Backer, L. C., ... & Rampal, P. (2020). Human health and ocean pollution. *Annals of global health*, *86*(1). doi: 10.5334/aogh.2831

Lee, A., Chaibakhsh, N., Rahman, M.B.A., Basri, M., & Tejo, B.A. (2010). Optimized enzymatic synthesis of levulinate ester in solvent-free system. *Industrial Crops and Products*, *32*(3), 246-251. https://doi.org/10.1016/j.indcrop.2010.04.022

Lee, K. E., Morad, N., Teng, T. T., & Poh, B. T. (2012). Development, characterization and the application of hybrid materials in coagulation/flocculation of wastewater: A review. *Chemical Engineering Journal, 203, 370–386.* doi:10.1016/j.cej.2012.06.109

Magdalane, C. M., Kaviyarasu, K., Vijaya, J. J., Siddhardha, B., Jeyaraj, B., Kennedy, J., & Maaza, M. (2017). Evaluation on the heterostructured CeO2/Y2O3 binary metal oxide nanocomposites for UV/Vis light induced photocatalytic degradation of Rhodamine-B dye for textile engineering application. *Journal of Alloys and Compounds*, *727*, 1324-1337. https://doi.org/10.1016/j.jallcom.2017.08.209

Mahmood, K. T., Mugal, T., & Haq, I. U. (2010). Moringa oleifera: a natural gift-A review. *Journal of Pharmaceutical Sciences and Research*, *2*(11), 775.

Mahmoud, D. K., Salleh, M. A. M., Karim, W. A. W. A., Idris, A., & Abidin, Z. Z. (2012). Batch adsorption of basic dye using acid treated kenaf fibre char: Equilibrium, kinetic and thermodynamic studies. *Chemical Engineering Journal*, *181*, 449-457. https://doi.org/10.1016/j.cej.2011.11.116

Mallevialle, J., Bruchet, A., & Fiessinger, F. (1984). How safe are organic polymers in water treatment?. *Journal-American Water Works Association*, *76*(6), 87-93. **https://doi.org/10.1002/j.1551-8833.1984.tb05354.x**

Mara, D. (2013). *Domestic wastewater treatment in developing countries*. Routledge.

Mareddy, A. R. (2017). Impacts on water environment, *Environmental Impact Assessment*. doi: 10.1016/b978-0-12-811139-0.00006-2.

Martyn, C. N., Osmond, C., Edwardson, J. A., Barker, D. J. P., Harris, E. C., & Lacey, R. F. (1989). Geographical relation between Alzheimer's disease and aluminium in drinking water. *The Lancet*, *333*(8629), 59-62. https://doi.org/10.1016/S0140-6736(89)91425-6

May, D. B., & Sivakumar, M. (2009). Prediction of urban stormwater quality using artificial neural networks. *Environmental Modelling & Software*, *24*(2), 296 302. http://doi.org/10.1016/j.envisoft.2008.07.004.

McRobb, C. M., & Holt, D. W. (2008). Methylene blue-induced methemoglobinemia during cardiopulmonary bypass? A case report and literature review. *The Journal of extra-corporeal technology*, *40*(3), 206.

Melesse, A., Steingass, H., Boguhn, J., Schollenberger, M., & Rodehutscord, M. (2012). Effects of elevation and season on nutrient composition of leaves and green pods of Moringa stenopetala and Moringa oleifera. *Agroforestry systems*, *86*, 505-518. https://doi.org/10.1007/s10457-012-9514-8

Melikoğlu, A. Y., Bilek, S. E., & Cesur, S. (2019). Optimum alkaline treatment parameters for the extraction of cellulose and production of cellulose nanocrystals from apple pomace. *Carbohydrate polymers*, *215*, 330-337. https://doi.org/10.1016/j.carbpol.2019.03.103

Meneghel, A. P., Gonçalves, A. C., Rubio, F., Dragunski, D. C., Lindino, C. A., & Strey, L. (2013). Biosorption of cadmium from water using *Moringa* (*Moringa oleifera* Lam.) seeds. *Water, Air, & Soil Pollution*, *224*(3), 1-13. doi:10.1007/s11270-012-1383-2.

Menkiti, M. C., & Ejimofor, M. I. (2016). Experimental and artificial neural network application on the optimization of paint effluent (PE) coagulation using novel Achatinoidea shell extract (ASE). *Journal of Water Process Engineering, 10, 172–187.* doi:10.1016/j.jwpe.2015.09.010

Merwad, A. E. (2018). Influence of Natural Plant Extracts in Reducing Soil and Water Contaminants. *Sustainability of Agricultural Environment in Egypt: Part I*, 161-188. doi:10.1007/698_2018_260.

Mishra, G., Singh, P., Verma, R., Kumar, S., Srivastav, S., Jha, K. K., & Khosa, R. L. (2011). Traditional uses, phytochemistry and pharmacological properties of Moringa oleifera plant: An overview. *Der Pharmacia Lettre*, *3*(2), 141-164.

Mistry, B. D. (2009). A handbook of spectroscopic data. *Chemistry*, *600*.

Mohamed, M. A., Salleh, W. N. W., Jaafar, J., Asri, S. M., & Ismail, A. F. (2015). Physicochemical properties of "green" nanocrystalline cellulose isolated from recycled newspaper. *Rsc Advances*, *5*(38), 29842-29849.**https://doi.org/10.1039/C4RA17020B**

Mofijur, M., Masjuki, H. H., Kalam, M. A., Atabani, A. E., Arbab, M. I., Cheng, S. F., & Gouk, S. W. (2014). Properties and use of Moringa oleifera biodiesel and diesel fuel blends in a multi-cylinder diesel engine. *Energy Conversion and Management*, *82*, 169-176. doi: 10.1016/j.enconman.2014.02.073.

Moriana, R., Vilaplana, F., & Ek, M. (2016). Cellulose nanocrystals from forest residues as reinforcing agents for composites: A study from macro-to nano-dimensions. *Carbohydrate polymers*, *139*, 139-149. https://doi.org/10.1016/j.carbpol.2015.12.020

Moulin, M., Mossou, E., Signor, L., Kieffer-Jaquinod, S., Kwaambwa, H. M., Nermark, F., Gutfreund, P., Mitchell, E. P., Haertlein, M., Forsyth, V.T., Rennie, A. R . (2019). Towards a molecular understanding of the water purification properties of Moringa seed proteins. *Journal of Colloid and Interface Science*, *554*. https://doi.org/10.1016/j.jcis.2019.06.071

Moyo, B., Masika, P. J., Hugo, A., & Muchenje, V. (2011). Nutritional characterization of Moringa (Moringa oleifera Lam.) leaves. *African Journal of Biotechnology*, *10*(60), 12925-12933. 10.5897/AJB10.1599

Muyibi, S. A., & Okuofu, C. A. (1995). Coagulation of low turbidity surface waters with *Moringa oleifera* seeds. *International Journal of Environmental Studies, 48(3-4), 263–273.* doi:10.1080/00207239508710996.

Myers, R.H., Montgomry, D.C., & Anderson-Cook, C.M. (2009). Response Surface Methodology and Product Optimization Using Designed Experimeents. Third edition. *Wiley Series In Probability and Statistics.*

Nand, V., Maata, M., Koshy, K., & Sotheeswaran, S. (2012). Water purification using moringa oleifera and other locally available seeds in Fiji for heavy metal removal. *International Journal of Applied*, *2*(5), 125-129. From 14-with-cover-page-v2.pdf (d1wqtxts1xzle7.cloudfront.net)

Nandi, B. K., Goswami, A., & Purkait, M. K. (2009). Adsorption characteristics of brilliant green dye on kaolin. *Journal of hazardous materials*, *161*(1), 387-395. https://doi.org/10.1016/j.jhazmat.2008.03.110

Naduparambath, S., Jinitha, T. V., Shaniba, V., Sreejith, M. P., Balan, A. K., & Purushothaman, E. (2018). Isolation and characterisation of cellulose nanocrystals from sago seed shells. *Carbohydrate polymers*, *180*, 13-20. https://doi.org/10.1016/j.carbpol.2017.09.088

Nayeripour, M., & Kheshti, M. (Eds.). (2011). *Sustainable growth and applications in renewable energy sources*. BoD–Books on Demand.

Ndabigengesere, A., Narasiah, K.S., & Talbot, B.G. (1995). Active agents and mechanism of coagulation of turbid waters using Moringa oleifera. *Water Research*, *29*(2), 703–710. https://doi.org/10.1016/0043-1354(94)00161-Y

Ndabigengesere, A., & Narasiah, K. S. (1998 a). Quality of water treated by coagulation using Moringa oleifera seeds. *Water research*, *32*(3), 781-791. https://doi.org/10.1016/S0043-1354(97)00295-9

Ndabigengesere, A., & Narasiah, K. S. (1998 b). Use of Moringa oleifera seeds as a primary coagulant in wastewater treatment. *Environmental Technology*, *19*(8), 789-800. https://doi.org/10.1080/09593331908616735

Niaounakis, M., & Halvadakis, C. P. (2006). Olive processing waste management: literature review and patent survey. Second edition. Elsevier publisher. The boulevard, Langford Lane Kidlington, Oxford, OX5 1GB UK. 495P.

Nuruddin, M., Chowdhury, A., Haque, S. A., Rahman, M., Farhad, S. F., Jahan, M. S., & Quaiyyum, A. (2011). Extraction and characterization of cellulose microfibrils from agricultural wastes in an integrated biorefinery initiative. *biomaterials*, *3*, 5-6. https://doi.org/10.1007/s10570-010-9481-z

Ofor, M. O., & Nwufo, M. I. (2011). The search for alternative energy sources: Jatropha and moringa seeds for biofuel production. *Journal of Agriculture and Social Research (JASR)*, *11*(2), 87-94.

Okuda, T., Baes, A. U., Nishijima, W., & Okada, M. (2001). Isolation and characterization of coagulant extracted from Moringa oleifera seed by salt solution. *Water research*, *35*(2), 405-410. https://doi.org/10.1016/S0043-1354(00)00290-6

Oladoja, N. A., & Pan, G. (2015). Modification of local soil/sand with Moringa oleifera extracts for effective removal of cyanobacterial blooms. *Sustainable Chemistry and Pharmacy*, *2*, 37-43.

Olatunji, M. A., Khandaker, M. U., Mahmud, H. E., & Amin, Y. M. (2015). Influence of adsorption parameters on cesium uptake from aqueous solutions-a brief review. *RSC advances*, *5*(88), 71658-71683. **https://doi.org/10.1039/C5RA10598F**

O'Melia, C. R. (1998). Coagulation and sedimentation in lakes, reservoirs and water treatment plants. *Water science and technology*, *37*(2), 129-135. https://doi.org/10.1016/S0273-1223(98)00018-3

Onoji, S. E., Iyuke, S. E., Igbafe, A. I., & Daramola, M. O. (2017). Hevea brasiliensis (rubber seed) oil: modeling and optimization of extraction process parameters using response surface methodology and artificial neural network techniques, Biofuels. https://doi.org/10.1080/17597269.2017.1338122

Öztürk, D., & Şahan, T. 2015. Design and optimization of Cu (II) adsorption conditions from aqueous solutions by low-cost adsorbent pumice with response surface methodology. *Polish Journal of Environmental Studies*, *24*(4), 1749-1756. doi: 10.15244/pjoes/40270

Pala, A., & Tokat, E. (2002). Color removal from cotton textile industry wastewater in an activated sludge system with various additives. *Water research*, *36*(11), 2920-2925. https://doi.org/10.1016/S0043-1354(01)00529-2

Pang, F. M., Kumar, P., Teng, T. T., Omar, A. M., & Wasewar, K. L. (2011). Removal of lead, zinc and iron by coagulation–flocculation. *Journal of the Taiwan Institute of Chemical Engineers*, *42*(5), 809-815. https://doi.org/10.1016/j.jtice.2011.01.009

Prasanna, N. S., & Mitra, J. (2020). Isolation and characterization of cellulose nanocrystals from Cucumis sativus peels. *Carbohydrate polymers*, *247*, 116706. https://doi.org/10.1016/j.carbpol.2020.116706

Parsons, S . A., Jefferson, B. (2006). Introduction to potable water treatment processes (No. 04 ; TD430, P3.). Blackwell Pub. doi:10.1002/9781444305470.

Pereira, F. S. G., da Silva, A. M. R. B., Galvão, C. C., de Lima, V. F., de Assunção Montenegro, L. G. L., de Lima-Filho, N. M., & da Silva, V. L. (2015). Moringa oleifera as sustainable source for energetic biomass. *International Journal of Chemistry*, *7*(2), 177.doi: 10.5539/ijc.v7n2p177

Pokhrel, D., & Viraraghavan, T. (2008). Organic arsenic removal from an aqueous solution by iron oxide-coated fungal biomass: An analysis of factors influencing adsorption. *Chemical Engineering Journal*, *140*(1-3), 165-172. https://doi.org/10.1016/j.cej.2007.09.038

Price, M. L. (2007). The moringa tree. *ECHO technical note*, *17391*, 1-19.

Primack, R. B. and Morrison, R. A. (2013). Extinction, Causes of', *Encyclopedia of Biodiversity: Second Edition*, 3, pp. 401–412. doi: 10.1016/B978-0-12-384719-5.00050-2.

Quesada, H. B., Cusioli, L. F., de O Bezerra, C., Baptista, A. T., Nishi, L., Gomes, R. G., & Bergamasco, R. (2019). Acetaminophen adsorption using a low-cost adsorbent prepared from modified residues of Moringa oleifera Lam. seed husks. *Journal of Chemical Technology & Biotechnology*, *94*(10), 3147-3157. doi: 10.1002/jctb.6121.

Qiu, H., Lv, L., Pan, B. C., Zhang, Q. J., Zhang, W. M., & Zhang, Q. X. (2009). Critical review in adsorption kinetic models. *Journal of Zhejiang University-Science A*, *10*(5), 716-724. https://doi.org/10.1631/jzus.A0820524

Qu, X., Alvarez, P. J., & Li, Q. (2013). Applications of nanotechnology in water and wastewater treatment. *Water research*, *47*(12), 3931-3946. https://doi.org/10.1016/j.watres.2012.09.058

Rafatullah, M., Sulaiman, O., Hashim, R., & Ahmad, A. (2010). Adsorption of methylene blue on low-cost adsorbents: a review. *Journal of hazardous materials*, *177*(1-3), 70-80. https://doi.org/10.1016/j.jhazmat.2009.12.047

Rakshit, A. K., Naskar, B., & Moulik, S. P. (2021). Stability of hydrophobic colloids: Perspectives and current opinion. *Journal of Dispersion Science and Technology*, *42*(4), 503-513.doi: 10.1080/01932691.2019.1700133.

Ranade, V. V., & Bhandari, V. M. (2014). Industrial Wastewater Treatment, Recycling, and Reuse-Past, Present and Future. In *Industrial Wastewater Treatment, Recycling and Reuse* (pp. 521-535). Elsevier Inc. 10.1016/B978-0-08-099968-5.00014-3

Razis, A. A., Ibrahim, M. D., & Kntayya, S. B. (2014). Health benefits of Moringa oleifera. *Asian pac J cancer prev*, *15*(20), 8571-8576. doi: 10.7314/APJCP.2014.15.20.8571.

Reddy, D. H. K., Harinath, Y., Seshaiah, K., & Reddy, A. V. R. (2010). Biosorption of Pb (II) from aqueous solutions using chemically modified Moringa oleifera tree leaves. *Chemical Engineering Journal*, *162*(2), 626-634. https://doi.org/10.1016/j.cej.2010.06.010

Reddy, D. H. K., Ramana, D. K. V., Seshaiah, K., & Reddy, A. V. R. (2011). Biosorption of Ni (II) from aqueous phase by Moringa oleifera bark, a low cost biosorbent. *Desalination*, *268*(1-3), 150-157. https://doi.org/10.1016/j.desal.2010.10.011

Reddy, D. H. K., Seshaiah, K., Reddy, A. V. R., & Lee, S. M. (2012). Optimization of Cd (II), Cu (II) and Ni (II) biosorption by chemically modified Moringa

oleifera leaves powder. *Carbohydrate Polymers*, *88*(3), 1077-1086. https://doi.org/10.1016/j.carbpol.2012.01.073

Renault, F., Sancey, B., Charles, J., Morin-Crini, N., Badot, P. M., Winterton, P., & Crini, G. (2009). Chitosan flocculation of cardboard-mill secondary biological wastewater. *Chemical Engineering Journal*, *155*(3), 775-783. https://doi.org/10.1016/j.cej.2009.09.023

Rondeau, V., Commenges, D., Jacqmin-Gadda, H., Dartigues, J. F. (2000). Relation between aluminum concentrations in drinking water and Alzheimer's disease: An 8-year follow-up study. *American Journal of Epidemiology*, *152*(1), 59–66. https://doi.org/10.1093/aje/152.1.59

Rosenwinkel, K. H., Weichgrebe, D., Meyer, H., & Wendler, D. (2001). Suspended solids from industrial and municipal origins. *Ecotoxicology and environmental safety*, *50*(2), 135-142.doi:10.1006/eesa.2001.2082.

Saini, R. K., Sivanesan, I., & Keum, Y. S. (2016). Phytochemicals of Moringa oleifera: a review of their nutritional, therapeutic and industrial significance. *3 Biotech*, *6*, 1-14. https://doi.org/10.1007/s13205-016-0526-3

Sajidu, S. M., Henry, E. M. T., Kwamdera, G., & Mataka, L. (2005). Removal of lead, iron and cadmium ions by means of polyelectrolytes of the Moringa oleifera whole seed kernel. *WIT Transactions on Ecology and the Environment*, *80*. doi:10.2495/WRM050261.

Sánchez-Machado, D. I., Núñez-Gastélum, J. A., Reyes-Moreno, C., Ramírez-Wong, B., & López-Cervantes, J. (2010). Nutritional quality of edible parts of Moringa oleifera. *Food analytical methods*, *3*, 175-180. https://doi.org/10.1007/s12161-009-9106-z

Saranya, P., Ramesh, S. T., & Gandhimathi, R. (2014). Effectiveness of natural coagulants from non-plant-based sources for water and wastewater treatment—A review. *Desalination and Water Treatment*, *52*(31-33), 6030-6039. https://doi.org/10.1080/19443994.2013.812993

Saritha, V., Srinivas, N., & Srikanth Vuppala, N. V. (2017). Analysis and optimization of coagulation and flocculation process. *Applied Water Science*, *7*, 451-460. doi: 10.1007/s13201-014-0262-y

Saravanan, A., Kumar, P. S., Jeevanantham, S., Karishma, S., Tajsabreen, B., Yaashikaa, P. R., & Reshma, B. (2021). Effective water/wastewater treatment methodologies for toxic pollutants removal: Processes and applications towards sustainable development. *Chemosphere*, *280*, 130595.doi: 10.1016/j.chemosphere.2021.130595.

Sazli, M. H. (2006). A brief review of feed-forward neural networks. *Communications Faculty of Sciences University of Ankara Series A2-A3 Physical Sciences and Engineering*, *50*(01).

Schulz, H., & Baranska, M. (2007). Identification and quantification of valuable plant substances by IR and Raman spectroscopy. *Vibrational Spectroscopy*, *43*(1), 13-25. https://doi.org/10.1016/j.vibspec.2006.06.001

Seghosime, A., Awudza, J. A. M., Richard, B., & Kwarteng, S. O. (2017). Comparative studies on proximate composition and phytochemical screening of mango, key lime, African star apple and African pear seeds as possible coagulant aids for water treatment. *American Journal of Environmental Sciences*, *13*(4), 325-333. doi:10.3844/ajessp.2017.325.333

Sengupta, M. E., Keraita, B., Olsen, A., Boateng, O. K., Thamsborg, S. M., Pálsdóttir, G. R., & Dalsgaard, A. (2012). Use of Moringa oleifera seed extracts to reduce helminth egg numbers and turbidity in irrigation water. *Water research*, *46*(11), 3646-3656. https://doi.org/10.1016/j.watres.2012.04.011

Shah, D. P., Jain, V. C., Daldavi, H. P., Ramani, V. D., Patel, K. G., Saralai, M. G., & Jani, G. K. (2011). A preliminary investigation of Moringa oleifera Lam gum as a pharmaceutical excipient. *International Journal of Pharmacy Research & Technology (IJPRT)*, *1*(1), 12-16. https://doi.org/10.31838/ijprt/01.01.03

Shak, K. P. Y., & Wu, T. Y. (2014). Coagulation–flocculation treatment of high-strength agro-industrial wastewater using natural Cassia obtusifolia seed gum: Treatment efficiencies and flocs characterization. *Chemical Engineering Journal, 256, 293–305.* doi:10.1016/j.cej.2014.06.093

Shan, T. C., Matar, M. A., Makky, E. A., & Ali, E. N. (2017). The use of Moringa oleifera seed as a natural coagulant for wastewater treatment and heavy metals removal. *Applied Water Science*, *7*(3), 1369-1376. doi: 10.1007/s13201-016-0499-8.

Sharifudin, S. A., Fakurazi, S., Hidayat, M. T., Hairuszah, I., Aris Mohd Moklas, M., & Arulselvan, P. (2013). Therapeutic potential of Moringa oleifera extracts against acetaminophen-induced hepatotoxicity in rats. *Pharmaceutical Biology*, *51*(3), 279-288. https://doi.org/10.3109/13880209.2012.720993

Shmeis, R. M. A. (2018). Water chemistry and microbiology. In *Comprehensive analytical chemistry* (Vol. 81, pp. 1-56). Elsevier.doi: 10.1016/bs.coac.2018.02.001.

Siddhuraju, P., & Becker, K. (2003). Antioxidant properties of various solvent extracts of total phenolic constituents from three different agroclimatic origins of drumstick tree (Moringa oleifera Lam.) leaves. *Journal of agricultural and food chemistry*, *51*(8), 2144-2155. https://doi.org/10.1021/jf020444+

Singh, S., Gaikwad, K. K., Park, S. I., & Lee, Y. S. (2017). Microwave-assisted step reduced extraction of seaweed (Gelidiella aceroso) cellulose nanocrystals. *International journal of biological macromolecules*, *99*, 506-510. https://doi.org/10.1016/j.ijbiomac.2017.03.004

Singh, G., & Patidar, S. K. (2020). Water quality restoration by harvesting mixed culture microalgae using *Moringa oleifera*. *Water Environment Research*, *92*(9), 1268-1282. doi:10.1002/wer.1322.

Sotheeswaran, S., Nand, V., Maata, M., & Koshy, K. (2011). Moringa oleifera and other local seeds in water purification in developing countries. *Research Journal of chemistry and environment*, *15*(2), 135-138.

Spellman FR. 2007. The Science of Water: Concepts and Applications. Second Edition CRC Press, *Taylor & Francis Group,* Boca Raton London New York.

Stone, A., Massey, A., Theobald, M., Styslinger, M., Kane, D., Tung, A., ... & Davert, E. (2011). Innovations that nourish the planet Africa's indigenous crops. *Africa's Indigenous Crops*, *23*.

Subha, E., Sasikala, S., & Muthuraman, G. (2015). Removal of phosphate from wastewater using natural adsorbents. *Int. J. ChemTech Res.*, *7*, pp 3095-3099. ISSN: 0974-4290.

Tahir, S. S., & Rauf, N. (2006). Removal of a cationic dye from aqueous solutions by adsorption onto bentonite clay. *Chemosphere*, *63*(11), 1842-1848. https://doi.org/10.1016/j.chemosphere.2005.10.033

Tang, X., Zheng, H., Teng, H., Sun, Y., Guo, J., Xie, W., ... & Chen, W. (2016). Chemical coagulation process for the removal of heavy metals from water: a review. *Desalination and water treatment*, *57*(4), 1733-1748.

Teh, C. Y., Budiman, P. M., Shak, K. P. Y., & Wu, T. Y. (2016). Recent advancement of coagulation–flocculation and its application in wastewater treatment. *Industrial & Engineering Chemistry Research*, *55*(16), 4363-4389. https://doi.org/10.1021/acs.iecr.5b04703

Toppo, R., Roy, B. K., Gora, R. H., Baxla, S. L., & Kumar, P. (2015). Hepatoprotective activity of Moringa oleifera against cadmium toxicity in rats. *Veterinary world*, *8*(4), 537. 10.14202/vetworld.2015.537-540

Tran, H. N., You, S. J., Hosseini-Bandegharaei, A., & Chao, H. P. (2017). Mistakes and inconsistencies regarding adsorption of contaminants from aqueous solutions: a critical review. *Water research*, *120*, 88-116. https://doi.org/10.1016/j.watres.2017.04.014

Trinh, T. K., & Kang, L. S. (2011). Response surface methodological approach to optimize the coagulation–flocculation process in drinking water

treatment. *Chemical engineering research and design*, *89*(7), 1126-1135. https://doi.org/10.1016/j.cherd.2010.12.004

Tsai, W. T., Hsu, H. C., Su, T. Y., Lin, K. Y., Lin, C. M., & Dai, T. H. (2007). The adsorption of cationic dye from aqueous solution onto acid-activated andesite. *Journal of Hazardous Materials*, *147*(3), 1056-1062. https://doi.org/10.1016/j.jhazmat.2007.01.141

Turner, A., & Millward, G. E. (2002). Suspended particles: their role in estuarine biogeochemical cycles. *Estuarine, Coastal and Shelf Science*, *55*(6), 857-883. https://doi.org/10.1006/ecss.2002.1033

United Nations. (2022a). United Nations World Population Prospects: The 2022 Revision Population Database.

United Nations. (2022b). United Nations sustainable development goals https://www.un.org/sustainabledevelopment/water-and-sanitation/ [Website] Accessed 20/05/2023.

US EPA. (1994). Method 200.8. Determination of Trace Eleements in Waters and Wastes By Inductively Coupled Plasama - Mass Spectrometry Revision 5.4. Environmental Monitoring Systems Laboratory, Office of Research and Development, U.S. Environmental Protection Agency, Cincinnati, Ohio 45268.

Vallejos, M. E., Felissia, F. E., Area, M. C., Ehman, N. V., Tarrés, Q., & Mutjé, P. (2016). Nanofibrillated cellulose (CNF) from eucalyptus sawdust as a dry strength agent of unrefined eucalyptus handsheets. *Carbohydrate polymers*, *139*, 99-105. https://doi.org/10.1016/j.carbpol.2015.12.004

Vanaja, M., Paulkumar, K., Baburaja, M., Rajeshkumar, S., Gnanajobitha, G., Malarkodi, C., ... & Annadurai, G. (2014). Degradation of methylene blue using biologically synthesized silver nanoparticles. *Bioinorganic chemistry and applications*, *2014*. https://doi.org/10.1155/2014/742346

Velázquez-Zavala, M., Peón-Escalante, I. E., Zepeda-Bautista, R., & Jiménez-Arellanes, M. A. (2016). Moringa (Moringa oleifera Lam.): potential uses in agriculture, industry and medicine. *Revista Chapingo. Serie horticultura*, *22*(2), 95-116. https://doi.org/10.5154/r.rchsh.2015.07.018

Verma, A. K., Dash, R. R., & Bhunia, P. (2012). A review on chemical coagulation/flocculation technologies for removal of colour from textile wastewaters. *Journal of environmental management*, *93*(1), 154-168.

Vieira, A. M. S., Vieira, M. F., Silva, G. F., Araújo, Á. A., Fagundes-Klen, M. R., Veit, M. T., & Bergamasco, R. (2010). Use of Moringa oleifera seed as a natural adsorbent for wastewater treatment. *Water, air, and soil pollution*, *206*, 273-281. https://doi.org/10.1007/s11270-009-0104-y

Vilaseca, M., López-Grimau, V., & Gutiérrez-Bouzán, C. (2014). Valorization of waste obtained from oil extraction in Moringa oleifera seeds: coagulation of reactive dyes in textile effluents. *Materials*, *7*(9), 6569-6584.

Vijayaraghavan, G., Sivakumar, T., & Kumar, A. V. (2011). Application of plant based coagulants for waste water treatment. *International Journal of Advanced Engineering Research and Studies*, *1*(1), 88-92.

Volesky, B. (1999). Biosorption for the next century. In *Process Metallurgy* (Vol. 9, pp. 161-170). Elsevier. https://doi.org/10.1016/S1572-4409(99)80104-7

Vunain, E., Masoamphambe, E. F., Mpeketula, P. M. G., Monjerezi, M., & Etale, A. (2019). Evaluation of coagulating efficiency and water borne pathogens reduction capacity of Moringa oleifera seed powder for treatment of domestic wastewater from Zomba, Malawi. *Journal of Environmental Chemical Engineering*, *7*(3), 103118.

Wang, S., Boyjoo, Y., Choueib, A., & Zhu, Z. H. (2005). Removal of dyes from aqueous solution using fly ash and red mud. *Water research*, *39*(1), 129-138. https://doi.org/10.1016/j.watres.2004.09.011

Wang, J., & Guo, X. (2020). Adsorption isotherm models: Classification, physical meaning, application and solving method. *Chemosphere*, *258*, 127279. https://doi.org/10.1016/j.chemosphere.2020.127279

Ward, J. S., Lapworth, D. J., Read, D. S., Pedley, S., Banda, S. T., Monjerezi, M., ... & MacDonald, A. M. (2020). Large-scale survey of seasonal drinking water quality in Malawi using in situ tryptophan-like fluorescence and conventional water quality indicators. *Science of the Total Environment*, *744*, 140674. doi: 10.1016/j.scitotenv.2020.140674

Webb, P. A. (2003). Introduction to chemical adsorption analytical techniques and their applications to catalysis. *Micromeritics Instrument Corp. Technical Publications*, 1-12.

Weng, C. H., & Pan, Y. F. (2007). Adsorption of a cationic dye (methylene blue) onto spent activated clay. *Journal of Hazardous Materials*, *144*(1-2), 355-362. https://doi.org/10.1016/j.jhazmat.2006.09.097

Wibowo, N., Nurcahyo, R., & Gabriel, D. S. (2022). Environmental awareness factor of used cell phones. *Global Journal of Environmental Science and Management*, *8*(1), 87-100.

World Health Organization. (2017). Progress on drinking water, sanitation and hygiene: 2017 update and SDG baselines.

World Health Organization. (2022). Drinking-Water detailed Fact Sheet. Available on https://www.who.int/en/news-room/fact-sheets/detail/drinking-water [Website] Accessed 20/05/2023.

Wu, Y., & Chen, J. (2013). Investigating the effects of point source and nonpoint source pollution on the water quality of the East River (Dongjiang) in South China. *Ecological indicators*, *32*, 294-304.doi : https://doi.org/10.1016/j.ecolind.2013.04.002

Xu, P., Zeng, G. M., Huang, D. L., Feng, C. L., Hu, S., Zhao, M. H., ... & Liu, Z. F. (2012). Use of iron oxide nanomaterials in wastewater treatment: a review. *Science of the total environment*, *424*, 1-10. https://doi.org/10.1016/j.scitotenv.2012.02.023

Yagub, M. T., Sen, T. K., Afroze, S., & Ang, H. M. (2014). Dye and its removal from aqueous solution by adsorption: a review. *Advances in colloid and interface science*, *209*, 172-184. https://doi.org/10.1016/j.cis.2014.04.002

Yamaguchi, N. U., Cusioli, L. F., Quesada, H. B., Ferreira, M. E. C., Fagundes-Klen, M. R., Vieira, A. M. S., ... & Bergamasco, R. (2021). A review of Moringa oleifera seeds in water treatment: Trends and future challenges. *Process Safety and Environmental Protection*, *147*, 405-420. https://doi.org/10.1016/j.psep.2020.09.044

Yang, G., & Wang, J. (2018). Kinetics and microbial community analysis for hydrogen production using raw grass inoculated with different pretreated mixed culture. *Bioresource technology*, *247*, 954-962. https://doi.org/10.1016/j.biortech.2017.09.041

Yargeau, V. (2012). Water and wastewater treatment: Chemical processes', *Metropolitan*
Sustainability: Understanding and Improving the Urban Environment, 1854, pp. 390–405. doi: 10.1533/9780857096463.3.390.

Yildiz, B. S. (2012). Water and wastewater treatment: Biological processes. In *Metropolitan Sustainability* (pp. 406-428). Woodhead Publishing. https://doi.org/10.1533/9780857096463.3.406

Yin, C. Y. (2010). Emerging usage of plant-based coagulants for water and wastewater treatment. *Process Biochemistry*, *45*(9), 1437-1444. https://doi.org/10.1016/j.procbio.2010.05.030

Yonten, V., Tanyol, M., Yildirim, N., Yildirim, N.C., & Ince, M. (2015). Optimization of Remazol Brilliant Blue R dye removal by novel biosorbentP. eryngiiimmobilized on Amberlite XAD-4 using response surface methodology. *Desalination and Water Treatment, 57(33), 15592 15602.* https://doi.org/10.1080/19443994.2015.1070760

Yusoff, M. A. M., Lee, C. W., & Bong, C. W. (2019). Analysis of water treatment by Moringa oleifera bioflocculant prepared via supercritical fluid extraction. *Polish Journal of Environmental Studies*, *28*(4), 2995-3002. https://doi.org/10.15244/pjoes/92119

Zaidi, N. S. (2019). Potential of fruit peels in becoming natural coagulant for water treatment. *International Journal of Integrated Engineering*, *11*(1). DOI: https://doi.org/10.30880/ijie.2019.11.01.017

Zaid, A. Q., & Ghazali, S. B. (2019). Dataset on physicochemical properties of particle-sized Moringa oleifera seed cake and its application as bio-coagulants in water treatment application. *Chemical Data Collections*, *24*, 100284. https://doi.org/10.1016/j.cdc.2019.100284

Zappi, D., Coria-Oriundo, L. L., Piccinini, E., Gramajo, M., Von Bilderling, C., Pietrasanta, L. I., Azzaroni, O., Battaglini, F. (2019). *The effect of ionic strength and phosphate ions on the construction of redox polyelectrolyte–enzyme self-assemblies. Physical Chemistry Chemical Physics, 21(41), 22947–22954.* doi:10.1039/c9cp04037d

Zhang, G., Hu, M., He, L., Fu, P., Wang, L., & Zhou, J. (2013). Optimization of microwave-assisted enzymatic extraction of polyphenols from waste peanut shells and evaluation of its antioxidant and antibacterial activities in vitro. *Food and Bioproducts Processing*, *91*(2), 158-168. doi:10.1016/j.fbp.2012.09.003.

Zheng, H., Feng, L., Gao, B., Zhou, Y., Zhang, S., & Xu, B. (2017). Effect of the cationic block structure on the characteristics of sludge flocs formed by charge neutralization and patching. *Materials*, *10*(5), 487. **https://doi.org/10.3390/ma10050487**

Zhigila, D. A., Mohammed, S., Oladele, F. A., & Sawa, F. B. (2015). Numerical analyses of leaf and fruit external morphology in Moringa oleifera LAM. *Jurnal Teknologi*, *77*(13).

Zouboulis, A. I., & Tzoupanos, N. (2010). Alternative cost-effective preparation method of polyaluminium chloride (PAC) coagulant agent: Characterization and comparative application for water/wastewater treatment. *Desalination*, *250*(1), 339-344.

Summary

The *MO* seeds, known for their coagulant effect were tested in dam water purification and wastewater treatment using coagulation-flocculation process. An evaluation via the optimisation of the influencing factors on this technique has been covered by using statistical methods such as RSM and artificial intelligence such as ANN. The dehulled and hulled *MO* seeds cake powder were used as coagulant, and the dose of coagulants has been fluctuated alongside fast and slow mixing of the jar test. Settling time has been tested too. All RSM and ANN models have been effective in the process description, with better performance of ANN models with R^2 0.96 at the IW and 0,99 at the OW. Both preparations of *MO* seeds cake powder were efficient in promoting the coagulation-flocculation process with better performance of the hulled seeds category. The waste of *MO* seeds peeling was recovered by synthesis of crystalline cellulosic nanoparticles (NPs). The synthetized NPs have homogenous porous structure, with a large specific surface area, and large porosity giving it a high adsorption capacity. The obtained NPs have been tested in methylene bleu adsorption (MB), and the process was found to be affected by the MB initial concentration, the NPs dosage and the pH of MB solution. The adsorption process fitted well to both pseudo first and second order model.

Résumé

Les graines de *MO*, connues pour leur effet coagulant, ont été évaluées dans la purification des eaux de barrage et le traitement des eaux usées en utilisant le processus de coagulation-floculation. Une évaluation via l'optimisation des facteurs d'influençant la technique a été réalisée à l'aide de méthodes statistiques telles que RSM et d'intelligence artificielle telle que ANN. Les poudres de tourteau de graines de *MO* décortiquées et non décortiquées ont été utilisées comme coagulants, et la dose de coagulants a été variée en même temps que l'agitation rapide et lente de l'essai en jar test. Le temps de décantation a également été varié. Tous les modèles RSM et ANN ont été efficaces dans la description du processus, avec une meilleure performance des modèles ANN, avec un R^2 de 0.96 à l'entrée et 0.99 à la sortie de la station. Les deux préparations de poudre de tourteau de *MO* se sont avérées efficaces pour promouvoir le processus de coagulation-floculation, avec une meilleure performance des graines décortiquées. Les déchets d'épluchage des graines de *MO* ont été valorisés par synthèse de nanoparticules cellulosiques cristallines (NPs). Les NPs synthétisées se caractérisent par une structure poreuse homogène, avec une grande surface spécifique et une grande porosité qui leur confère une grande capacité d'adsorption. Les NPs obtenues ont été testées dans l'adsorption du bleu de méthylène (BM), et le processus s'est avéré être affecté par la concentration initiale de BM, le dosage des NPs et le pH de la solution de BM. Le processus d'adsorption s'est bien adapté au modèle du pseudo-premier ordre et du pseudo-second ordre.

ملخص

تم اختبار بذورالمورينجا أوليفيرا المعروفة بخصائص التلبد وتأثيرها في تنقية مياه السدود ومعالجة مياه الصرف الصحي باستخدام عملية التلبد والتخثر. تم تقييم العوامل المؤثرة على هذه التقنية باستخدام الأساليب الإحصائية مثل طريقة سطح الاستجابة والذكاء الاصطناعي مثل الشبكة العصبية الاصطناعية. تم استخدام مسحوق البذورغير منزوع القشر والمُقشر كمخثر.تم استعمال عدة جرعات من المخثرين المدروسين مع الخلط السريع والبطيء و وقت الاستقرار لاختبار الجرة. كان اداء جميع النماذج فعال مع فعالية قصوى لطريقة الشبكة العصبية الاصطناعية بمعمل تحديد 0.96عند مدخل المحطة و 0.99 في المياه الخارجة منها, مع العلم ان اداء المخثر منزوع القشر كان اكثر فعالية. من جهة اخرى تم استرداد نفايات تقشير بذورالمورينجا أوليفيرا من اجل استغلالها في تصنيع النانوجسيمات. و قد ثثبت ان هذه الاخيرة تتميز ببنية مسامية متجانسة ، مع مساحة سطح محددة كبيرة و التي تمنحها قدرة امتصاص عالية و هي ذات طبيعة سليلوزية بلورية. لقد تم اختبار قدرة هذه الجسيمات على امتصاص ازرق الميثيلين. و قد ثبت ان هذه العملية تتأثر بتركيزمحلول ازرق الميثيلين, بحموضة المحلول و كذلك جرعة النانوجسيمات المستعملة. و قد اثبتت دراسة حركية عملية الامتصاص ان العملية تخضع لكلا نموذجي الحركية و المتمثلين في نموذج الدرجة الاولى و الثانية.